UNIVERSITY OF OKLAHOMA

GRADUATE COLLEGE

MAPPING AND ANALYZING URBAN GROWTH: A STUDY TO IDENTIFY DRIVERS OF URBAN GROWTH IN WEST AFRICA

A DISSERTATION

SUBMITTED TO THE GRADUATE FACULTY

in partial fulfillment of the requirements for the

Degree of

DOCTOR OF PHILOSOPHY

By

PRADEEP ADHIKARI
Norman, Oklahoma
2016

MAPPING AND ANALYZING URBAN GROWTH: A STUDY TO IDENTIFY DRIVERS OF URBAN GROWTH IN WEST AFRICA

A DISSERTATION APPROVED FOR THE
DEPARTMENT OF GEOGRAPHY AND ENVIRONMENTAL SUSTAINABILITY

BY

_____
Dr. Kirsten M. de Beurs, Chair

_____
Dr. David Sabatini

_____
Dr. Renee McPherson

_____
Dr. Aondover Tarhule

_____
Dr. Yang Hong

Acknowledgements

First of all, I would like to express my sincere gratitude to my advisor Dr. Kirsten M. de Beurs for the continuous support during my Ph.D. study and research, for her patience, and for her motivation. Her guidance steered me on the right path in this journey. Thank you Dr. de Beurs!

I would like to extend my sincere thanks to the rest of my committee members: Dr. David Sabatini, Dr. Renee McPherson, Dr. Aondover Tarhule, and Dr. Yang Hong for their insightful questions and encouragement along the way. Such questions and probing helped me to widen my research from various perspectives. I also thank my fellow students from the Landscape Land Use Change Institute for the stimulating discussions and comments on my research, presentations and write-ups. Additionally, I would also like to extend my gratitude to the faculty, staff and students of the department for their support and help, directly or indirectly during my graduate study.

My parents, Jeevan and Saraswati, who are living on the other side of the globe, are the constant source of encouragement throughout for which I am always grateful. Last but not least, I thank my wife Kabita and children Pranshu and Pranjal for their continuous love and support. They played various roles including counsellors wherever needed, and kept me motivated during my study and research. This journey would not have been completed without their support and sacrifice.

Table of Contents

List of Tables

CHAPTER 4

List of Figures

CHAPTER 1

CHAPTER 2

CHAPTER 3

CHAPTER 4

Abstract

Urban area expansion is one of the most powerful anthropogenic forces changing the earth‘s surface. Such changes are happening at much faster rates in African and Asian cities. Several interconnected but distinct processes like increase in population concentration and extensive alteration of the landscape are associated with urban area expansion. Therefore, understanding the urban area expansion and its drivers is a key task to devise a plan for sustainable urban development. In this study we mapped and analyzed urban area growth of six mid to large size cities of West Africa.

In land cover studies, growth in urban land use are characterized by the declines in cropland. So, firstly we evaluated twelve freely available, remotely sensed land cover and land use (LCLU) datasets at the eco-region, country, and pixel levels in West Africa to estimate croplands. The result shows a very high variability of estimated cropland at all levels. Despite this variability, datasets having a finer spatial resolution and representing a similar time period—specifically data from the International Institute for Applied Systems Analysis-International Food Policy Research Institute (IIASA-IFPRI), Global Land Cover-SHARE(GLC-SHARE), Moderate Resolution Imaging Spectroradiometer-UMD (MODIS-UMD), Global Cropland Extent, Moderate Resolution Imaging Spectroradiometer-UMD (MODIS-IGBP), and GLOBCOVER (GlobCover V23)—estimated comparable cropland areas at eco-region and country levels. The countrywide cropland area, obtained from the selected datasets, when compared with the sum of arable land and permanent crop area obtained from the Food and Agriculture Organization (FAO), showed high coefficient of determination (R^2>0.95) for IIASA-IFPRI, and GLC-SHARE. At the pixel level, at the original

resolution, the newer datasets have a comparable user's accuracy (UA>53%) and producer's accuracy (PA>46%), except for the Global Cropland Extent data. Overall, two datasets – IIASA-IFPRI and GLC-SHARE– performed better in the region to estimate the cropland area at all levels.

Next, we used Landsat MSS, TM and ETM+ images to map the urban land area in six West African cities for four different time steps from the early-1970s to 2010. The selected cities are Kumasi of Ghana, Daloa of Cote d'Ivoire, Abuja and Kano in Nigeria, Kindia of Guinea, and Ouagadougou of Burkina Faso. They also represent three different eco-regions: Eastern Guinean Forest, Guinean Forest-Savanna Mosaic, and West Sudanian Savanna of West Africa. We found that all the cities, except Daloa, have a large number of non-urban pixel converted to urban in the past three to four decades. The growth of the urban areas was high, 13 to 54%, but the growth trajectories were not consistent. For example, the rate of urban growth has been declining in Abuja and Ouagadougou in recent years while Kumasi has been growing consistently at a much higher rate since 1975 and was still growing about 13% annually, between 2005 and 2010. Also, most of the cities have shown a higher rate of growth of urban land use than population except Abuja and Ouagadougou. These cities revealed higher population growth, (10.7 to 15.8%) than urban land use growth, which varies from 3.0 to 4.5%. We did not observe any similarities in the growth of cities from the same eco-region.

Finally, we identified that Normalized Difference Vegetation Index (NDVI) and distance to the urban area showed strong associations with the growth of six cities in West Africa. The six cities include Kumasi, Daloa, Abuja, Kindia, Ouagadougou, and

Kano. We found that none of the factors showed a consistent association with urban land use. Out of the six cities, Ouagadougou and Kano showed some level of agreement in associating the urban growth with NDVI at different time periods. In the rest of the cities, proximity parameters such as distance to the nearest urban area and distance to the core city area showed some level of association to urban growth. These findings shows that the process of conversion of urban land use is unique for a city at a given time period.

Chapter 1: Introduction

Urban area expansion, one of the most powerful anthropogenic forces changing the earth‘s surface (Dawson et al. 2009; Cui and Shi 2012), is associated with several interconnected but distinct processes like increase in population concentration and extensive alteration of the landscape (McDonnell and Pickett 1990). The literature treats urbanization differently in different contexts (Hope 1942; Satterthwaite et al. 2010; Marcotullio and Solecki 2013; Seto et al. 2013). Some define urbanization as a movement of people from rural to urban areas with population growth equating to urban migration (DESA/UN 2011) while others argue that urbanization is the process which covers some aspect of a region’s population, economy, or built infrastructure (Seto et al. 2011).

Since 2010, more people live in urban than in rural areas around the world (UN 2011). It is expected that by 2050, more than 60 percent of the global population will live in urban areas. However, the level of urbanization differs greatly across the world. On the one hand, the population of many of the countries in Europe, Latin America and the Caribbean, Northern America and Oceania is mostly urban. On the other hand, despite an increase in the rate of urbanization around the world since 1950, the majority of the population in countries in Africa and Asia (except China) remain mostly rural (DESA/UN 2011; Cui and Shi 2012; Seto et al. 2013). Major changes in urban population are projected to take place in developing countries in Africa and Asia (Satterthwaite et al. 2010; DESA/UN 2011) likely altering the landscapes greatly.

Historically, urban hubs around the world have been the center of economic and social development, but urbanization has also negatively affected Earth’s environment

(Hope 1942; Satterthwaite et al. 2010; Rodriguez 2008; Marcotullio and Solecki 2013). As urban centers grow, the increasing concentration of people and economic activities demand further development of housing and public infrastructures (Thapa and Murayama 2009) changing the urban landscape. Several studies have investigated impacts of such development on the biota and physical environment (McDonnell and Pickett 1990; Lambin et al. 2001; Kalnay and Cai 2003; Alberti 2005; Satterthwaite et al. 2010; Tian et al. 2011; Marcotullio and Solecki 2013). One of the serious impacts of urbanization according to those studies is on land use and land cover (LULC) in and around the urban centers including encroachment on croplands (Tian et al. 2011). Furthermore, LULC changes, associated with urban development, are considered one of the most disturbing processes and are the causes of changes in mesoscale weather patterns, water resources, and biodiversity (McDonnell and Pickett 1990; Kalnay and Cai 2003; Alberti 2005; Liu et al. 2010). There is also evidence of changes in composition and structure of ecological communities associated with urban land use (Posa and Sodhi 2006; Sadler et al. 2006).

Traditionally, migration from rural to urban areas is credited for urbanization. The classic push and pull factors working in tandem with strong links to economic development are the prime reason of such movement of the human population. But urbanization in developing countries including countries in Sub-Sahara Africa (SSA) does not show the same level of economic improvement in the urban area as has been found in the developed countries (Barrios et al. 2006). Recent studies in China show that government policies have played a key role in the migration of people and the growth of urban areas (Cui and Shi 2012). The growth of urban population in West

Africa is also attributed to high population growth and migration from the rural area (UNEP 2012). The economy is the primary driver for urbanization in developing regions, including West Africa (UNEP 2012; Barrios et al. 2006; DESA/UN 2011). Shortfall in crop production affecting livelihood, lack of services (e.g. health and education) and poor security situations are some of the common push factors while higher employment opportunities, better services and security are the main pull factors (AEO/UNEP, date; Barrios et al 2006; DESA/UN 2011). An increasing number of studies on rural urban migration in SSA also show climate as an important factor (Barrios et al. 2006; Parnell and Walawege 2011) along with social and economic factors for the movement of people to urban areas. In a region like West Africa where the agricultural sector employs 60 percent of the active labor force as subsistence farmers (Jalloh et al. 2013), changes in the rainfall amount and onset of rainfall play a significant role. A poor harvest due to such changes means a likely loss of livelihood for these farmers. This situation has caused movement of people from rural areas to the nearby urban areas looking for jobs and improved livelihoods (Barrios et al. 2006).

There are many studies of urban growth around the world using remote sensing data (Mundia and Aniya 2005; Seto et al. 2011; Attua and Fisher 2011; Forkuor and Cofie 2011; Weng 2012; Karolien et al. 2012; Kamh et al. 2012; Brinkman et al. 2012; Linard et al. 2013; Wania et al. 2014). But the number of studies vary across the regions of the world. Seto et al. (2011) did a meta-analysis of studies that monitored changes in urban land-use using remote sensing for the period between 1988 and 2008. They listed 326 case studies around the world meeting their criteria. The majority of the studies were carried out in China, North America, Europe, and South West Asia. In Africa, they

found only twenty nine studies addressing urban expansion (Seto et al. 2011). Yeboah (2000, 2003) also mentions that urban expansion in Africa had not been adequately studied. However, the situation is changing as an increasing number of studies are being carried out focusing on the expansion of urban and peri-urban area in Africa in recent years (Karolien et al. 2012, Attua and Fisher 2011, Forkuor and Cofie 2011, Kamh et al. 2012, Brinkman et al. 2012, Linard et al. 2013, Wania et al 2014). Below, I will summarize some of the research that has focused on urban expansion in West Africa. One of the commonalities of these studies is the use of Landsat imagery at several time steps. Another commonality is the focus on the expansion of just *one* city disregarding the development of other cities in the region.

Mundia and Aniya (2005) studied the land use/ cover changes and urban expansion of Nairobi City, Kenya using Landsat Multi-spectral Scanner (MSS), Thematic Mapper (TM) and Enhanced Thematic Mapper plus (ETM +) images for 1976, 1988 and 2000. They found that for the period from 1976 to 2000, the urban area grew by about 50 square kilometers. They also identified economic growth and proximities to transportation routes as the major factors for urban growth.

Karolien et al. (2012) used Landsat images from 1989, 1995, 2003 and 2010 to map and analyze the urban growth of Kampala, Uganda. In the study, a logistic regression model for the growth of Kampala was developed, and it revealed the presence of roads, accessibility of city center, and distance to the existing built-up area as the controlling factors of the growth of the city. They also predicted the future urban growth for three alternative scenarios.

Attua and Fisher (2011) used Landsat data 1985 to 2003, to study the urban expansion of the New Juaben municipality in Ghana. The study found that the urban core expanded by 10% and the periurban areas expanded by 25% over the period at the expense of open woodlands, tree, grass, and crop areas. They also found that the prime drivers of land-cover changes are demographic changes and past microeconomic policies.

Forkuor and Cofie (2011) used Landsat data from 1974, 1986, and 2000 to study the land use and land cover change in Freetown, Sierra Leone, and found an astounding growth of the urban area by more than 140% for the period 1974 to 2000. The change occurred at the loss of agriculture areas, grasslands, forests, and barren lands.

Kamh et al. (2012) evaluated the urban land cover change in the Hurghada, Egypt using Landsat 7 ETM+, Landsat 5TM and Advanced Space borne Thermal Emission and Reflection Radiometer (ASTER) data from 1987, 2000 and 2005. They used post-classification comparison of the urban expansion and found expansion of the urban area by 40 square kilometers for the period 1987 to 2005.

Brinkman et al. (2012) used a Corona (KH-4B) panchromatic image and Landsat (TM and ETM) data in combination with geographical and demographic data to study landscape transformation processes (LTP) in four different cities of West Africa. They mapped four LTP processes namely urbanization, crop expansion, deforestation, and land abandonment for the cities and surrounding area for the period from 1986 to 2009 on the basis of common classification of the Landsat and Corona images.

Linard et al. (2013) studied the spatial pattern of urban growth in twenty large cities of Africa using the Atlas of urban expansion available from the Lincoln Institute

of Land Policy (http://www.lincolninst.edu/) and Landsat images from the 1990s and 2000s. They classified Landsat images into built-up and non-built-up pixels. They used travel time to core business district, distance to nearest urban pixels and slope as the covariates to model the urban growth in those cities.

Wania et al. (2014) mapped the built-up area changes in the city of Harare, Zimbabwe with Spot-2 and Spot-5 for the period 2004-2010 at 10m spatial resolution. They investigated the change in built-up area with the change in population density and observed a good correlation between these two parameters. They analyzed the change at the grid and administrative levels.

Most of the research on urban land cover change in Africa presented above is primarily focused on *one* city. These studies map the land cover for different time period (s) using remote sensing data, mainly Landsat data along with some ancillary data and analyze the change in urban growth over certain time period(s). None of the studies so far have taken a comprehensive look at urban growth. For example, they do not investigate the interplay of environmental and socio-economic factors in the growth urban land use of a city, let alone cities across the various ecoregions of West Africa. In addition, none of the studies have looked into any similarities or differences in the urban growth of the cities within West Africa. This study attempts to fill this gap.

A review of existing land cover change studies including the expansion of urban area or urban land use shows that such studies have focused mainly on spatio-temporal changes on land cover in an area or a region (Mundia and Aniya 2005; Seto et al. 2011; Attua and Fisher 2011; Forkuor and Cofie 2011; Weng 2012; Karolien et al. 2012; Kamh et al. 2012; Brinkman et al. 2012; Linard et al. 2013; Wania et al. 2014) as

described in previous paragraphs. A comprehensive analysis of environmental and socio-economic parameters could help our understanding of the process and drivers of urban area expansion. For example, about 60 percent of active labor force depends on subsistence agriculture in the study region. Since agricultural productivity is highly dependent on favorable climatic conditions (i.e., good and timely onset of rainfall, suitable temperature), any variability on climate impends the livelihood of subsistence farmers triggering the movements of more people to the cities causing the physical growth of cities in the region. Thus, I postulate that studying urban growth of cities from three different eco-regions: Eastern Guinean Forest, Guinean Forest-Savanna Mosaic, and West Sudanian Savanna representing five different countries (Burkina Faso, Cote d'Ivoire, Ghana, Guinea, and Nigeria) within West Africa will help to better explain the nature of urban growth in the region. Furthermore, urban growth analysis based on cities across the eco-regions will help researchers to identify factors affecting the urban growth among the cities of West Africa. I am interested in studying if those factors vary across the eco-regions and/or countries.

Research questions and hypothesis

The overarching research question is: How has the urban land use expanded and what are the reasons of such expansion in the region? More precisely this research attempts to answer the following specific questions.

1. How have publically available land cover and land use datasets mapped and quantified agriculture land use in West Africa? How does this data quantify agriculture land use in the various eco-regions of West Africa?

2. What is the rate of urban land use change for the selected nine West African cities since 1970s based on remote sensing data?
3. Do environmental factors (e.g. Normalized Difference Vegetation Index-NDVI and precipitation anomalies) play a role in the expansion of the urban land use in the selected cities of West Africa? If so, how?
4. Do socio-economic factors (e.g. population growth, security, and human influence index) play a role in the expansion of urban land use in the selected cities of West Africa? If so, how?
5. Are the same causal factors responsible for expansion of urban land use of the cities within an eco-region? If so, do they influence the urban land use expansion equally or differently?

To address these research questions, I propose the following hypothesis:

Null hypothesis (H_0): If the growth of cities within specific eco-regions of West Africa are driven by the same environmental factors, then changes in these environmental factors will result in similar expansion of urban expansion of these cities within the ecoregions leading to comparable urban land use.

Alternative hypothesis (H_1): Other factors, such as national policies and localized socio-economic factors play a more significant role in the urban expansion of cities within specific eco-regions, resulting in cities within ecoregions to reveal urban land use expansion at differential rates.

Study area

The study area covers the fifteen contiguous countries (Figure 1.1) of West Africa (referred as West Africa) from Sub-Sahara Africa (SSA). This region of Africa has witnessed the most severe and longest droughts in the world since the late 1970s (Druyan, 2011; Wang and Eltahir, 2000). The general climate in the region is dictated by the tropical continental air mass, dry and dusty from the Sahara Desert and another mass of tropical maritime air, warm and humid from the south Atlantic forming a convergence zone (the Inter Tropical Convergence Zone or ITCZ). The ITCZ also dominates the annual rainfall variability in the region (AIACC, 2006). This region of Africa has a population of a little over 300 million people as of 2010 and is expected to reach 570 million in 2050 and 735 million by the end of 21st century (DESA/UN 2011). The average urban population growth rate since 1950 is the second highest compared to the other regions of Africa. In 1900 the growth rate was 5% which rose to 12% in 1950, 28% in 1980 and 17% in 2000 (Fuwape and Onyekwelu 2010). I selected six cities from four eco-regions (Olson et al 2001) of West Africa for detailed study (Figure 1.2 and Table 1.1).

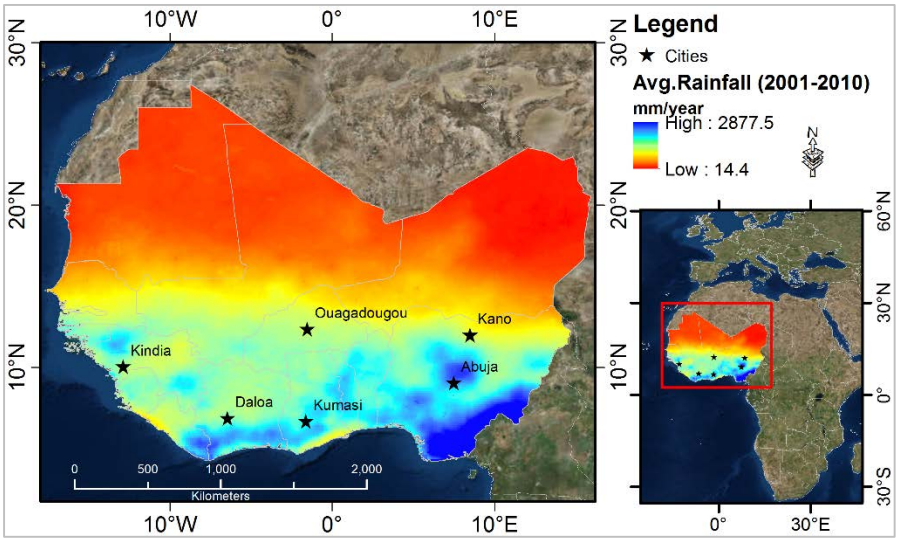

Figure 1.1. Study area of West Africa and selected cities.

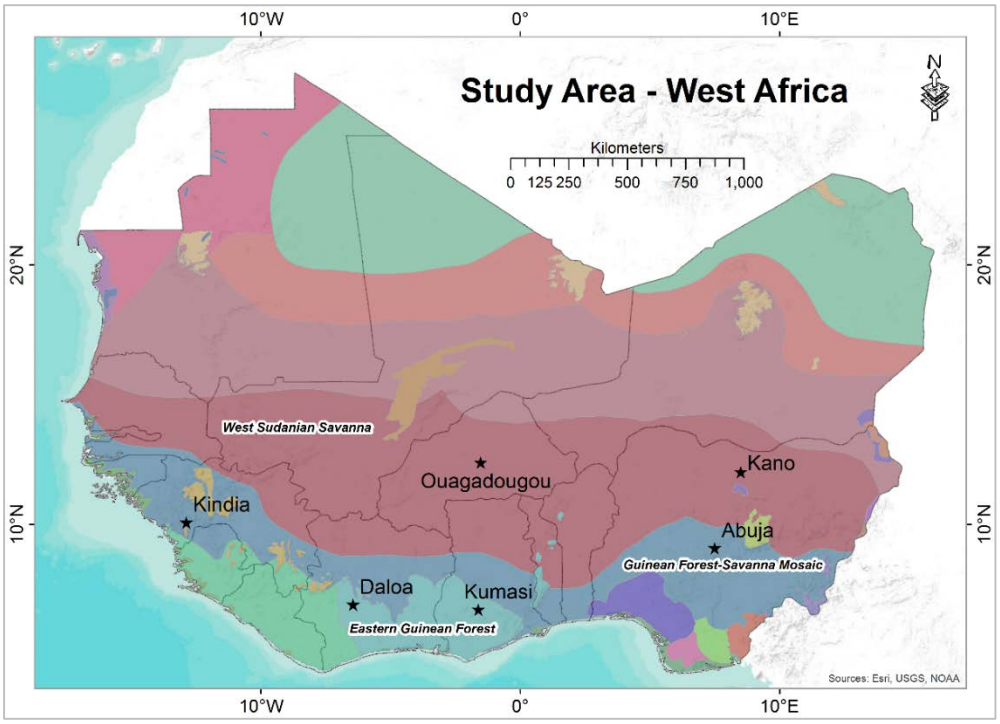

Figure 1.2. Selected cities and their eco-regions in West Africa.

Table 1.1. Salient features of selected cities.

Cities	Countries	Eco-regions	Mean annual rainfall (mm, for 2001-10)	Population (for 2000 in '000)*	Population (for 2010 in '000)*
1.Kumasi	Ghana	Eastern Guinean Forest	1,146	1,187	1,935
2.Daloa	Cote d'Ivoire		1,026	185	248
3.Abuja	Nigeria	Guinean Forest-Savanna Mosaic	1,436	833	2,153
4.Kindia	Guinea		730	96	135
5.Ouagadougou	Burkina Faso	West Sudanian Savanna	812	921	1,911
6.Kano	Nigeria		712	2,602	3,271

**Sources: DESA/UN, 2011 and Institut National de la Statistique*

The selected six cities are some of the medium to large and fastest growing cities in West Africa and are from five different countries: Ghana, Cote d'Ivoire,

Nigeria (two), Guinea, and Burkina Faso. In terms of eco-regions, the cities are from four eco-regions of West Africa: Eastern Guinean Forest, Guinean Forest-Savanna Mosaic, and West Sudanian Savanna of West Africa. Although by definition an ecoregion has a relatively uniform climate with unique ecological communities (Olson et al. 2001), climatic parameters like annual rainfall may vary within the same ecoregion (Table 1.1). Therefore, at least two cities from the same eco-region with different annual rainfall patterns are selected for this study. In addition, as urban growth may have been affected as a result of government's land policy (Wu et al. 2011) the selected cities capture any variability that exist in the region both in terms of climate and land policy. A brief description about the cities is given below.

Kumasi, Ghana

Kumasi was founded in 1680 and developed into a major commercial hub during the British rule (Fynn 1971; Dickson 1969). The British rule, which started in 1890, the city grew and became second to Accra—the capital city of Ghana—in terms of land area, population and economic activity (Adu Boahen 1964). The first city plan of Kumasi was laid out by the British administration in 1896 (Urban Design Lab/Earth Institute 2012). The city of Kumasi turned into a major commercial hub primarily due to major road connections to the other West African cities in Cote d'Ivoire, Togo and Burkina Faso (Baker 2008). The growth of Kumasi originally occurred radially as the result of arterial roads in the city. In modern times, the passage of the Town and Country Planning Ordinance, Cap 84, marked the genesis of an organized urban

development of Kumasi in 1945 (Urban Design Lab/Earth Institute 2012; Kasanga and Kotey 2001).

Kumasi, situated in a wet semi-equatorial zone, has bi-modal rainfall distributions with two peaks (Nkrumah et al. 2014). The major rainfall season is from April to July (about 160 to 225mm/month) followed by a minor rainfall season that occurs between September and mid-November (60-175mm/month) (Maoulidi 2010; Nkrumah et al., 2014). The average temperature in the city varies from 24°C to 27 °C (ClimaTemps 2016). The central location of the city and its milder climatic conditions have contributed to the high rate of migration to the city (Cobbinah and Amoako 2012) and its expansion. The completion of the Volta River Dam Project in 1970 also contributed to the growth of urban population in Ghana including the city of Kumasi (d'Auria and De Meulder 2011; d'Auria 2012). In 2013, the population in Kumasi has found to have grown at 5.4 % annually, the fastest in Ghana causing the growth in the outskirts of the city as well (Amoateng et al. 2013). According to a 2010 estimate the city has the area of about 21,400 ha (Ghana Statistical Service 2014). The outskirts have become the preferred places for residential and commercial development due to the relatively low land values (Drabkin 1977; Cobbinah and Amoako 2012; Amoateng et al. 2013). The physical development of the area is going on in a haphazard manner at the cost of prime agriculture land surrounding the city (Amoateng et al. 2013). Scattered or dispersed development is the most common sprawl type happening in Kumasi (Cobbinah and Amoako 2012).

In terms of city amenities, Kumasi is not different from any other third world city in Africa and Asia. The pace of the population growth has outpaced the

development of infrastructure for better public health and safety (Urban Design Lab/Earth Institute 2012; Cobbinah and Amoako 2012) as a result roads are very congested, and the water and sanitation network in the city become inadequate.

Figure 1.3. A view of Central Market, Kumasi, Ghana. (Photo credit: Ian Bacon, Univ. of Oregon, 2014)

Figure 1.4. A view of an outskirt area of Kumasi, Ghana. (Photo credit: Ian Bacon, Univ. of Oregon, 2014)

Daloa, Cote d'Ivoire

Daloa is the third largest city of Cote d'Ivoire in terms of population size. Currently, the city serves as the capital of the Haut Sassamdra region of Cote d'Ivoire (Daddieh 2012). Daloa became a French military post in 1903 (Daloa 2016). Daloa was granted the status of a medium-sized town, called "normal exercise" commune, through a law in late 1955 along with six other towns (Attahi 1989). Despite such arrangements, the communes such as Daloa lacked resources even to prepare the city master plan (Attahi 1989). During the Ivoirian civil war that lasted from 2002 to 2007, and again from 2010-2011, the city became the battleground for the rebels, mainly representing Muslim northerners and government security forces, dominated by the Christian southerner (Daddieh 2012).

The city of Daloa falls on the forest agro-ecological zones of Cote d'Ivoire and receives average annual rainfall of 1,300mm to 2,540mm and is humid year around (Erenstein et al. 2006; Aregheore 2009). The average temperature varies from 24°C to 27 °C (Climate-Data, 2016). So the seasons in the city are less clearly marked (Aregheore 2009).

The population of Daloa rose from 20,000 in 1960 to 112, 000 in 1988 (Population Statistics 2016). Due to the development of the plantation sector the economy of Cote d'Ivoire has attracted foreign labors since the colonial times (ICMPD and IOM 2015). Daloa receives a good share of such migrants from drier areas to the north who are attracted by the labor opportunities in the cocoa and coffee plantations in the region (Erenstein et al. 2006). The city is a local trading center for rice, cassava, cocoa and coffee (Daloa 2016).

Abuja, Nigeria

The city of Abuja is located in the central part of Nigeria. Abuja was designated as the capital city in 1976 by a military government decree (Ikoku, 2004; Abubakar and Doan, 2010). All Federal Government institutions and diplomatic missions were relocated to Abuja from Lagos during the 1990s (Ikoku, 2004). The city area is hilly and dissected terrain at 760m from the mean sea level (Balogun, 2001). Abuja receives about 1630 mm rainfall annually while the mean annual temperature ranges from 26°C to 30°C (Fanan et al. 2011).

Abuja was initially developed based on a master plan devised in 1976 so as to avoid problems associated with the unplanned growth in other Nigerian cities (Imam et al., 2008). The city is planned in such a way that the central area, which has a layout in the form of a grid, extends east-west while the residential areas are planned in the north and south of the city (Ebo 2006). But while implementing the original plan, the Nigerian Government had to change the resettlement policies to address the concern of indigenous people living outside the first phase of the master plan (Ebo, 2006). So, many provisions of the original plans were revised or not implemented.

Despite the objectives of the creation of a modern, spacious, and functional city with an emphasis on preserving the nature and environmental quality, a 1999 review of the Abuja master plan found that the city is dysfunctional and physically worsening (Adama, 2012; Ikoku 2004; Ebo, 2006). The city saw rapid growth in its population, from 379,000 in 1991 to 1.4 million in 2006 (Adama, 2012). The physical deterioration in the city is attributed to the poor management of solid waste, however, some argue that population growth alone does not explain the failure to solid waste management but

it is an issue of urban governance (Adama 2012). Also, in recent decades, several suburbs of the city have seen a proliferation of squatter settlements mainly driven by rural migration and very high housing prices in the city (Abubakar 2014). Furthermore, the pace of urban development is slow compared to the rate of population growth (Abubakar 2014; Ujoh et al. 2010). This creates sub-urban areas without adequate basic infrastructure and social amenities creating very poor living conditions (Adama 2007; Imam et al. 2008).

Kindia, Guinea

The city of Kindia in Guinea was established in 1904 as a collection point for agriculture produce on the railroad and became a primary trading center for rice, cattle, fruits and palm oil (Kindia 2016).

According to the latest population data Kindia has a population of 117,062 which is the fourth largest in Guinea (GeoNames 2016). The city has a tropical, sub-hum climate with an average annual rainfall that varies from 1,900 to 3,600 mm and average annual temperature of about 26°C (Camara et al. 2011; Climate-Data 2016). The rainy season in the city lasts six months, from April to September.

The surrounding area of the city of Kindia has a majority population depend on farming, which shows the importance of agriculture in the local economy. The share of agriculture contribution in the economy of the region is about 80% (Camara et al. 2011). In addition to the farming, a significant bauxite mining is done near Kindia (Bah 2014; Kindia 2016).

The city amenities are poor. The region of Kindia has little over 55% coverage of improved drinking water sources (ACAPS 2015). In recent years, international development agencies such as the World Bank are supporting the city for the inner roads and sewer systems (The World Bank 2006).

Ouagadougou, Burkina Faso

Ouagadougou, the capital city of Burkina Faso, was founded in the 15th century and developed into a trading and business center (Skinner 1974). The city is a part of the Soudano-Sahelian eco-region and has a tropical savannah climate (Santos and LeGrand 2002) with decreasing gradient of average annual rainfall from south, with average annual rainfall of about 900mm, to the north, with an average annual rainfall of less than 500mm (Offerle et al. 2005; Henry et al. 2004). The rain falls during a single wet season from May to September (Henry et al. 2004). The mean air temperature in the city varies from 23°C to 34°C (Offerle et al. 2005). During the dry season, January to March, the climate of the city is very dry. During this time, dusty wind resulting from the Harmattan wind blows from the Sahara (Offerle et al. 2005).

In 1962, the population of Ouagadougou was about 60,000 (Skinner 1974), which grew to about 1.9 million in 2010 (DESA/UN 2011). The growth is expected to continue in future. Being one of the two largest urban centers in Burkina Faso, Ouagadougou has attracted the largest percentage share of migrants from the rural area, within and outside the country, over the past decades (Henry et al. 2004; Beauchemin and Schoumaker 2005). The rural to urban migration is attributed to the environmental conditions, primarily to an insufficient or late onset of rainfall hampering agriculture

production. As Burkina Faso has experienced long droughts, mainly in the early 1970s and in the mid-1980s, migration from the rural to the urban centers are also taken as a survival strategy by the people (Henry et al. 2004; Guilmoto 1998).

Kano, Nigeria

The city of Kano is located between latitude 11° 55’24” N to 12° 3’ 53” N and longitude 8°27’42” E to 8° 36’42” E (Dankani 2013). Kano, located in the semi-arid savannah belt, has a distinct wet and dry seasons (Lynch et al. 2001). The wet season lasts about five months from May to September, with August being the wettest month. The annual rainfall varies from 600 to 1200 mm. The mean annual temperature varies from 26°C to 32°C (Mohammed et al. 2015). There is little variation in temperature, compared to the rainfall, but the mean temperature value could be cooler during the Harmattan period (Gwadabe 2012). A network of rivers and rivulets including Challawa, Kano, and Jakara Rivers drains the city (Gwadabe 2012).

Kano was established in the 9th century and its planning and development started in the period 1095-1134 (Barau 2006; Dankani 2013). In 1820, Kano had the population of about 30 to 40 thousand people (Minjibir 2012). According to the 2006 census, the population of the metropolitan Kano was 2.2 million which is the second largest in Nigeria after Lagos (National Population Commission, 2006). Currently, the city serves as the capital of Kano State and is an important commercial and administrative center of northern Nigeria (Barau 2006).

A twenty year development plan was prepared in 1963 (Home, 1986) and revised in 1976, 1980 and 1990 (Dankani 2013). But this plan had been marred by

shortcomings related to procedural, technical, financial and enforcement issues (Dankani 2013). In 1963, the plan intended to expand to the southwest and indicated the future road network and neighborhoods. This is only partly implemented The urban landscape of Kano has gone through several changes from the cluster of indigenous buildings and structures to Islamic architecture, and to British colonist's changes in built environment including land development policies (Barau et al. 2008). The city has two settlement patterns: traditional nucleated pattern with irregularly shaped houses with narrow streets and a modern nucleated pattern where houses are rectangular or square shaped and attached with wider streets (Gwadabe 2012).

As other major cities of Nigeria, Kano also lacks efficient management of solid waste generated in the city. The rate of generation of solid waste has outpaced the development of infrastructure and efficiencies of solid wastes management practices (Nabegu and Mustapha 2015) threatening the well-being of the public at large in the city (Butu and Mshelia 2014).

Methodology

To accomplish the objectives of this research, the following tasks are accomplished.

1. Examine the agriculture land use in West Africa based on available global land cover land use datasets.
2. Map and analyze the urban growth of the six selected cities of West Africa.
3. Investigate the relationship of environmental and socio-economic factors and the urban growth.

4. Compare the factors of urban growth in the selected cities across the same and different eco-regions of West Africa.

This study primarily uses remote sensing and geographic information systems to map and analyze the land cover in West Africa and logistic regression to understand the drivers of the urban growth. The details about the methodology are presented in each chapters in details.

Organization of dissertation

The dissertation chapters are structured as standalone manuscripts for the publication in professional journals. Chapter one provides an introduction to the topic including research questions, hypothesis, study area, and tasks. Chapter two, compares twelve global and regional Land cover and Land use (LCLU) datasets to estimate cropland. This chapter has been submitted to the *International Journal of Remote Sensing* for publication and is under review. Chapter three maps and analyzes the growth in urban land use in the selected six West African cities and is formatted for submission to *Land Use Science*. Chapter four identifies factors responsible for the growth of urban land use in the cities analyzed in chapter three. This chapter is formatted for submission to the journal of *Urban Ecosystems.* Finally, in chapter five I summarize conclusions obtained in the previous chapters and propose future research.

Literature cited

ACAPS (2015). Guinea: Country profile, available from http://acaps.org/img/documents/c-acaps-country-profile-guinea-29012015.pdf , accessed on March 03, 2016.

Adu Boahen, A. (1964). Britain, the Sahara, and the western Sudan, 1788–1861. Oxford Studies in African Affairs xiii, 268 pp., 4 maps. Oxford, Clarendon Press, 1964.

Amoako, Clifford, with David Korboe (2011). Historical Development, Population Growth and Present Structure of Kumasi. In Adarkwa, op. cit. 35-54.

Aregheore, E.M. (2009).Country pasture/forage resources profile, Cote d'Ivoire, Food and Agriculture Organisation.

Attahi, K. (1989). Cote d'Ivoire: An evaluation of urban management reforms in *African Cities in Crisis Managing Rapid Urban Growth*, Richard E. Stern and Rodney R. White (eds.) Westview Press.

Bah, M. D. (2014). Mining for peace: diamonds, bauxite, iron ore and political stability in Guinea. *Review of African Political Economy*, *41*(142), 500-515.

Baker, G. (2008). Assessing Infrastructure Constraints on Business Activity in Kumasi Ghana, MCI and VCC Working paper series on Investment in the Millennium Cities No. 3/2008 available from http://mci.ei.columbia.edu/files/2012/12/Kumasi_Infrastructure.pdf accessed on February 20, 2016

Balogun O (2001). The Federal Capital Territory of Nigeria: A Geography of its Development. University Press, Ibadan.

Butu, A. W., & Mshelia, S. S. (2014). Municipal solid waste disposal and environmental issues in Kano metropolis, Nigeria. *British Journal of Environmental Sciences*, *2*(1), 1-16.

Camara, M., Wen, Y., Wu, H., Diakite, M., Gerson, K. K., & Wang, H. (2011). Impact assessment of women farmer activity on poverty reduction and food security: a case of Kindia region/Guinea. *Journal of Agricultural Science*, *3*(4), 141.

Climate-Data (2016). http://en.climate-data.org/ accessed on March 02, 2016.

ClimaTemps (2016). http://www.kumasi.climatemps.com/ accessed on February 28, 2016.

Cui, L and J Shi (2012). Urbanization and its environmental effects in Shanghai, China. *Urban Climate* 2: 1-15.

d'Auria, Viviana, and Bruno De Meulder (2011). Dam[ned] landscapes: re-envisioning the Volta River Project's unsettled territories. *Journal of Landscape Architecture* (Autumn 2011): 54-69.

d'Auria, Viviana (2012). Developing Urbanism[s] in Development: Five Episodes in the Making of the Volta River Project in [Post] colonial Ghana 1945-76. Unpublished doctoral dissertation. Leuven: Katholieke Universiteit, Leuven.

Daddieh, C. K. (2016). Historical dictionary of Cote d'Ivoire, 3rd edition, Rowman and Littlefield, London, 2016.

Daloa. (2016). In ***Encyclopedia Britannica***. Retrieved from http://www.britannica.com/place/Daloa , accessed on March 02, 2016

Dankani, I. M. (2013). Constraints to sustainable physical planning in metropolitan Kano. *International Journal of Management and Social Sciences Research*, *2*(3), 34-42.

Dawson, RJ, J W Hall, S L Barr, M Batty, A L Bristow, S Carney, A Dagoumas, S Evans, A Ford, H Harwatt, J Köhler, M R Tight, C LWalsh, and A M Zanni (2009). A blueprint for the integrated assessment of climate change in cities. Tyndall Working Paper 129, pp. 26.

DESA/UN (2011) Population Distribution, Urbanization, Internal Migration and Development: An International Perspective, Department of Economic and Social

Affairs, Population Division of the United Nations available from www.unpopulation.org.

Dickson, K. B (1969). A Historical Geography of Ghana, Cambridge University Press.

Drabkin, D. H. (1977) *Land Policy and Urban Growth*, London: Pergamon Press.

Ebo, I.N. (2006). City design and social exclusion: Abuja, Nigeria in review, Master Thesis submitted to the Massachusetts Institute of Technology available from https://dspace.mit.edu/handle/1721.1/37664 accessed on February, 2016.

Erenstein, O., Oswald, A., & Mahaman, M. (2006). Determinants of lowland use close to urban markets along an agro-ecological gradient in West Africa. *Agriculture, Ecosystems & Environment*, *117*(2), 205-217.

Fanan, U, K.I. Dlama and I. O. Oluseyi (2011). Urban expansion and vegetal cover loss in and around Nigeria's Federaal Capital City, *Journal of Ecology and the Natural Environment*, Vol 3(1), 1-10.

Fyn, J. K. (1971). Asante and Its Neighbors 1700-1807, Northwestern University Press.

Ghana Statistical Services (2014). 2010 Population and Housing Census, District Analytical Report, Kumasi Metropolitan, available from http://www.statsghana.gov.gh/docfiles/2010_District_Report/Ashanti/KMA.pdf , accessed on March 05, 2016.

GeoNames (2016). http://www.geonames.org/GN/largest-cities-in-guinea.html accessed on March 04, 2016.

Guilmoto, C. Z. (1998). Institutions and migrations. Short-term versus long-term moves in rural West Africa. *Population Studies*, *52*(1), 85-103

Gwadabe, Salisu (2012). Road Transport Problems in Kano Metropolis, Nigeria. A Master Degree Thesis submitted to the Ahmadu Bello University, Zaria, Nigeria available on http://kubanni.abu.edu.ng:8080/jspui/bitstream/123456789/787/1/ROAD%20TRANSPORT%20PROBLEMS%20IN%20KANO%20METROPOLIS,%20NIGERIA.pdf, accessed on February, 2016.

Henry, S., Schoumaker, B., & Beauchemin, C. (2004). The Impact of Rainfall on the First Out-Migration: A Multi-level Event-History Analysis in Burkina Faso. *Population and Environment*, *25*(5), 423–460. Retrieved from http://www.jstor.org/stable/27503895

Hope T (1942) Process of Urbanization, *Social Forces*, Vol. 20 (3), Pp311-316, available from http://heinonline.org

International Centre for Migration Policy Development, Vienna – Austria and the International Organization for Migration (Regional Office for West and Central Africa), Dakar – Senegal (2015). A Survey on Migration Policies in West Africa.

Kindia. (2016). In ***Encyclopedia Britannica***. Retrieved from http://www.britannica.com/place/Kindia on March 03, 2016.

Maoulidi, M. (2010). A Water and Sanitation Needs Assessment for Kumasi, Ghana http://mci.ei.columbia.edu/files/2014/04/16_KumasiWatSan-NA-Sep2010.pdf accessed on February 20, 2016

Marcotullio, P J and W Solecki (2013). What is a city? An essential definition for sustainability. *Urbanization and Sustainability*, Springer: 11-25.

McDonnell, M J and S T Pickett (1990). Ecosystem structure and function along urban-rural gradients: an unexploited opportunity for ecology. *Ecology*: 1232-1237.

Minjibir, N.A. (2012). Ancient Kano city relics and monuments: Restoration as strategy for Kano city development. A Master Degree Thesis submitted to the Ahmadu Bello University, Zaria, Nigeria available on http://kubanni.abu.edu.ng:8080/jspui/handle/123456789/2569, accessed on February, 2016.

Mohammed, M. U., Abdulhamid, A., Badamasi, M. M., & Ahmed, M. Rainfall Dynamics and Climate Change in Kano, Nigeria. *Journal of Scientific Research & Reports, Vol 7(5): 386-395.*

Nabegu, A. B., & Mustapha, A. (2015). Institutional constrainst to Municipal solid waste Mananagemnt in Kano Metropolis, Nigeria. *International Journal of Innovative Environmental Studies Research*, *3*(3), 13.

Population Statistics (2016). http://www.populstat.info accessed on March 02, 2016.

Satterthwaite, D., G. McGranahan, et al. (2010). Urbanization and its implications for food and farming. *Philosophical Transactions of the Royal Society B: Biological Sciences* 365(1554): 2809-2820.

Seto, K C, M Fragkias, B Güneralp, and M K Reilly (2011). A meta-analysis of global urban land expansion. PLoS ONE, 6 (8), e23777.

Seto, K C, S Parnell, et al. (2013). A Global Outlook on Urbanization. Urbanization, Biodiversity and Ecosystem Services: Challenges and Opportunities, in Urbanization, Biodiversity and Ecosystem Services: Challenges and Opportunities: A Global Assessment, T. Elmqvist et al. (eds.), DOI 10.1007/978-94-007-7088-1_1, Springer 9-12

Skinner E.P. 1974. African urban life: The transformation of Ouagadougou. Princeton University Press.

Thapa, R. B. and Y. Murayama (2009). Examining spatiotemporal urbanization patterns in Kathmandu Valley, Nepal: Remote sensing and spatial metrics approaches. *Remote Sensing* 1(3): 534-556.

Ujoh, F., I. D. Kwabe and O. O. Ifatimehin (2010). Understanding urban sprawl in the Federal Capital City, Abuja: Towards sustainable urbanization in Nigeria, *Journal of Geography and Regional Planning*, Vol. 3(5), pp. 106-113.

Urban Design Lab/Earth Institute (2012). Re-Cultivating the Garden City of Kumasi, Blaustein, S., C. Goitia, G. Mehta eds, Colombia University.

Chapter 2: An Evaluation of Multiple Land Cover Datasets to Estimate Cropland Area in West Africa

Pradeep Adhikari and Kirsten M. de Beurs

Department of Geography and Environmental Sustainability, University of Oklahoma, 100 E Boyd St, Suite 510, Norman, OK 73019, USA

(Submitted to *International Journal of Remote Sensing*, under review)

Abstract: West Africa is one of the fastest growing regions of the world and depends heavily on rain-fed agriculture for its food production. This study evaluates twelve freely available land cover and land use (LCLU) datasets at the eco-region, country, and pixel levels in West Africa to estimate croplands. The selected datasets are primarily derived using remote sensing data, representing different time periods and using various classification schemes. The result shows a very high variability of estimated cropland at all levels. Despite this variability, datasets having a finer spatial resolution and representing a similar time period—specifically data from the International Institute for Applied Systems Analysis-International Food Policy Research Institute (IIASA-IFPRI), Global Land Cover-SHARE(GLC-SHARE), Moderate Resolution Imaging Spectroradiometer-UMD (MODIS-UMD), Global Cropland Extent, Moderate Resolution Imaging Spectroradiometer-UMD (MODIS-IGBP), and GLOBCOVER (GlobCover V23)—estimated comparable cropland areas at eco-region and country levels. The countrywide cropland area, obtained from the selected datasets, when compared with the sum of arable land and permanent crop area obtained from the Food

and Agriculture Organization (FAO), showed high coefficient of determination (R^2>0.95) for IIASA-IFPRI, and GLC-SHARE. At the pixel level, at the original resolution, the newer datasets have a comparable user's accuracy (UA>53%) and producer's accuracy (PA>46%), except for the Global Cropland Extent data. Overall, two datasets – IIASA-IFPRI and GLC-SHARE– performed better in the region to estimate the cropland area at all levels.

Keywords: land cover and land use; cropland; arable land; eco-region; West Africa

Introduction

The importance of land cover datasets in ecosystem assessment, bio-diversity conservation, and environmental modelling are well known (Giri et al., 2005; Roy et al., 2015). With the advancement of remote sensing techniques, land cover mapping at various scales has gained momentum and many regional and global land cover datasets are currently available. Still, many developing countries have not been able to use this technology to create (and update) their land cover and land use (LCLU) data because of the cost associated with the acquisition and processing of satellite data (Giri 2012; Fritz et al. 2010). This situation is slowly changing. Since 2001, yearly land cover data from MODIS has been available for the entire world at 500 m resolution. Additionally, much finer resolution (30 m) data from Landsat sensors has been used to map the LCLU of any region of the world as these images have been freely available since December 2008 (Gong et al. 2013). Although the Landsat data are available freely, the processing of data requires expertise on radiometric and atmospheric corrections and resources that

many developing countries are lacking (Giri 2012). One of the ways to fill this gap in LCLU data is to use freely available global and regional land cover land use datasets. But these datasets were created for different purposes at different time periods employing different algorithms to classify LCLU types (Loveland et al., 2000; Ramankutty, 2004; Hansen et al., 2000; Mayaux et al., 2003; Bicheron et al., 2008; Pitman et al., 2010; FAO, 2011; Defourny et al., 2012). As a result, there are inconsistencies among these datasets, which can partly be attributed to differences in land cover typology, time, limited accuracy of land cover classifications, and the use of various environmental properties (like climate, topography, human influence) for discriminating land cover and land use types (Defourny et al., 2012; Townsend et al., 1991).

Several studies have compared and investigated inconsistencies of LCLU datasets at global, regional, and country levels (Fritz et al., 2010; Hensen and Reed, 2000; Giri et al., 2005; McCallum et al., 2006; de Beurs and Ioffe, 2013). In general, these comparisons were carried out for a particular land cover class or for multiple land cover classes among the selected datasets themselves, globally or regionally. Sometimes the selected datasets were compared with national / subnational statistical data for some land cover classes (e.g. forest or cropland area). The following paragraph provides a brief account of these comparisons.

Hansen and Reed (2000) compared the International Geosphere-Biosphere Program Data and Information System (IGBP-DISCover), which was based on 1992-1993 Advanced Very High Resolution Radiometer (AVHRR) data, and the University of Maryland (UMD) 1 Km land cover maps. Both of these datasets are derived using

data from the same satellite sensor. They found that the global area totals of aggregated vegetation types were very similar with a per-pixel agreement of about 75% while for tall *versus* short/no vegetation, the per-pixel agreement was about 85%. However transition zones around core areas differed significantly, resulting in high regional variability between the datasets. Individual class agreement between the two datasets was about 50%. Giri et al. (2005) compared the Global Land Cover 2000 (GLC-2000) that used SPOT vegetation data (Fritz et al., 2003) and the MODIS global land cover data for the year 2000 for 17 classes of the IGBP. They found agreement at the class aggregate level for all classes except for savannas/shrublands and wetlands. Disagreement between the datasets was observed because the comparison was made at the detailed land cover classes. McCallum et al. (2006) compared four satellite derived datasets: International Geosphere Biosphere Project (IGBP) (Loveland et al., 2000), University of Maryland (UMD) (Hansen and Reed, 2000), GLC-2000 (Fritz et al., 2003) and MODIS (Strahler et al., 1999). They reported a reasonable agreement in total area and spatial pattern at a global level among the four datasets. However, at the individual class level, the agreement of the spatial distribution was reduced to 82% (in South America), 11% (in Africa) and 4% (in Asia). McCallum et al. (2006) concluded that when global datasets were used at a continental or regional level, agreement decreased considerably. Fritz et al. (2010) compared four global and regional land cover datasets to determine their suitability for monitoring croplands in Africa: GLC-2000 (Fritz et al., 2003), the MODIS land cover product (MOD12V1) with 17 classes of the IGBP, the Center for Sustainability and the Global Environment (SAGE) Cropland data (Leff et al., 2004) and the AFRICOVER data (from the FAO) based on visual

interpretation of Landsat TM data (Fritz et al., 2010). They found that the MODIS data underestimated the cropland compared to FAO statistics (AFRICACOVER), whereas GLC-2000 overestimated cropland in countries located at the northern transition zone of subtropical shrublands and semi-desert areas. Compared to GLC-2000 and MODIS datasets, the SAGE data estimations were poor at the regional scale. de Beurs and Ioffe (2013) evaluated three global datasets and compared classified croplands with the census data for twenty-two oblasts and republics of Russia. They found that the MODIS-IGBP and MERIS GlobCover 2009 quantified cropland very similarly and compared more favorably with the agricultural census data than the Global Cropland Extent dataset.

In this study we expand on previous studies and evaluate twelve LCLU datasets. The list is representative of LCLU datasets currently available in the public domain being used in research around the world. It is difficult for the scientific community, planners, and natural resource managers to choose one dataset over another without knowing their strengths and weaknesses for a specific geographic region. Furthermore, some of these datasets are also being used to update or create newer LCLU datasets (Latham et al., 2014). Therefore, the objective of this paper is to evaluate twelve LCLU datasets, representing various time periods and to find their suitability to estimate cropland area in West Africa. Here, we focused on croplands because of their importance in land cover studies. Declines in cropland are mainly characterized by the expansion of urban and/or other impervious areas into cropland, while cropland expansion typically occurs at the cost of grasslands, savannahs and forests (Holmgren, 2006). More specifically, this study analyzes accuracies of the land cover data from

different time periods to represent cropland at the eco-region, country, and pixel levels in West Africa. This evaluation is expected to help the scientific community identify the existing limitations of cropland maps derived from global classification data. In addition, we expect that highlighting the errors and uncertainties in these dataset will result in improved attention to classification techniques to map cropland using remote sensing data in regions like West Africa where croplands are often relatively small and sometimes ephemeral. Furthermore, the result from this study could help natural resource managers to make an informed decision in selecting a particular dataset for use in West Africa.

This paper is organized as follows: The first section provides background information and objectives of the study. The second section describes the study area followed by data and methods in the third and fourth sections, respectively. The fifth section provides results and discussion followed by the conclusions of the study at the end.

Study Area

The study area (Figure 2.1) consists of the fifteen contiguous countries of Western Africa referred to as West Africa hereafter. It is a part of Sub-Saharan Africa (SSA). Most of the countries in the region have experienced long droughts (Tarhule and Woo, 1997; Jalloh et al., 2013; EM-DAT; UCD) and are vulnerable to climate change. As of 2014, West Africa has a population of a little over 340 million people and is expected to reach more than 800 million people in 2050 (DESA/UN, 2014), making it one of the fastest growing regions of the world.

The region heavily depends on rain-fed agriculture which extends from the Atlantic coast to the east of Nigeria (Droogers et al., 2001). The climate in the study area is driven by a tropical continental air mass, dry and dusty from the Sahara Desert, and another mass of tropical maritime air, warm and humid from the South Atlantic. These form a convergence zone called the Inter Tropical Convergence Zone (ITCZ) that causes the annual rainfall variability (Druyan, 2011; AIACC, 2006) in the region (Figure 1).

An eco-region is a relatively large unit of land or water containing a unique community of species and environmental settings (Olson et al., 2001). There are twenty-six terrestrial eco-regions, with areas varying from about 3 kilo hectares (KHa) to 163.18 million hectares (MHa), in West Africa (Olson et al., 2001). In this study, eight eco-regions, each with an area of more than 10 MHa were selected. These eight eco-regions together cover more than ninety-four percent of West Africa (Figure 2.2, Table 2.1).

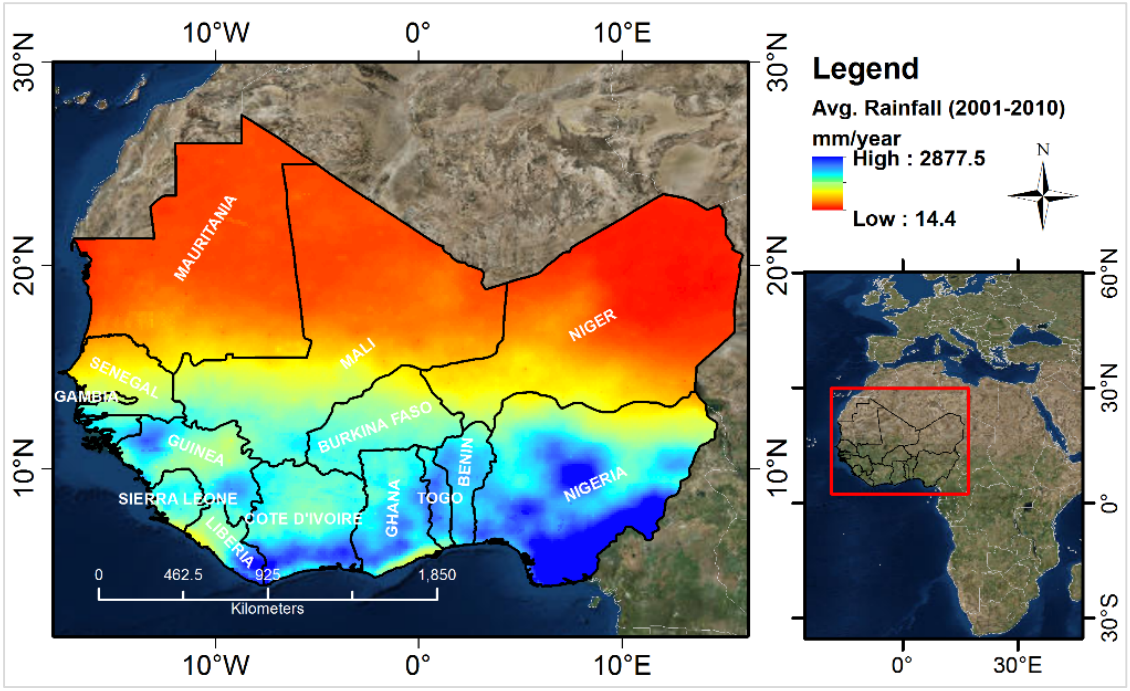

Figure 2.1. The study area, West Africa extends from 4º 13' N to 27º 22' N, and 17º 34' W to 15º 56' E. It is surrounded by the Sahara desert to the North and the Atlantic Ocean to the South and West. The map also shows the spatial rainfall variability in the region for the period 2001-2010 (Data sources: FEWSNET; ESRI).

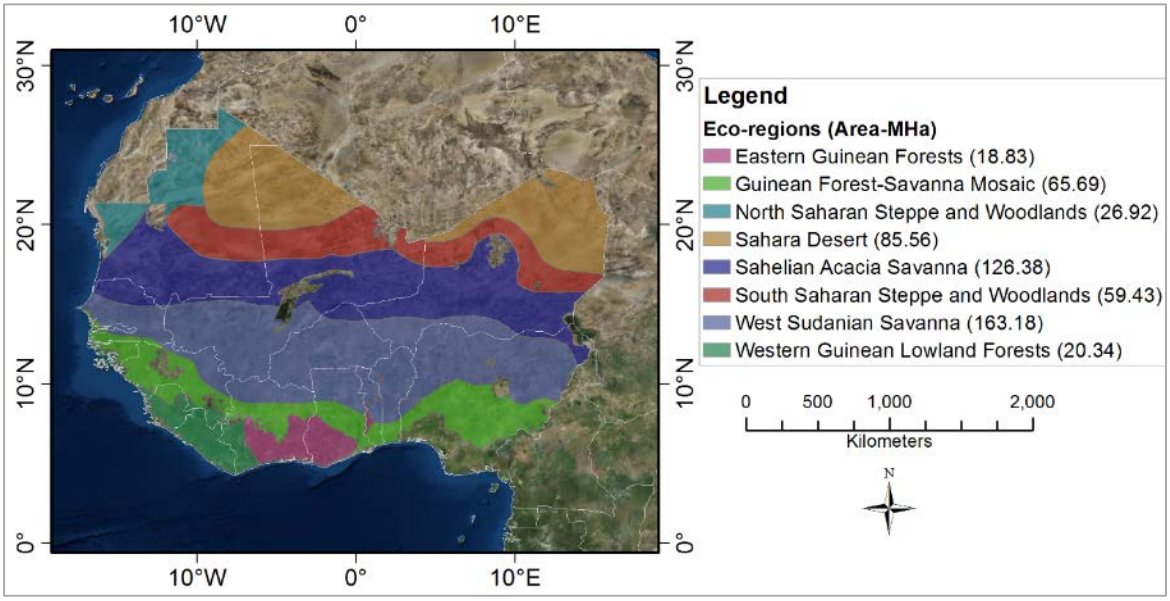

Figure 2.2. The selected eight eco-regions in West Africa (Data sources: Olson et al., 2001; ESRI)

Table 2.1. Selected eight eco-regions in West Africa

Eco-region	Elevation(in meters)	Climate	Population density/Urban centers
Eastern Guinean Forest (EGF)	50-400	Two distinct wet and dry seasons; Annual Rainfall 1,000-2,500 mm	High population density/Daloa (Cote d'Ivoire) and Abidjan (Cote d'Ivoire), and Kumasi (Ghana)
Guinean Forest-savanna Mosaic (GFM)	60-800; some mountains go beyond 1,100 m	Tropical; Average annual rainfall 450-2,400mm; Maximum temperature ranges from 30-35°C while minimum ranges from 20-25°C	High population density in the eastern part of the region/ Abuja (Nigeria), Accra (Ghana), Bouake (Cote d'Ivoire)
North Saharan Steppe and Woodlands (NSSW)	50-450	Rainfall from the Mediterranean caused by depressions in the Sahara desert; 50-100mm; Some years there is no rainfall at all. Highest temperature ranges from 40-45°C, evaporation exceeds rainfall	Sparsely populated
Sahara Desert (SD)	220-650	Hottest region of the world; max temperature above 50°C in some months; Virtually no rainfall	No significant settlements; some nomadic population
Sahelian Acacia Savanna (SAS)	200-400	Tropical; Monthly mean max 33-36°C, min 18-21°C; Annual rainfall 600 mm in the south while it is about 200 mm in the north	Low population density/Aleg (Mauritania), Agadez (Niger)
South Saharan Steppe and Woodlands (SSSW)	100-200	The mean annual temperature in Sahelian portion of the ecoregion is between 26°C and 30°C. Annual rainfall 100-200mm; Rainfall in this ecoregion is insufficient for rain-fed agriculture	Sparsely populated
West Sudanian Savanna (WSS)	200-400	Tropical; Strongly seasonal; Mean monthly maximum temperature 30-33°C, minimum temperature 18-21°C; Annual rainfall 1,000mm in the south which decreases to 600mm in the north	High population density/ Thies (Senegal), Ouagadougou (Burkina Faso), Tamale (Ghana) and Kano (Nigeria)
Western Guinean Lowland Forests (WGLF)	50-500; some mountains beyond 500 m	Warm and humid; Wettest parts of West Africa; Annual rainfall up to 3,300 mm; Temperature ranges from 30-33°C during dry season and 12-21°C during wet season.	Pockets of area along the coast in the south are densely populated/ Kenema (Sierra Leone), Nzerekore (Guinea), San Pedro (Cote d'Ivoire)

Sources: Olson et al. (2001), EoE, and WWF

Data

Twelve freely available LCLU datasets were evaluated in this study (Table 2.2). All the datasets except the Regional Cropland Intensity and AFRICA COVER have global coverage. The Regional Cropland Intensity data was prepared for West Africa only while AFRICA COVER data was available for the entire continent of Africa. The datasets represented different time periods from the early 1990s to 2013. They were also representative of various land cover classification systems. The spatial resolution of the datasets varied from 300 meters to 10 kilometers. The MODIS land cover datasets (MODIS-IGBP and MODIS-UMD) were the only datasets that have been available on a yearly basis since 2001. All other datasets were produced for a particular year only once, or sometimes with a gap of a couple of years after the first production. The majority of the datasets had both pure and mosaic pixels classified as croplands. Most of the datasets used remote sensing data to map land cover, with the exception of the Regional Cropland Intensity data, which infused ancillary data, such as population density and agriculture census/inventory with the cultivation intensity data derived from Landsat and Normalized Difference Vegetation Indices from AVHRR (Ramankutty, 2004). The IIASA-IFPRI and GLC-SHARE data infused satellite data from various sensors and the total cropland area was matched to the global food and agriculture statistics available from the United Nations Food and Agriculture Organization (FAOSTAT) for 2005 (Fritz et al., 2015; Latham et al., 2014). A high resolution land cover dataset, with a spatial resolution of 30m × 30m, produced using the Landsat imagery is available from Gong et al. (2013). Although this dataset is much finer

resolution than the rest of the twelve datasets we compared them with the rest to estimate the country level cropland area.

To visually evaluate the data we homogenized (Fritz and See, 2008) all the datasets by assigning a “1” to pure cropland pixels and a “0” to non-cropland pixels. For pixels with a mix of cropland and other LCLU types, fractional values varying from 0.1 to 0.9 were assigned to all datasets except for the Regional Cropland Intensity and the Global Cropland Extent datasets. The Regional Cropland Intensity dataset already has pixels with fractional values of crop intensity, while the Global Cropland Extent dataset provides the probability value of a pixel being a cropland. For the other datasets, the fractional values were based on the descriptions of the land cover classification system in each of the land cover datasets (Table 2). For example, in the case of AFRICA COVER, one of the land cover classes is ‘croplands with open vegetation’. Pixels in this class contain 30% cropland mixed with natural vegetation (Mayaux et al. 2003). So, for this class, we assigned a value of 0.3. For the country and regional level analysis described below, if a pixel was assigned a fractional crop value (e.g. 0.3) we took only 0.3 of the total area of the pixel as the estimated cropland area.

We used the Food and Agriculture Organization (FAO) of the United Nations data for the country level analysis. The FAO has compiled time-series data since the 1960s relating to global food and agricultural statistics (FAOSTAT). We used the sum of the country level arable land and permanent crop area as a variable and analyzed its relationship with the estimated cropland from the selected classification datasets. The arable land gives the land area with temporary agriculture while the permanent crop area gives land area cultivated with long-term crops (FAOSTAT). For this part of the

analysis, we matched the year of the arable and permanent crop area with the year for which the selected LCLU datasets were available. For example, we matched the UMD-AVHRR estimated cropland area (1992-1994) with the FAOSTAT data from 1993. FAOSTAT only provides arable land and permanent crop area data until 2012, so we used the 2012 data for the comparison of the GLC-SHARE estimated cropland area of the year 2014.

Table 2.2. The global LCLU datasets used in the study.

Data	Sensors	Resolution (km)	Classification Schemes	Reference period	References/Sources
Regional Cropland Intensity	Not Applicable	10	Cultivation intensity 0-100%	Early 1990s	Ramankutty (2004)
IGBP-DISCover	AVHRR	1	IGBP (17 classes) that includes Croplands (100%) and Cropland Natural Vegetation Mosaic (60% max)	1992-1993	Loveland et al. (2000)
IGBP-SiB*	AVHRR	1	IGBP SiB (16 classes) that includes Agriculture (100%) or C3 Grassland	1992-1993	Loveland et al.(2000)
UMD-AVHRR*	AVHRR	1	Simplified IGBP (14 classes) that includes a cropland (100%)class	1992-1994	Hansen et al.(2000)
AFRICA-COVER	SPOT-Vegetation	1	Five major classes with 27 sub-classes that include croplands (>50%), cropland with open woody vegetation (30%), irrigated cropland (100%) and tree cropland (100%)	2000	Mayaux et al. (2003)
LADA-FAO	Not Applicable	1	Eight major land use systems with 37 sub-systems that include five different systems for agriculture: moderate intensive (max 50%) and high intensive (100%) agricultures, agriculture-large scale irrigation (100%) and agriculture-protected (100%)	2000	FAO (2011)
IIASA-IFPRI	Integrated global, regional and national cropland maps including GlobCover 2005, MODIS v.5	1	Cropland percentage 0-100%	2005	Fritz et al. (2015), Geo-Wiki Project
Global Cropland Extent	MODIS	1	Cropland probability (1 to 100%)	2008	Pittman et al. (2010)
GlobCover V23	MERIS	0.30	FAO Land Cover Classification (22 classes) that includes irrigated (100%), rain-fed (100%), mosaic (50-70%) croplands and mosaic vegetation (with 20-50% cropland)	2009	Bicheron et al.(2008)
MODIS-IGBP	MODIS	0.50	IGBP (17 classes) that includes cropland (100%) and cropland/natural vegetation mosaic (50% max)	2010	Friedl et al. (2010)
MODIS-UMD*	MODIS	0.50	Simplified IGBP (14 classes) that includes cropland (100%) class	2010	Friedl et al.(2010)
GLC-SHARE (v1.0_2014)	Fusion of various remotely sensed global, regional, national land cover data including MODIS, AFRICA-COVER	1	Combination of Land Cover Classification System and System of Environmental-Economic Accounting (11 classes) that include a cropland class (100%)	2014	Latham et al. (2014)

* Only pure pixels are classified as croplands.

Methods

We extracted the cropland data and calculated the total cropland area in the study domain for all eco-regions and countries. The variability in the countrywide estimated area was determined by the coefficient of variation (CV), which measures the dispersion of the data (e.g. cropland area) from the mean value obtained from all the datasets for an ecoregion or a country (Bruin, 2006). A high CV indicates greater dispersion and uncertainty of the data to estimate the cropland. To minimize the effect of time gaps among datasets, we chronologically grouped them into three groups: Early 1990s, 2000s, and around 2010. We calculated the CV for each group separately. Furthermore, we also compared the countrywide estimated cropland with the sum of the country level arable land and permanent crop area data obtained from FAOSTAT.

Pixel level validation

We validated the original datasets with imagery from Google Earth™. The Google Earth™ images were selected for validation because they are available at high spatial resolution of at least 15 m, and they are updated regularly, every one to three years (Google Earth Help). Furthermore, these images are better alternatives for validation if the area is large and field data are not available. For the collection of Google Earth™ data points, we used the extent of West Africa as the sampling frame. We randomly collected 1,000 pixels, at 1 Km × 1 Km grids and visually determined the land cover class for each grid. For each pixel a maximum of three dominating land cover classes (selected from impervious surface, grass and herbaceous, trees and forest, soil and barren, water, cropland, and wetlands) with estimated percentage of land cover

were assigned based on visual interpretation (Figure 3). We omitted samples with poor resolution or those that were contaminated by clouds and replaced these samples with visually distinguishable samples. The collected cropland samples include both agricultural and fallow land. We identified 215 (with 1 Km × 1 Km resolution) as cropland (50% or more cropland) in the set of 1,000 randomly selected points. All of the cropland points sampled from Google Earth™ were from the year 2000 or later. Among them, about 80% were from the year 2008 or later (Table 2.3).

Table 2.3. Time stamps on randomly selected 1 Km × 1 Km Google Earth™ cropland points

2007 or earlier	2008-2013	No dates	Total
24	172	19	215

Finally, we calculated the user's and producer's accuracies (Congalton, 1991; See et al., 2013):

$$\text{Overall accuracy (OA)} = \frac{\sum_{i,j=1}^{n} x_{i,j}}{\sum_{i=1}^{n}\sum_{j=1}^{n} x_{i,j}} \times 100 \quad \text{----- (1)}$$

$$\text{User's accuracy (UA)} = \frac{x_{i,i}}{\sum_{j=1}^{n} x_{i,j}} \times 100 \quad \text{----- (2)}$$

$$\text{Producer's accuracy (PA)} = \frac{x_{j,j}}{\sum_{j=1}^{n} x_{i,j}} \times 100 \quad \text{----- (3)}$$

$$\text{Kappa (k)} = \frac{N\sum_{i=1}^{n} x_{i,i} - \sum_{i=1}^{n}(G_i C_i)}{N^2 - \sum_{i=1}^{n}(G_i C_i)} \times 100 \quad \text{----- (4)}$$

Where i and j are the cropland class from the selected datasets and sampled pixels from the Google EarthTM imagery, respectively, and N is the total pixels including cropland and non-cropland classes, Ci are the total number of classified pixels

(by the selected datasets) to cropland class, and Gi are the total number of ground truth pixels (obtained from Google EarthTM imagergy) belonging to cropland class.

Figure 2.3. Two data pixels (1 Km × 1 Km) collected using the Google Earth™. The pixel on the left panel shows a mix of two dominating land cover classes, cropland and fallow land (about 70%), and grass and herbaceous (about 30%). The pixel on the right panel also shows a mixed pixel with cropland and fallow land (80%), trees and forest (10%) and buildings (10%).

Results and Discussion

Cropland areas estimated by the twelve datasets were first mapped at their original resolutions (Figure 2.4). Although these datasets represent cropland at different times, we see certain patterns in the region. We observed that most of the datasets have identified croplands in the south and southeast of the study area, including the coastal areas. The Regional Crop Intensity identified the largest area of cropland among all datasets. The IGBP-SiB identified croplands along the coastal regions in the south only. The IGBP-DISCover, AFRICA-Cover, LADA-FAO, GlobCover V23, MODIS-IGBP,

MODIS-UMD and GLC-SHARE have a swath of area identified as cropland just south of the Sahara desert, which is the area with rain-fed agriculture (Jalloh et al. 2013). The IIASA-IFPRI shows cropland primarily in the East Central and coastal area of West Africa. The Global Cropland Extent, however, showed high probability of croplands across the south and a small pocket of area in the East Central part (North Western Nigeria).

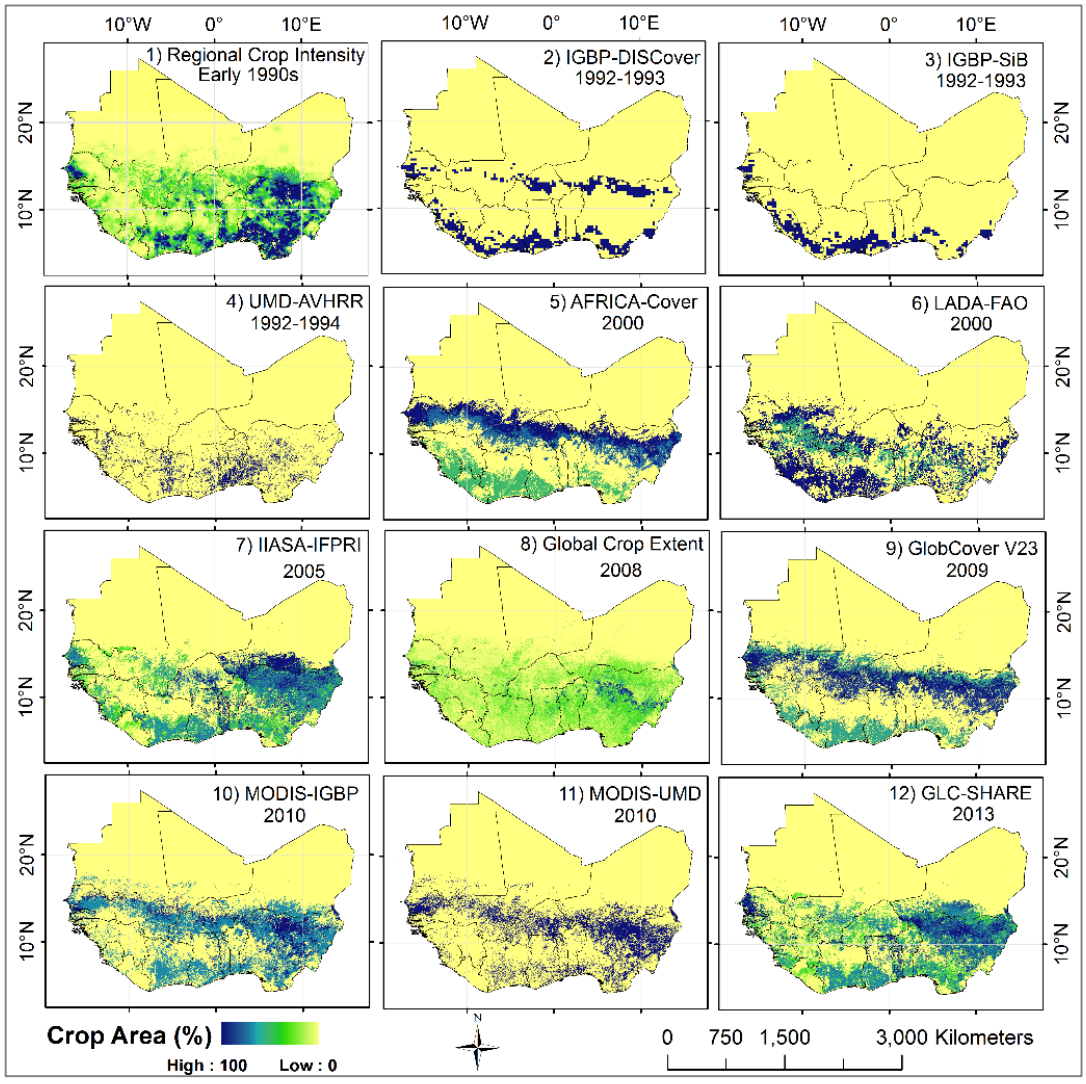

Figure 2.4. Cropland map from the global LCLU datasets.

Eco-region level

None of the datasets showed cropland in the NSSW and SD eco-regions. Therefore, these two eco-regions were excluded from this analysis. Overall, there is a high variability in estimated cropland across all eco-regions at all time periods (Table 2.4). We observed that the estimates from datasets from the early 1990s and 2000s varied widely. Cropland estimation varied more than 50% across all eco-regions in the datasets that were from the early 1990s. The datasets from the 2000s also showed wide variability except for the EGF, and WGLF eco-regions. The variability was smallest for the datasets from around 2010. Across the different time periods, we did not find any increasing or decreasing trend in estimated cropland area. For example, in WSS, the cropland area ranged from 16 MHa – estimated by the Regional Crop Intensity (early 1990s) data – to 60 MHa estimated by AFRICA-COVER in the 2000s. For the same eco-region, the GlobCover V23 (around 2010) estimated cropland to be around 58 MHa. In contrast, the cropland area in the EGF eco-region was 10.57 MHa, according to the IGBP-DISCover dataset in the early 1990s, and 10.71 MHa according to the LADA-FAO from the 2000s. Despite a 10 year gap, the cropland area remained virtually unchanged in the region. For the same region, the maximum cropland area estimated a decade later (around 2010) was 30% lower (7.54Mha). The newer datasets have less variability in estimating cropland compared to the older datasets from the early 1990s or 2000s.

Country level

The estimated cropland area varied widely in the twelve datasets at the country level as well (Table 2.5). In the datasets from the early 1990s, the CV ranges from 20-107% for all countries, and it was the highest for Gambia (107%) and Benin (100%). For most countries, datasets from the 2000s have a low CV compared to the 1990s datasets, with some exceptions, such as Guinea, Guinea-Bissau, Mauritania, and Niger. The datasets from around 2010 have a low CV for most countries compared to the datasets from the 1990s. Liberia revealed a CV of 139%, which was the highest among all countries. In addition, eight other countries had a CV of 50% or more. The uncertainties in cropland estimation around 2010 decreased compared to the uncertainties in the datasets from the early 1990s. We also compared these data with the cropland area obtained from Gong et al. (2013). We found that the Gong et al. (2013) data highly underestimated cropland area in West Africa. For example, only 0.02% of the FAO's Arable Land and Permanent Cropland data are identified in Gong et al. (2013) data for Sierra Leone as cropland area. This number is only 11%, the highest among the countries in the study area, for Guinea-Bissau. For countries such as Nigeria and Senegal, the 30m data from Gong et al. (2013) identified only 2.86% and 2.27% of the FAO data as cropland area respectively. As the countrywide cropland area obtained from Gong et al. (2013) were too low we did not use the data for further analysis.

We also investigated how estimated cropland areas compare with the sum of the arable land and permanent cropland obtained from FAOSTAT. As mentioned earlier, we matched the reference year of the estimated cropland areas with the year of the sum of the arable land and permanent cropland data for each country (Table 2.6). We

observe that over the years, arable land and permanent cropland data have changed, but the changes were not consistent. For example, in the case of Benin, arable land and permanent cropland value increased from 1.77 MHa (1993) to 2.65 MHa in the year 2000. In contrast, the value decreased to 2.9 MHa in 2009 compared to 2.97 MHa in 2005.

A linear regression between the estimated cropland areas (X-axis) with the sum of arable land and permanent cropland areas (Y-axis), from the FAOSTAT showed R^2 values of 0.52 or greater (significant at 0.05 level) (Figure 2.5). The IIASA-IFPRI has the best R^2 at 0.99 followed by the GLC-SHARE (R^2=0.89), Global Cropland Extent (R^2=0.74), and Regional Cropland Intensity (R^2=0.58). Most of the data since 2005 have R^2 values 0.52 or greater. For this analysis, we dropped Nigeria as it presented much larger cropland area as a result of its size and thus skewed the regression results.

The slope of the regression line for the datasets varies from 0.10 to 1.56. The LADA-FAO has the lowest slope of 0.10. The IIASA-IFPRI and GLC-SHARE have slopes of 0.97 (R^2=0.99) and 1.46 (R^2=0.89), respectively, which show their better agreement with the sum of the arable land and permanent cropland data than the rest of the datasets, which is expected. As mentioned earlier FAOSTAT cropland statistics for 2005 are used to produce IIASA-IFPRI and GLC-SHARE (Fritz et al., 2015; Latham et al., 2014). Cropland area estimated from remotely sensed data alone mapped the arable and permanent cropland relatively poorly in the study area compared with the results from multiple, fused data sources.

Table 2.4. Estimated cropland area (MHa) and coefficient of variation (CV) at the eco-region level.

Eco-regions* (Arranged alphabetically)	Area (MHa)	Early 1990s				2000s		Around 2010						CV (%)		
		Regional Crop Intensity	IGBP-DISCover	IGBP-SiB	UMD-AVHRR	AFRICA-COVER	LADA-FAO	IIASA-IFPRI	Global Cropland Extent	GlobCover V23	MODIS-IGBP	MODIS-UMD	GLC-SHARE (Beta)	Early 1990s	2000s	Around 2010
Eastern Guinean Forests (EGF)	18.83	1.79	6.72	10.57	3.56	0.00	10.71	7.54	0.30	5.12	6.27	4.66	6.90	59	100	46
Guinean Forest-Savanna Mosaic (GFM)	65.69	2.86	3.33	4.66	13.50	3.34	9.70	13.82	10.27	7.32	15.08	12.62	13.84	71	49	22
Sahelian Acacia Savanna (SAS)	126.38	1.19	0.42	0.37	0.17	8.39	4.87	9.01	2.35	5.96	6.17	4.29	6.52	72	27	36
West Sudanian Savanna (WSS)	163.18	16.30	13.64	1.56	11.04	60.33	42.26	48.67	32.95	58.08	53.18	56.63	47.67	52	18	17
Western Guinean Lowland Forests (WGLF)	20.34	0.75	6.13	8.98	0.81	0.00	11.09	3.90	0.53	3.86	1.97	1.48	3.60	85	100	51

* NSSW, SD, and SSSW eco-regions do not have cropland so are excluded from this table.

Table 2.5. Estimated cropland area (MHa) and coefficient of variation (CV) at the country level.

Country (Arranged alphabetically)	Area (MHa)	Early 1990s				2000s		Around 2010						CV (%)		
		Regional Crop Intensity	IGBP-DISCover	IGBP-SiB	UMD-AVHRR	AFRICA-COVER	LADA-FAO	IIASA-IFPRI	Global Cropland Extent	GlobCov V23	MODIS-IGBP	MODIS-UMD	GLC-SHARE	Early 1990s	2000s	Around 2010
Benin	12.10	1.99	0.30	0.30	0.32	2.59	2.05	3.08	1.78	3.28	4.17	2.37	2.87	100	12	25
Burkina Faso	27.38	4.16	4.97	0.00	4.99	12.73	16.79	5.25	4.31	17.89	15.72	7.56	5.23	59	14	58
Cote D'Ivoire	32.67	7.03	6.06	6.70	0.32	13.96	15.19	6.75	1.77	12.85	13.09	3.80	6.22	55	4	57
Gambia	1.10	0.18	0.47	0.00	0.04	0.69	0.66	0.34	0.28	0.7	0.73	0.59	0.34	107	2	37
Ghana	24.15	4.90	6.25	5.96	0.31	7.46	7.72	6.89	1.99	8.62	9.58	4.64	6.18	55	2	40
Guinea	24.74	1.55	1.38	1.68	0.17	3.11	6.52	2.58	1.15	4.75	2.34	1.18	3.62	50	35	49
Guinea-Bissau	3.46	0.34	0.15	0.07	0.08	1.2	0.31	0.52	0.13	1.18	0.55	0.42	0.54	69	59	56
Liberia	9.42	0.66	4.03	4.27	0.01	6.11	5.55	0.58	0.10	3.84	0.39	0.19	0.56	86	5	139
Mali	125.14	4.73	2.43	0.15	7.80	24.40	23.69	4.87	5.71	25.26	18.92	13.38	5.99	75	1	62
Mauritania	103.86	0.50	0.07	0.07	0.78	9.07	2.47	0.44	0.19	3.73	2.39	3.65)	0.41	85	57	84
Niger	119.03	5.22	1.19	0.00	2.69	9.51	2.14	14.67	7.19	3.26	11.88	11.38	8.93	86	63	38
Nigeria	91.06	43.77	18.26	5.27	12.74	39.81	42.89	38.06	21.68	49.01	58.19	38.33	35.44	72	4	28
Senegal	19.21	2.67	3.63	2.06	3.08	9.53	11.16	3.17	1.06	11.96	8.77	5.56	4.68	20	8	61
Sierra Leone	7.15	0.58	2.48	2.74	0.02	4.74	5.47	1.54	0.51	3.73	1.24	0.41	1.48	81	7	74
Togo	5.86	2.55	0.66	0.62	0.10	0.75	0.68	2.57	1.05	1.16	2.62	1.24	2.21	95	5	37

Table 2.6. Sum of arable land and permanent crop (AL&PC) over the years.

Country	Sum of Arable and Permanent Cropland, AL & PC (in MHa)					
	1993	**2000**	**2005**	**2008**	**2010**	**2012**
Benin	1.77	2.65	2.97	2.90	2.89	3.15
Burkina Faso	3.50	3.77	4.97	6.07	6.07	6.07
Cote D'Ivoire	6.50	6.60	7.00	7.40	7.40	7.40
Gambia	0.17	0.29	0.34	0.38	0.46	0.45
Ghana	4.40	6.10	6.80	7.30	7.32	7.40
Guinea	3.35	2.79	3.42	3.54	3.60	3.70
Guinea-Bissau	0.39	0.55	0.53	0.53	0.55	0.55
Liberia	0.50	0.61	0.62	0.63	0.66	0.71
Mali	3.14	4.60	5.75	5.91	6.41	7.01
Mauritania	0.44	0.50	0.41	0.41	0.46	0.41
Niger	13.00	14.00	14.18	15.00	15.20	16.00
Nigeria	34.90	41.00	42.40	42.40	39.70	41.70
Senegal	3.07	3.11	3.23	3.70	3.91	3.42
Sierra Leone	0.61	0.61	1.61	1.51	1.73	1.90
Togo	2.30	2.63	2.25	2.55	2.67	2.85

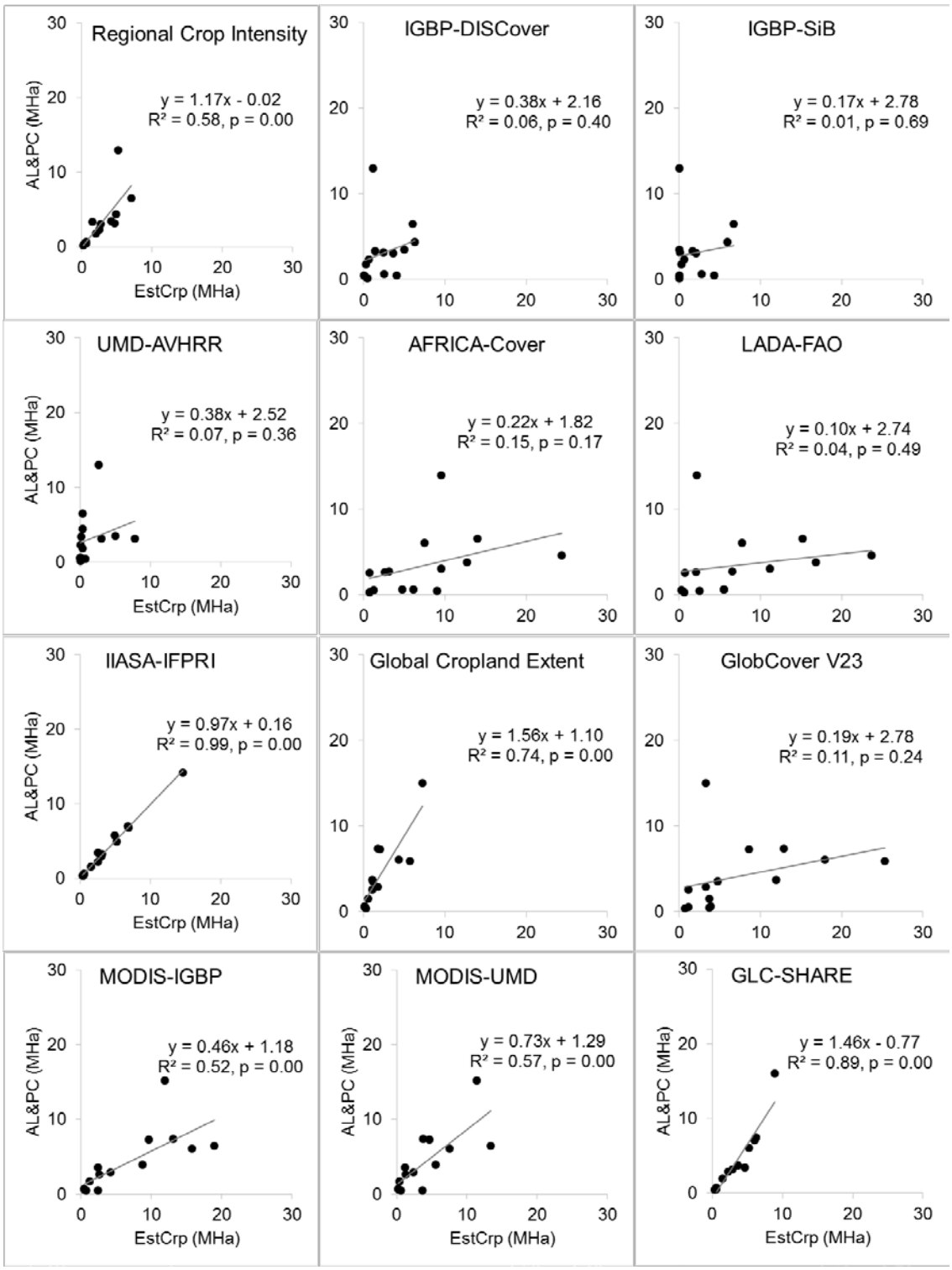

Figure 2.5. Country wide estimated cropland area (EstCrp) estimated by the selected datasets (X-axis) vs sum of arable land and permanent crop area (AL&PC) from FAOSTAT (Y-axis). The regression showed $R^2 \geq 0.52$ (significant at $p<0.05$) for six datasets: Regional Cropland Intensity, IIASA-IFPRI, Global Cropland Extent, MODIS-IGBP, MODIS-UMD and GLC-SHARE.

Pixel level

We investigated the agreement of the cropland pixels with the points collected from the Google Earth™ images. As most of the validation points collected were from 2005 or later, we evaluated the accuracy of the datasets with reference year 2005 or later for this part of the analysis (Table 7). We calculated the accuracies of the original datasets against the cropland pixels collected using Google Earth™ images. The user's accuracies of the original datasets were found to be in the range of 53-93% while the producer's accuracies varied from 47-70% except for the Global Cropland Extent data which is only 6%. This result is less than what is reported in the literature for most of the selected data (Table 7) except for MODIS-IGBP. The accuracies for MODIS-IGBP are close to the reported value. Any deviations between reported accuracies and our calculated accuracies are likely due to sampling strategy used to collect validation points from Google Earth™. Furthermore, reported accuracies were based on sample points from various parts of the world, not just West Africa.

Table 2.7. Accuracies (%) of the datasets to estimate cropland in West Africa.

Data	Ref. Year	Reported Accuracy	Accuracies in West Africa			
			UA	PA	Overall	Kappa
IIASA-IFPRI	2005	Overall: 82 (Fritz et al., 2015)	62.07	50.23	82.70	0.45
Global Cropland Extent	2008	Not available	92.86	6.05	79.70	0.09
GlobCover V23	2009	61<UA <99, 66 <PA<91 (Bicheron et al., 2008)	59.41	46.98	81.70	0.41
MODIS-IGBP	2010	28<UA<93, 61< PA <83 (Friedl et al., 2010)	52.98	70.23	80.20	0.48
MODIS-UMD	2010	Not available	58.58	46.05	81.40	0.40
GLC-SHARE	2014	UA 95, PA 89 (Latham et al., 2014)	68.76	50.23	84.40	0.49

In general, we found that the newer datasets (around 2010) have performed better in estimating the cropland. They have the high UA, PA, OA and Kappa values. More specifically, IIASA-IFPRI and GLC-SHARE were found to be the best. The variability at the regional and country levels (except in the case of Liberia and Senegal) was less in the case of these datasets. Furthermore, the estimated cropland areas were comparable with the sum of arable land and permanent cropland at the country level.

Cropland data agreement

We recognize the fact that all twelve datasets represent different reference periods. Despite this constraint, we tried to understand where in West Africa the data agreed or disagreed in predicting croplands. We summed up the cropland area of all twelve datasets in West Africa. Theoretically, neglecting any change in cropland, a value of 12 for pixels in the resulting raster means all datasets agree to classify those pixels as cropland (Figure 6), but only 25 pixels have a value of 11 from the entire study area.

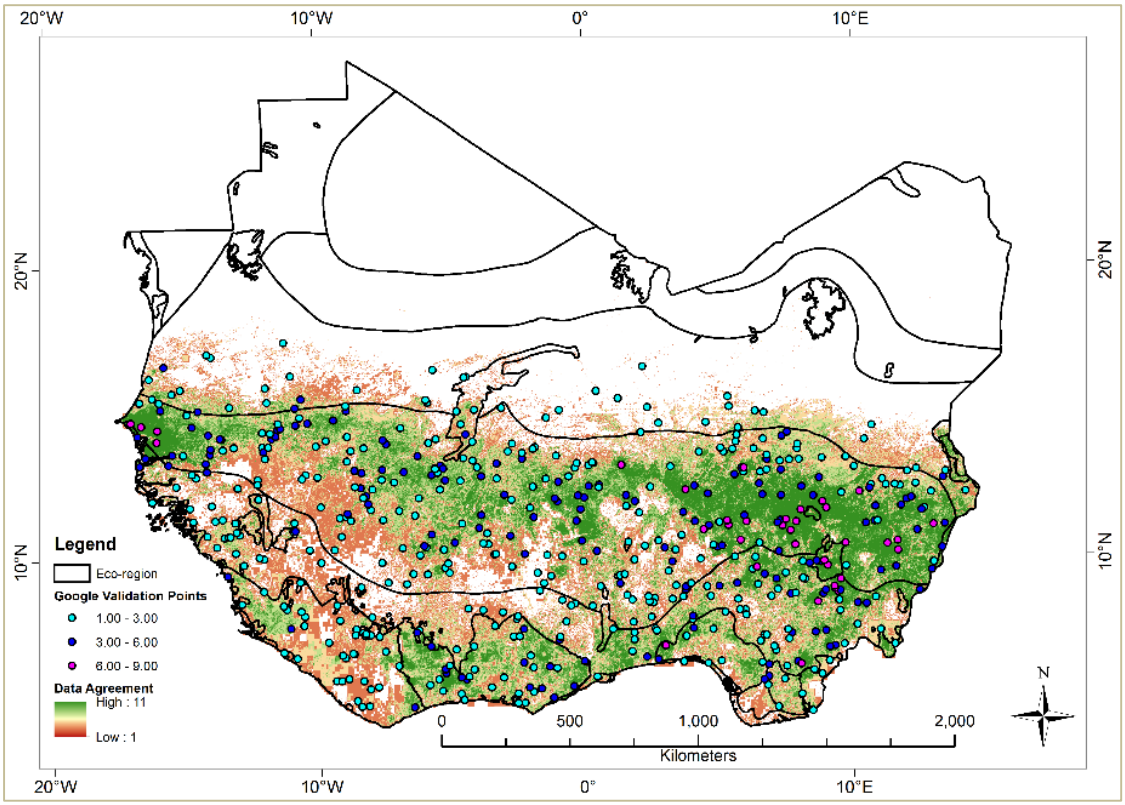

Figure 2.6. Agreement/disagreement of datasets to identify croplands in the study area.

The areas where most of the data agreed were along the West Sudanian Savanna, Guinean Forest-Savanna Mosaic, and Eastern Guinean Forest eco-region bands. Only 11% of the pixels agreed among six or more datasets. In the case of the 215 Google Earth™ pixels, where croplands are the dominant land use (out of 1,000 random samples), only 48 pixels (i.e. 22%) revealed agreement between six to nine datasets (indicated as purple dots in Figure 6). Out of these 48 pixels, 32 were from the year 2010 to 2013. This shows that the Google Earth™ points have better agreement with the newer datasets, as they are from the same time period.

Conclusions

This study evaluated twelve LCLU datasets to estimate the cropland in West Africa. Despite limitations in the sampling strategy, homogenizations and aggregation, discrepancies that we found in this study were not new (Giri et al., 2005; Fritz et al., 2010). The datasets were from different time periods and used different sensors and techniques to acquire and classify remote sensing images (Xie et al. 2008). In addition, variability in the datasets to estimate cropland is also attributed to agricultural areas mixed with significant non-agricultural land cover classes and low agriculture intensity (Xie et al., 2008; Ramankutty and Foley, 1999; Mayaux et al., 2004). These complexities were also evident in this study, especially when we collected 1,000 Google Earth™ data points.

The eco-region and country level analysis showed high variability in cropland estimation. At the pixel level, the IIASA-IFPRI and GLC-SHARE showed better user's and producer's accuracies as well as better Kappa values. In general, this study showed the limitations of using remotely sensed global land cover and land use products to estimate cropland area in a region like West Africa with a complex land cover system.

Furthermore, cropland is defined differently in each dataset. In IGBP-DISCover, AFRICA-COVER, LADA-FAO, GlobCover, MODIS-IGBP, and GLC-SHARE data croplands are combined into mixed classes while IGBP-SiB, UMD-AVHRR, and MODIS-UMD present croplands only as pure pixels. The share of cropland in each mixed pixel varies (Fritz et al., 2003; Mayaux et al., 2003). Also, while classifying the images different thresholds on the spectral profile were used to identify land covers

including cropland (Mayaux et al., 2003) which is also a source of uncertainty in cropland area estimations.

In addition, detecting agriculture in Africa is challenging due to farming system and the spatial pattern of croplands (Mayaux et al., 2003). The majority of farms in Sub Saharan Africa are small, with 60% less than a hectare and 95% less than 5 hectares, which makes it difficult to map cropland at 1 Km × 1 Km resolution (Lowder et al, 2014; Mayaux et al., 2003; Gallego et al., 2010). However, we found that even the much finer data from Gong et al. (2013) underestimated the cropland areas for the countries in West Africa, which clearly indicate limitation of current classification algorithm.

In recent years attempts are made to correctly map cropland are at regional level (Lavreniuk et al., 2015, Matton et al., 2015). Lavreniuk et al. (2015) used multilayer perceptrons to obtain land cover map for Ukraine using Landsat imagery with overall accuracy of 97%. Similarly, Matton et al. (2015) mapped annual cropland in different agro-systems using global land cover data as the baseline data (without field data) with an overall accuracy of more than 85%. Such techniques have potential to be utilized in the region like West Africa too.

In this study, newer datasets provided more accurate cropland estimates. This can be attributed to continuously improving sensor technology and algorithms to interpret the collected remotely sensed data and methodological changes like the fusion of various remote sensing data. Further, collection of training data has significantly improved both in terms of quality and quantity in recent years, compared with the

1990s, contributing to better classification of land cover classes (Fritz et al., 2015; See et al., 2013).

In conclusion, we observed that the IIASA-IFPRI and GLC-SHARE datasets were better in estimating cropland at all levels in the study area. Both IIASA-IFPRI and GLC-SHARE datasets were the ones which infused multiple, remotely sensed land cover products and directly tied their results to the FAO statistics. The IIASA-IFPRI also used crowdsourced data for better training (Fritz et al., 2015). Therefore, data fusion, the collection of better training data and improvement in image classification techniques help improve the accuracy of cropland mapping in a region like West Africa in the future.

Literature cited

AIACC. Food security, climate variability and climate change in Sub Saharan West Africa, A final report submitted to Assessments of Impacts and Adaptations to Climate Change AIACC), Project No AF 23, International START Secretariat, Washington DC, 2006. Available online from www.start.org, accessed on January 2014.

Bicheron, P.; Defourny, P.; Brockmann, C.; Schouter, L.; Vancutsem, C.; Huc, M.; Bontemps, S.; Leroy, M.; Achard, F.; Herold, M. *et al.* (2008). GLOBCOVER Products Report Description and Validation Report; MEDIAS: Toulouse, France, 2008.

Bruin, J. 2006. newtest: command to compute new test. UCLA: Statistical Consulting Group. http://www.ats.ucla.edu/stat/mult_pkg/faq/general/coefficient_of_variation.htm/ accessed on April-September 2015.

Congalton, R.G. A review of assessing the accuracy of classifications of remotely sensed data. *Remote Sensing of Environment*, 1991, 37(1), 35–46.

de Beurs, K.M.; Ioffe, G. Use of Landsat and MODIS data to remotely estimate Russia's sown area. *Journal of Land Use Science*, 2013, DOI: 10.1080/1747423X.2013.79803.

Defourny, P.; Bontemps, S. Revisiting Land-Cover Mapping Concepts in Remote Sensing of Land use and Land Cover: Principles and Applications, Giri C. P (ed.), CRC Press. 2012; pp 49–63.

DESA/UN. Population Distribution, Urbanization, Internal Migration and Development: An International Perspective, Department of Economic and Social Affairs, Population Division of the United Nations, 2014; pp 32. Available online from www.unpopulation.org accessed on January 2015.

Droogers, P.; Seckler, D.; Makin, I. Estimating the potential of rain-fed agriculture Vol. 20. IWMI, 2001; pp 21.

Druyan, L.M. Studies of 21st-century precipitation trends over West Africa. *International Journal of Climatology* 2011, 31(10), 1415–1424.

Encyclopedia of Earth (EoE): http://www.eoearth.org, accessed on January-April 2015.

ESRI, DigitalGlobe, GeoEye, Earthstar Geographics, CNES/Airbus DS, USDA, USGS, AEX, Getmapping, Aerogrid, IGN, IGP, Swisstopa, and the GIS User Community.

Famine Early Warning Systems Network (FEWSNET): http://www.fews.net/ assessed on January-March, 2012.

FAOSTAT: http://faostat3.fao.org accessed on March 2014-July 2015.

Food and Agriculture Organization (FAO). Land degradation assessment in Drylands: Methodology and results, A. Woodfine (ed.), Rome, 2011; pp 84.

Friedl, M.A.; Sulla-Menashe, D.; Tan, B.; Schneider, A.; Ramankutty, N.; Sibley, A.; Huang, X. MODIS Collection 5 global land cover: Algorithm refinements and characterization of new datasets. *Remote Sensing of Environment*, 2010, 114, 168–182.

Fritz, S. and See, L. Identifying and quantifying uncertainty and spatial disagreement in the comparison of Global Land Cover for different applications. *Global Change Biology*, 2008, 14, 1057–1075, doi: 10.1111/j.1365-2486.2007.01519.x

Fritz, S., Bartholome, E., Belward, A., Hartley, A., Stibig, H.J., Eva, H.; Defourny, P. Harmonization, Mosaicking and Production of the Global Land Cover 2000 Database (Beta Version), Luxembourg, Office for Official Publications of the European Communities, 2003; EUR 20849 EN.

Fritz, S.; See, L.; Rembold F. Comparison of Global and Regional Land Cover Maps with Statistical Information for the Agricultural Domain in Africa. *International Journal of Remote Sensing*, 2010, 31(9), 2237–56.

Fritz, S; See, L; McCallum, I., et al. Mapping global cropland and field size, 2015 *Global Change Biology*, 1980-1992, doi:10.1111/gcb.12838.

Gallego, F.J., Carfagna, E., Baruth, B., 2010. Accuracy objectivity and efficiency of remote sensing for agricultural statistics. In: Benedetti, R., Bee, M., Espa, G., Pier-simoni, F. (Eds.), Agricultural Survey Methods. John Wiley & Sons, pp. 193–211.

Geo-Wiki Project, http://beta-hybrid.geo-wiki.org/ accessed on March 2014-July 2015.

Giri, C P. Brief Overview of Remote Sensing of Land Cover in Remote Sensing of Land Use and Land cover: Principles and Application, Giri C P (ed.), CRC Press, New York, 2012; pp 3–12.

Giri, C., Zhu, Z.; Reed, B. A comparative analysis of the Global Land Cover 2000 and MODIS land cover data sets. *Remote Sensing of Environment*, 2005, 94(1), 123–132.

Google Earth Help, https://support.google.com/earth/answer/187961?hl=en accessed on August 2015.

Hansen, M.; DeFries, R.; Townshend, J.R.G.; Sohlberg, R. Global land cover classification at 1Km resolution using a decision tree classifier, *International Journal of Remote Sensing*, 2000, *21*, 1331–1365.

Hansen, M.C.; Reed, B. A comparison of the IGBP DISCover and University of Maryland 1 km global land cover products, *International Journal of Remote Sensing*, 2000, 21(6–7), 1365–1373

Holmgren, P. Global Land Use Area Change Matrix: Input to GEO-4. FAO, 2006; pp 9

Jalloh, A.; Nelson, G.C.; Thomas, T.S.; Zougmoré, R.B.; Roy-Macauley, H. eds. West African agriculture and climate change: a comprehensive analysis. *Intl Food Policy Res Inst*, 2013.

Latham, J.; Cumani, R; Rosati, I.; Bloise, M. FAO Global Land Cover (GLC-SHARE) Beta-Release 1.0 Database, FAO, 2014.

Lavreniuk, M., Kussul, N.; Skakun, S.; Shelestov, A.; Yailymov, B. Regional retrospective high resolution land cover for Ukraine: Methodology and results. In Geoscience and Remote Sensing Symposium (IGARSS), 2015 IEEE International, pp. 3965-3968. IEEE, 2015.

Leff, B., Ramankutty, N.; Foley, J.A. Geographic distribution of major crops across the world. *Global Biogeochemical Cycles*, 2004, *18*, 1–27.

Lowder, S.K.; Skoet, J.; Singh, S. What do we really know about the number and distribution of farms and family farms in the world? Background paper for The State of Food and Agriculture 2014, ESA Working Paper no. 14-02, available from http://www.fao.org/docrep/019/i3729e/i3729e.pdf accessed on March 28, 2016.

Loveland, T.; Reed B.; Brown, J.; Ohlen, D.; Zhu, Z.; Yang, L.; Merchant, J.W. Development of a global land cover characteristics database and IGBP DISCover from 1 Km AVHRR data, *International Journal of Remote Sensing*, 2000, 21 (6–7), 1303–1330.

Matton, N.; Canto, G.S.; Waldner, F.; Valero, S.; Morin, D.; et al., 2015. An Automated Method for Annual Cropland Mapping along the Season for Various Globally-Distributed Agrosystems Using High Spatial and Temporal Resolution Time Series. Remote Sensing, 7(10), pp.13208-13232.

Mayaux, P.; Bartholomé, E.; Massart, M.; Cutsem, C.V.; Cabral, A.; Nonguierma, A; Diallo, O.; *et al.* A land cover map of Africa, The European Commission 2003; pp 16.

Mayaux, P; Bartholomé, E.; Fritz, S.; Belward, A. A new land-cover map for Arica for the year 2000. *Journal of Biogeography*, 2004, *31*, 861–877.

McCallum, I.; Obersteiner, M.; Nilsson, S.; Shvidenko, A. A spatial comparison of four satellite derived 1Km global land cover datasets. *International Journal of Applied Earth Observation and Geo-information*, 2006, 8(4), 246–255.

Olson, D.M.; Dinerstein, E.; Wikramanayake, E.D.; Burgess, N.D.; Powell, G.V.; Underwood, E.C.; Kassem, K.R. Terrestrial ecoregions of the world: a new map of life. *Bioscience* 2001, 51(11), 933–938.

Pittman, K.; Hansen, M.C.; Becker-Reshef, I.; Potapov, P.V.; Justice, C.O. Estimating Global Cropland Extent with Multi-year MODIS Data. *Remote Sensing* 2010, 2(7), 1844–1863.

Ramankutty, N. Croplands in West Africa: A Geographically Explicit Dataset for Use in Models. *Earth Interactions*, 2004, 8(23), 1–22.

Ramankutty, N.; Foley, J.A. Estimating historical changes in global land cover: Croplands from 1700 to 1992. *Global Biogeochemical Cycles*, 1999, 13, 997–1027.

Roy, Parth S.; Roy, A.; Joshi, P.K et al. Development of Decadal (1985–1995–2005) Land Use and Land Cover Database for India. *Remote Sensing* 7.3, 2015, 2401-2430.

See, L.; McCallum, I.; Fritz, S. et al. Mapping cropland in Ethiopia using crowdsourcing. *International Journal of Geosciences* 4.06, 2013, 6.

Strahler, A.; Muchoney, D.; Borak, J.; Friedl, M. ; Gopal S.; Lambin, E.; Moody, A. MODIS land cover product: Algorithm Theoretical Basis Document (ATBD) Version 5.0 Boston University, USA 1999; pp 66.

Tarhule, A; Woo, M.K. Towards an interpretation of historical droughts in northern Nigeria. *Climatic Change*, 1997, 37(4), 601–616.

The International Disaster Datasets (EM-DAT) http://www.emdat.be/ accessed on February 2015.

Townshend, J.; Justice, C.; Li, W.; Gurney, C.; McManus, J. Global land cover classification by remote sensing: present capabilities and future possibilities. *Remote Sensing of Environment*, 1991, 35(2), 243–255.

Uppsala Conflict Database (UCD) http://www.ucdp.uu.se/gpdatabase/search.php accessed on February 2015.

World Wildlife Fund (WWF): https://www.worldwildlife.org/, accessed on January-April, 2015

Xie, Y.; Sha, Z.; Yu, M. Remote sensing imagery in vegetation mapping: a review. *Journal of Plant Ecology*, 2008, 1(1), 9–23.

Chapter 3: Mapping and Analysis of Urban Expansion in West African Cities

Pradeep Adhikari and Kirsten M. de Beurs

Department of Geography and Environmental Sustainability, University of Oklahoma, 100 E Boyd St, Suite 510, Norman, OK 73019, USA

(To be submitted to *Journal of Land Use Science*)

Abstract: Urban area expansion is one of the most powerful anthropogenic forces bringing changes to the earth's surface. Such changes are happening at much faster rates in Asian and African cities than elsewhere. In this study, we used Landsat MSS, TM and ETM+ images to map the urban land area in six West African cities for four different time steps from the early-1970s to 2010. The selected cities are Kumasi of Ghana, Daloa of Cote d'Ivoire, Abuja and Kano in Nigeria, Kindia of Guinea, and Ouagadougou of Burkina Faso. These cities are some of the small to large size cities with a medium to high rate of population growth in West Africa. They also represent three different eco-regions: Eastern Guinean Forest, Guinean Forest-Savanna Mosaic, and West Sudanian Savanna of West Africa. We found that all the cities, except Daloa, have a large number of non-urban pixel converted to urban in the past three to four decades. The growth of the urban areas was high, 13 to 54%, but the growth trajectories were not consistent. For example, the rate of urban growth has been declining in Abuja and Ouagadougou in recent years while Kumasi has been growing consistently at a much higher rate since 1975 and was still growing about 13% annually, between 2005 and 2010. Also, most of the cities have shown a higher rate of growth of urban land use

than population except Abuja and Ouagadougou. These cities revealed higher population growth, (10.7 to 15.8%) than urban land use growth, which varies from 3.0 to 4.5%. We did not observe any similarities in the growth of cities from the same eco-region.

Keywords: Urban land use; Urban growth; Cities; West Africa; Landsat,

Introduction

Urban area expansion is one of the most powerful anthropogenic forces changing the earth's surface (Dawson et al., 2009; Cui and Shi, 2012). Such expansion is associated with several interconnected but distinct processes such as an increase in population concentration and extensive alteration of the landscape due to infrastructure development (McDonnell and Pickett 1990). However, literature treats urbanization differently depending on contexts (Hope 1942; Satterthwaite et al. 2010; Marcotullio and Solecki 2013; Seto et al. 2013). For example, some limit urbanization to just the movement of people from rural to urban areas with population growth equating to urban migration (DESA/UN 2011) while others argue that urbanization encompasses processes which cover some aspect of a region's population, economy, or built infrastructure (Seto et al., 2011). In this research, we use urbanization as a process where built infrastructures have expanded changing the earth's surface from one land cover or land use type to the urban land use type.

There is no doubt that population growth is one of the most important drivers of urban area expansion. Since 2010, more people live in urban than in rural areas around the world (DESA/UN 2011). It is expected that by 2050, more than 60 percent of the

global population will live in urban areas. However, the level of such growth in urban population differs markedly across the world. On the one hand, the population of many of the countries in Europe, Latin America and the Caribbean, Northern America and Oceania is mostly urban. On the other hand, the majority of the population in countries in Africa and Asia (except China) remains mostly rural (DESA/UN 2011; Cui and Shi 2012; Seto et al. 2013). So, in coming decades major changes in urban population are projected to take place in developing countries of Africa and Asia (Satterthwaite et al., 2010; DESA/UN, 2011) likely altering the landscapes greatly.

Historically, urban hubs have been the center of economic and social development but urbanization has also negatively affected Earth's environment (Hope, 1942; Satterthwaite et al., 2010; Rodriguez, 2008; Marcotullio and Solecki, 2013). As urban centers grow, the increasing concentration of people and economic activities demand further development of housing and public infrastructures (Thapa and Murayama, 2009) changing the urban landscape. Several studies have investigated impacts of such development on the biota and physical environment (McDonnell and Pickett, 1990; Lambin et al., 2001; Kalnay and Cai, 2003; Alberti, 2005; Satterthwaite et al., 2010; Tian et al., 2011; Marcotullio and Solecki, 2013). One serious impact of urban development is the land use and land cover (LULC) change in and around the urban centers including encroachment on croplands (Tian et al., 2011). LULC changes associated with urban development are considered one of the most disturbing processes and are the cause of changes in mesoscale weather patterns, water resources and biodiversity (McDonnell and Pickett, 1990; Kalnay and Cai, 2003; Alberti, 2005; Liu et al., 2010). There is also evidence of changes in composition and structure of ecological

communities associated with urban land use (Posa and Sodhi, 2006; Sadler et al., 2006). Therefore, study of the expansion of urban land use holds a significant importance. This study aims to provide evidence for urban land use growth in West African cities and to quantify their growth so that authorities and land managers, both at the national and regional levels, can devise strategies balancing the urban growth with conservation efforts and socio-economic challenges facing the country and the region.

There are many urban growth studies around the world using remote sensing data (Mundia and Aniya, 2005; Seto et al., 2011; Attua and Fisher, 2011; Forkuor and Cofie, 2011; Weng, 2012; Karolien et al., 2012; Kamh et al., 2012; Brinkman et al., 2012; Linard et al., 2013; Wania et al., 2014). But the number of studies varies across the regions of the world. Seto et al. (2011) performed a meta-analysis of studies that monitored changes in urban land-use using remote sensing for the period between 1988 and 2008. They listed 326 case studies around the world meeting their criteria. The majority of the studies was carried out in China, North America, Europe and South West Asia. In Africa, they found only twenty-nine studies addressing urban expansion (Seto et al., 2011). Yeboah (2000, 2003) also mentions that urban expansion in Africa has not been adequately studied. However, the situation is changing as recently an increasing number of studies has been carried out focusing on the expansion of urban and peri-urban area in Africa in recent years (Karolien et al., 2012; Attua and Fisher, 2011; Forkuor and Cofie 2011; Kamh et al., 2012; Brinkman et al., 2012; Linard et al., 2013; Wania et al., 2014). One of the commonalities of these studies, in Africa, is the use of multi-temporal Landsat imagery.

Most of the research on urban land cover change in Africa presented above is primarily focused on one city. These studies map the land cover for the different time period(s) using remote sensing data, mainly Landsat imagery, along with some ancillary data and analyze the change in urban growth over a certain time period(s). None of the studies so far have taken a comprehensive look at urban growth across the region of West Africa. Therefore, the objective of this study is to quantify and compare the growth of urban land use in six different cities in West Africa using Landsat imagery for multiple time periods between the early-1970s and 2010.

Materials and Methods

Study area

The study area covers six cities from five countries and three eco-regions in West Africa (Fig. 3.1).

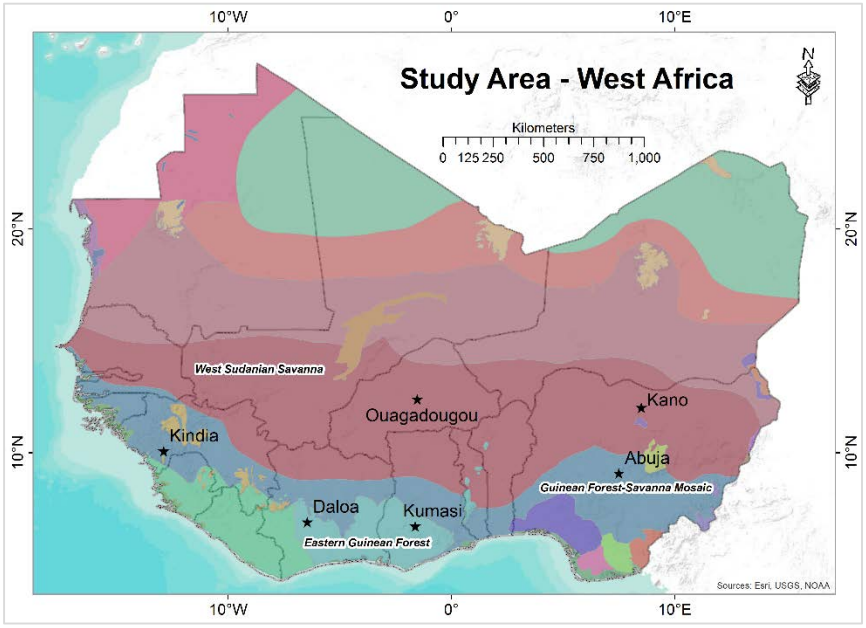

Figure 3.1. Selected cities in West Africa. Also shown are the eco-regions (Olson et al. 2001) in West Africa.

The selected six cities are a representative mix of small to large size cities in West Africa. They are from five different countries: Ghana, Cote d'Ivoire, Nigeria, Guinea, and Burkina Faso. The cities are selected in such a way that at least two cities are from the same eco-region: Eastern Guinean Forest (EGF), Guinean Forest-Savanna Mosaic (GFM), and West Sudanian Savanna (WSS) in West Africa (Table 3.1). Although by definition an ecoregion has a relatively uniform climate with unique ecological communities (Olson et al. 2001), climatic parameters like annual rainfall vary within the same ecoregion.

To capture such variabilities at least two cities from the same eco-region with different annual rainfall are selected for this study. In addition, as urban growth may have been affected as a result of governmental policies (Wu et al., 2011) the selected cities capture variability that exists in the region both in terms of climate and land policy. The selected cities had populations as low as 96 thousand (Kindia) to more than two million (Kano) in 2000. The population in the cities has grown substantially for the period 2000-2010. Abuja grew the most with 15.8% followed by Ouagadougou's 10.7% and Kumasi 6.3%. Among the six cities Kano grew the least, by 2.6%.

Table 3.2. Features of selected cities for the study of urban land use growth.

Cities	Countries	Eco-regions	Mean annual rainfall (mm, for 2001-10)	Population (for 2000 in '000)*	Population (for 2010 in '000)*	Annual rate of pop. growth (%)
1. Kumasi	Ghana	Eastern Guinean Forest	1,146	1,187	1,935	6.3
2. Daloa	Cote d'Ivoire		1,026	185	248	3.4
3. Abuja	Nigeria	Guinean Forest-Savanna Mosaic	1,436	833	2,153	15.8
4. Kindia	Guinea		730	96	135	4.1
5. Ouagadougou	Burkina Faso	West Sudanian Savanna	812	921	1,911	10.7
6. Kano	Nigeria		712	2,602	3,271	2.6

**Sources: DESA/UN, 2011 and http://www.citypopulation.de*

Data

Landsat data are obtained from the Earth Resources Observation and Science Center (EROS) (http://glovis.usgs.gov/). First, scenes without any cloud contaminations are selected using the web-filter available on the EROS website. Ideally, a minimum of two scenes— one each from wet and dry seasons— were obtained. If there was not at least a scene without cloud cover every four to five years then scenes with cloud cover up to ten percent —avoiding clouds just above the city and its immediate vicinity— were acquired (Figure 3.2).

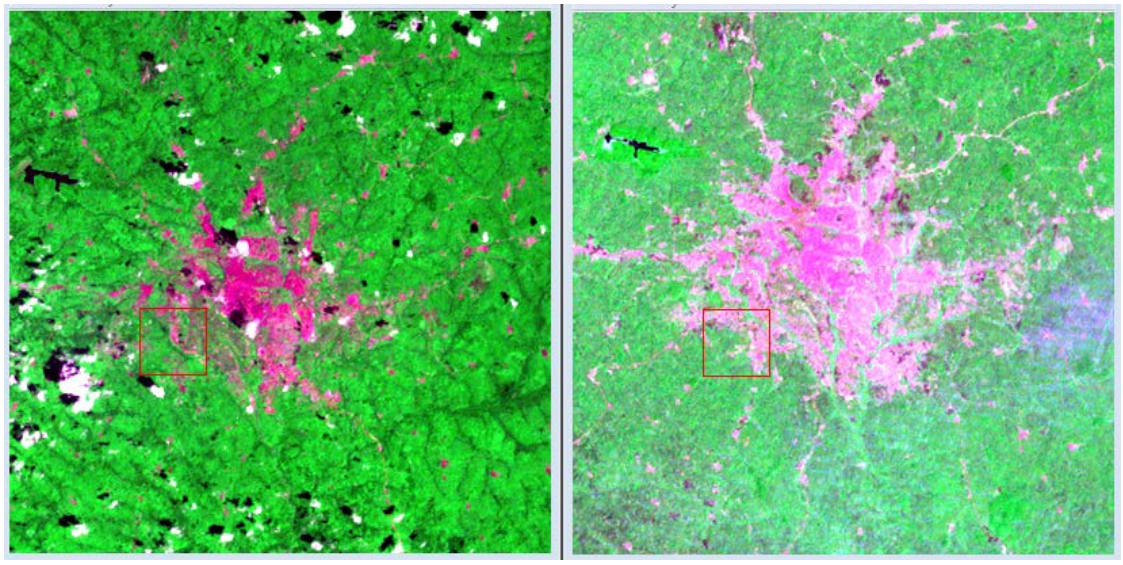

Figure 3.2. Landsat image (raw image without atmospheric correction) of 1973 (left panel) and 1986 (right panel) over Kumasi, Ghana. Due to different sensors used in different Landsat missions the types of spectral bands acquired varied among different Landsat missions. The image on left panel has bands 5(Red), 7(Near Infrared) and 4 (Green) while the image on right panel has bands 2(Red), 4(Near Infrared) and 1 (Green).There is some cloud contamination on the 1973 image (left panel).

A list of Landsat path and rows for the selected urban centers along with the years and number of scenes that have been acquired for this study is provided below (Table 3.2).

Table 3.2. Landsat path and rows, years of acquisition, number of scenes and sensors used in the acquisition.

Cities/Country	Landsat path/row (WRS-1)WRS-2	Years of acquisition (No. of scenes/Satellites*)
Kumasi, Ghana	(209/55)194/55	1973 (1/LM1), 1986 (3/LM5), 2005 (3/LE7), 2010 (2/LE7)
Daloa, Cote d'Ivoire	(212/55)197/55	1986 (1/LM5), 1991 (1/LT4), 2000 (2/LE7), 2008 (1/LE7),
Abuja, Nigeria	(203/54)189/54	1986 (3/LM5), 1990 (4/LT4 and LM4), 2001 (2/LE7), 2005 (4/LE7)
Kindia, Guinea	(217/53)202/53	1990 (1/LT4), 1995(1/LT5), 2000 (2/LE7), 2005 (5/LE7), 2010 (8/LE7)
Ouagadougou, Burkina Faso	(210/51)195/51	1975 (5/LM2), 1980 (4/LM3), 1986 (9/LT5), 1990 (1/LT5), 2000 (8/LE7), 2005 (11/LE7), 2010 (8/LE7)
Kano, Nigeria	(202/52)188/52	1975 (2/LM2), 1985 (5/LT4-5), 2000 (3/LE7), 2010 (6/LE7)

**Satellites LM2-5: Landsat 2, 3, 4 or 5 MultiSpectral Scanner (MSS); LT 4-5: Landsat 4 or 5 Thematic Mapper ™; LE 7: Landsat 7 Enhanced Thematic Mapper plus (ETM+). The spatial resolution of Landsat product varies. Landsat 1 and 2 have a spatial resolution of 80m. Landsat 3 has a spatial resolution of 40 meters and Landsat 4 through 8 have a spatial resolution of 30 meters.*

Methods

Mapping the urban area involves the following four steps: data preprocessing, image classification, accuracy assessment, and mapping the area. The process of mapping the urban growth is explained based on a case study to map the city of Kumasi, Ghana in this section. The process is summarized in a flow chart (Figure 3.3).

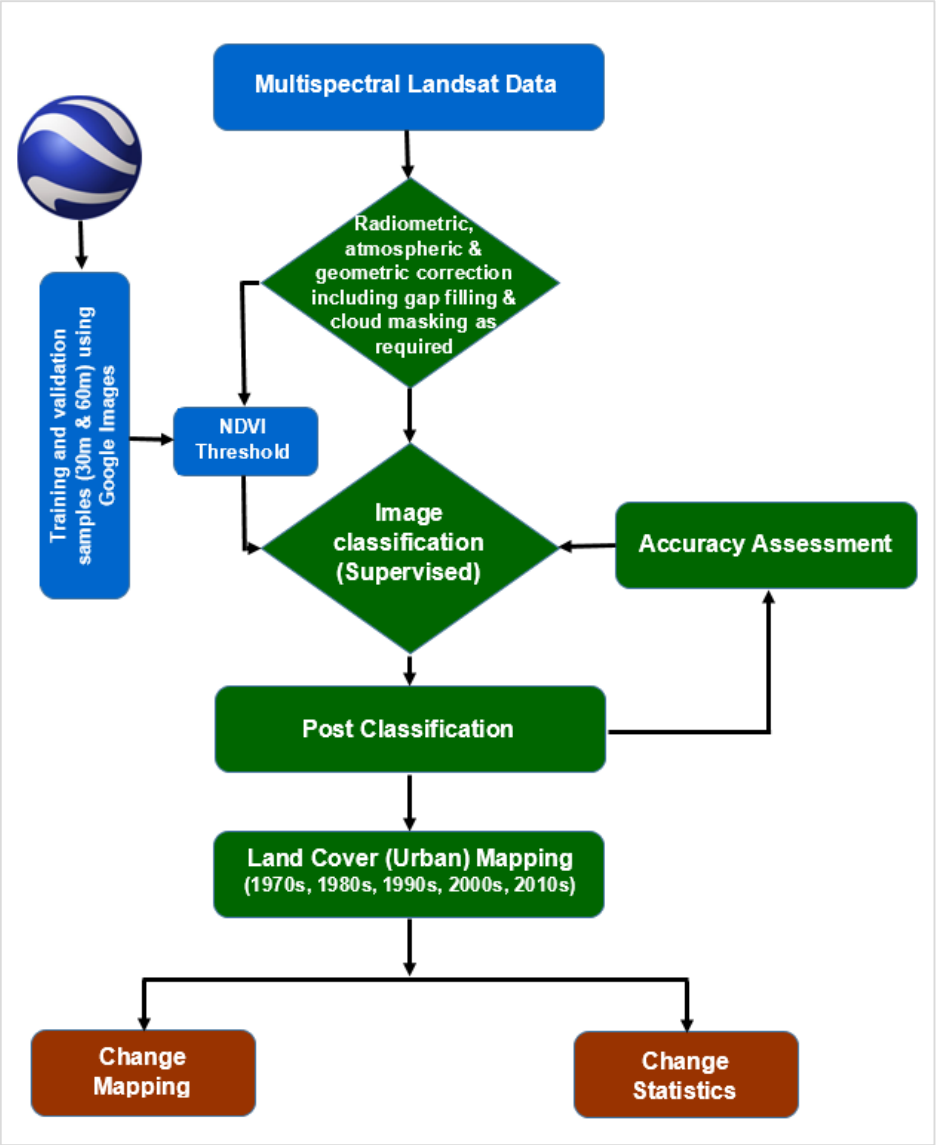

Figure 3.3. Flow chart of mapping and analyzing urban growth in West Africa.

Data preprocessing

The Landsat images for this research cover the entire period of the Landsat mission. There are only four spectral bands in Landsat Multispectral Scanner (MSS) series 1 to 5 while there are seven spectral bands in Landsat Thematic Mapper (TM). In the Landsat Enhanced Thematic Mapper Plus (ETM+) there are eight spectral bands including the panchromatic band. The selected Landsat images were radiometrically

and atmospherically corrected. The Landsat MSS images were corrected using Fast Line-of-sight Atmospheric Analysis of Spectral Hypercubes (FLAASH). The Landsat TM and ETM+ images were corrected using the Landsat Ecosystem Disturbance Adaptive Processing System (LEDPAS) (Vermote et al., 1997; Masek et al., 2013). Some of images, especially images from the early 1970s, were geometrically corrected using a base map to maintain proper alignment. Also in case of images with clouds, cloud cover and associated shadows were masked using an unsupervised classification technique (Irish et al., 2006).

Since 2003 the Scan Line Corrector (SLC) on Landsat 7 failed causing a series of gaps on the Landsat scenes. The SLC-off effects are more significant along the edges than at the center of the scenes (Chen et al., 2011). There were several scenes from 2005 to 2010 in the list presented in table 3.2 with gaps. We filled gaps using the Delaunay triangulation (Lee and Schachter, 1980; de Berg, 2002) of surface fitting algorithm, based on the neighboring pixel values (Liu et al., 1999) which is available in ENVI 5.1, an image analysis software.

Image classification

Broadly speaking there are three types of image classification techniques. They are pixel-based, sub-pixel based, and object-based techniques (Li et al., 2014). In pixel based techniques unsupervised and supervised classifiers are some of the widely used classifiers. In unsupervised classifier, clustering algorithms are used to classify the image based on spectral signatures (Jansen, 2007). While in using the supervised

classifier, training pixels are required to create representative parameters for each land cover class (Jansen, 2007). The most commonly used supervised classification is maximum likelihood classification which assumes that each spectral class can be described by a multivariate normal distribution (Otukei and Blaschke, 2010). But the accuracy of maximum likelihood classification depends on correct estimation of the mean vector and the covariance matrix for each spectral class based on training pixels (Richards, 1993; Jansen, 2007). Generating a satisfactory classification image from remotely sensed data depends on many factors: (a) the characteristics of the study area, (b) availability of suitable remotely sensed data, ancillary and ground reference data, (c) proper use of variables and classification algorithms, (d) the analyst's experience, and (e) available time (Lu and Weng, 2005). Therefore, there is no single method which performs better than others to classify land cover and land use (including urban land use) in all circumstances (Seto et al., 2011). Various methods have been employed to classify images for urban land use based on multispectral and hyperspectral remote sensing data (Herold and Roberts, 2010; Fan and Fan, 2014). They include decision tree, supervised and unsupervised maximum likelihood classifier, neural network, regression tree model, and spectral unmixing (Rashed et al., 2001; Yang et al., 2003; Bauer et al., 2004; Xian and Crane, 2005; Lee and Lathrop, 2006; Lu and Weng, 2006; Mohapatra and Wu, 2008;Wu, 2009; Hu and Weng, 2009). In this study, we used the maximum likelihood classification algorithm. The classification process involves three steps: defining the training pixels, extraction of signatures from the identified training pixels and classification of the image.

We collected training and validation pixels using Google Earth™ imagery. The Google Earth™ images were selected because they are available at high spatial resolution of at least 15 m, and are updated regularly —every one to three years (Google Earth Help). Furthermore, these images are better alternatives for training and validation if the area is large and field data are hard to come by because of their accuracy (Potere 2008; Knorn et al.2009). For the collection of Google Earth™ data pixels, we used the extent of the Landsat scenes that covered the selected cities as the sampling frame. We randomly collected about three thousand pixels each, at 30 m and 60 m. For each grid cell we assigned a maximum of three dominating land cover classes from eleven possible classes —Buildings, Paved roads, Unpaved roads, Airports, Grass and herbaceous, Tree and forest, Croplands, Fallow lands, Soil and barren, Water bodies and Wetlands (Figure 3.4). We replaced pixels with poor resolution or cloud contamination. The majority of the pixels were from images of the year 2010 or later.

Figure 3.4. Two data points (30 m × 30 m) collected using the Google Earth™. The pixel on the left panel shows a mix land cover classes, cropland (70%) and grass and herbaceous near Abuja, Nigeria. The pixel on the right panel shows a mixed pixel with buildings (80%) and unpaved roads (20 %) near Kano, Nigeria.

Only pixels with 50% or more of the same land cover class were retained for training and validation. After filtering out pixels not meeting the criteria, we aggregated some of the land cover classes. We grouped buildings, paved roads, unpaved roads and airports to a new class called impervious. Similarly, the croplands and fallow croplands were combined. Water bodies and wetlands pixels were grouped as water. Furthermore, if there were less than 10 pixels for a certain land cover type, we dropped that land cover class during classification. The number of pixels for the six resulting land cover classes over the selected cities varied (Table 3.3). After filtering the total number of pixels left for training and validation was much lower, as much as 68% less (such as in Abuja) than the originally collected three thousand pixels.

Table 3.3. Land cover land use class (LULC) and number of pixels from Google Earth ™ images retained for training and validation.

Types of LULC collected using Google images	Adopted LULC for training and validation	Number of Pixels (*30 m × 30 m*) retained *					
		Kumasi	Daloa	Abuja	Kindia	Ouagadougou	Kano
1. Buildings	1. Impervious	(20) 72	157	65	32	(29) 45	55
2. Paved roads							
3. Unpaved roads							
4. Airports							
5. Grass and herbaceous	2.Grass	(65) 432	1741	169	1526	(1051) 1594	976
6. Trees and forest	3.Forest	(104) 798	354	281	254	(121) 59	100
7. Croplands	4.Croplands	(199) 514	127	310	146	(643) 708	1414
8. Fallow lands							
9. Soil and barren	5.Soil	(24) 40	13	134	26	(40) 423	84
10. Water bodies	6.Water	Not enough samples	34	24	189	(21) 29	46
11. Wetlands							
Total number of pixels retained		(412) 1856	2426	983	2173	(1905) 2858	2675

**The numbers in the parenthesis are number of pixels for 60 m × 60 m grids*

Studies have shown effective use of Normalized Difference Vegetation Index (NDVI) (Masek et al., 2000; Gillies et al., 2003; Baur et al., 2004) to distinguish vegetated (e.g. croplands or grassland) and non-vegetated area (impervious surface such as a road or residential area). To increase class separability values, we used an NDVI threshold to further refine the quality of collected pixels. NDVI is derived from the red to near-infrared (NIR) reflectance ratio as follows (Eq. 3.1).

$$\mathrm{NDVI} = \frac{\mathrm{NIR} - \mathrm{RED}}{\mathrm{NIR} + \mathrm{RED}} - - - - - (3.1)$$

Here, NIR and RED are the percentages of near-infrared and red light reflected by the vegetation and captured by satellite sensors (Karnieli et al., 2010). We used the NIR and RED bands from the Landsat images to calculate the NDVI.

Based on the filtered training pixels, we calculated the spectral separability — measured by the Jeffries-Matusita Transformed Divergence separability, using the separability tool available in ENVI 5.1. Standard separability values vary from 0 to 2 with a value closer to 2 showing higher separability. The spectral separability for the training data 1.5 or more. Approximately two third of the pixels for each land cover class were used for training and the remainder one third pixel were used for validation. Based on the refined training pixels, the images are classified into five different classes as listed in table 3.4.

Table 3.4. NDVI threshold used for refining ground truth pixels collected using Google Earth.

Cities	Land Cover Classes					
	Impervious	Soil and barren	Croplands	Grass	Forest	Water
1. Kumasi	0.0-0.20 (13)	0.20- 0.30 (16)	0.3- 0.45 (52)	0.46- 0.69 (22)	0.69 or more (89)	Not enough samples
2. Daloa	0.07-0.20 (44)	Not enough samples	0.20 to 0.27 (30)	0.27 – 0.35 (377)	0.35 or more (195)	-0.08 to 0.06 (25)
3. Abuja	0.08-0.14 (30)	0.19-0.22 (40)	0.25-0.35 (57)	0.35- 0.40 (29)	0.35 or more (64)	0.0 or less (25)
4. Kindia	0.11-0.25 (46)	Not enough samples	0.25-0.38 (38)	0.38-0.45 (199)	0.45 or more (179)	-0.28 to 0.09 (131)
5. Ouagadougou	0.1-0.16 (13)	0.16-0.2 (201)	0.18-0.22 (144)	0.22-0.25 (223)	0.25 or more (33)	-0.44 to 0.01 (23)
6. Kano	0.06-0.10 (56)	0.11-0.18 (21)	0.18-0.21 (612)	0.22-0.25 (204)	0.26 or more (38)	-0.34 to 0.04 (46)

The number in ( ) are the number of pixels retained for training and validation meeting the NDVI threshold criteria.

Accuracy assessment

The accuracy of the classification is determined based on a confusion matrix. A confusion matrix is calculated using ground truth pixels collected from Google Images. In deriving a confusion matrix, the location and class of each ground truth pixel with the corresponding location and class in the classification image are determined. The overall accuracy is obtained by summing the number of correctly classified pixels and dividing by the total number of pixels. The producer accuracy is a measure indicating the probability that the classifier has labeled a pixel into a certain class given that the ground truth is that class. User accuracy is a measure indicating the probability that a pixel is in a class given that the classifier has labeled the pixel into that class (Jensen, 2005). The Kappa statistics (Lillesand et al., 2006) is calculated using equation (3.2).

$$k = \frac{\mathrm{N}\sum_{i=1}^{r} x_{ii} - \sum_{i=1}^{r}(x_{i+}.x_{+i})}{N^2 - \sum_{i=1}^{r}(x_{i+}.x_{+i})} - - - - - (3.2)$$

Where,

R = number of rows in the error matrix,

x_{ii} = number of observations in row i and column x,

x_{i+} = number of observation in row i

x_{+i} = number of observations in column i, and

N = number of observation within the matrix.

Change analysis

After image classification we categorized each pixel into either urban or non-urban. A box of 30 Km × 30 Km containing the city is used to extract urban and non-urban pixels for mapping and further analysis of the cities and their surroundings. Furthermore, to maintain the consistency of the classified images to represent urban pixels, it is assumed that if a pixel is classified as urban at the beginning (e.g. 1973 in the case of Kumasi or 1986 in the case of Daloa) then the pixel remains urban in subsequent years.

Results

Urban land use maps

The overall accuracy of the classified images varies from 67% to 98% and the Kappa statistics varies from 0.54 to 0.98 (Table 3.5). The urban land area in each city has grown over the past several decades (Figures 3.5-3.10). In general, cities expanded either along the road network or around the core city area. The city of Kumasi primarily expanded first nearer to the road network and along the city periphery. The city of Daloa, Kindia and Ouagadougou grew on the city fringes rather than along the roads. The situation is different in Abuja. The urban area grew within the core city area as well as expanded along the roads. The city of Kano also followed a similar pattern of growth around the city and expanding along the road network. We also observed that there were some pockets of the area along the roads in the cities where new built-up areas had emerged. Such development was visible in all cities except in Daloa and Kindia.

Table 3.5. Accuracy assessments of classified images.

Cities	Image Year	Kappa coefficient	Overall accuracy (%)
Kumasi	1973	0.66	75.34
	1986	0.54	67.82
	2005	0.74	80.85
	2010	0.77	83.52
Daloa	1986	0.79	85.92
	1991	0.98	98.85
	2000	0.80	88.85
	2008	0.81	85.75
Abuja	1986	0.94	94.87
	1990	0.97	97.54
	2001	0.98	98.70
	2005	0.97	97.28
Kindia	1990	0.65	74.34
	1995	0.76	80.12
	2005	0.87	89.64
	2010	0.91	90.27
Ouagadougou	1975	0.93	95.12
	1986	0.73	79.50
	2005	0.86	89.27
	2010	0.85	88.32
Kano	1975	0.90	91.23
	1985	0.86	88.56
	2000	0.95	94.54
	2010	0.92	93.12

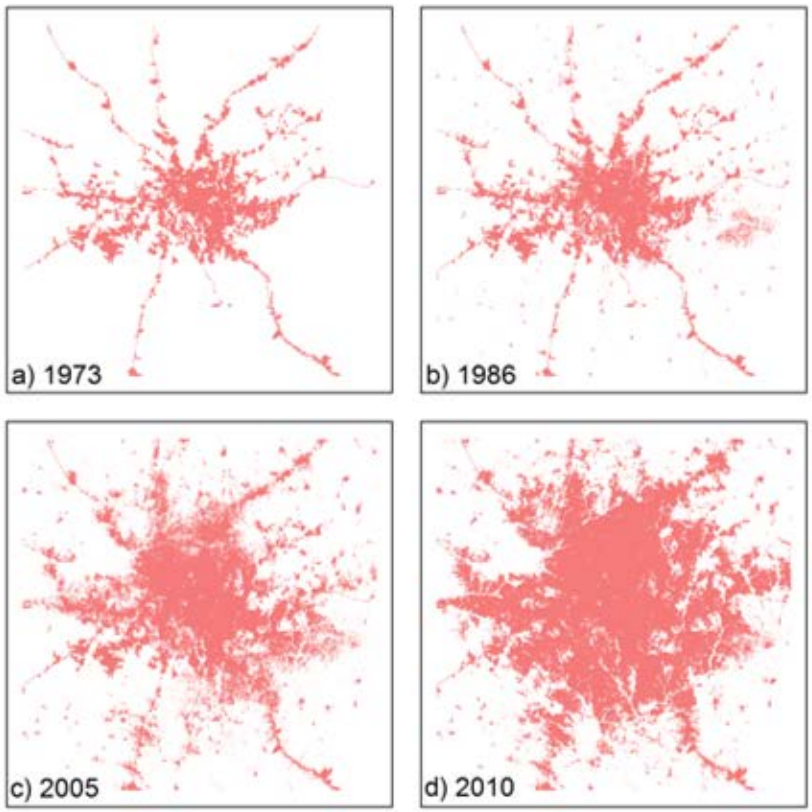

Figure 3.5. Urban area of the city of Kumasi, Ghana.

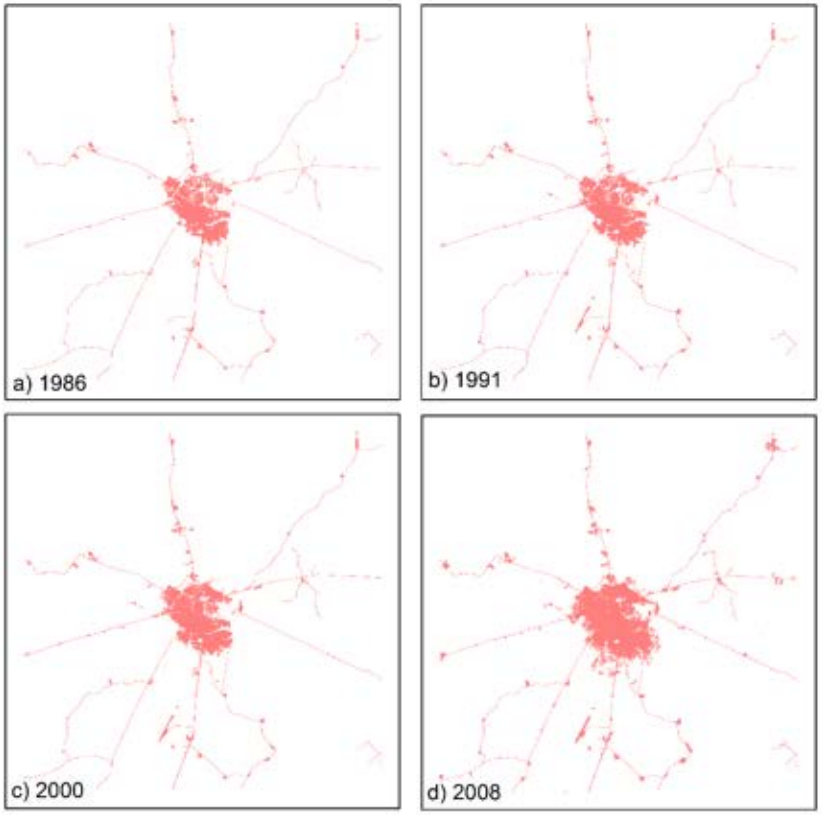

Figure 3.6. Urban area of the city of Daloa, Cote d'Ivoire.

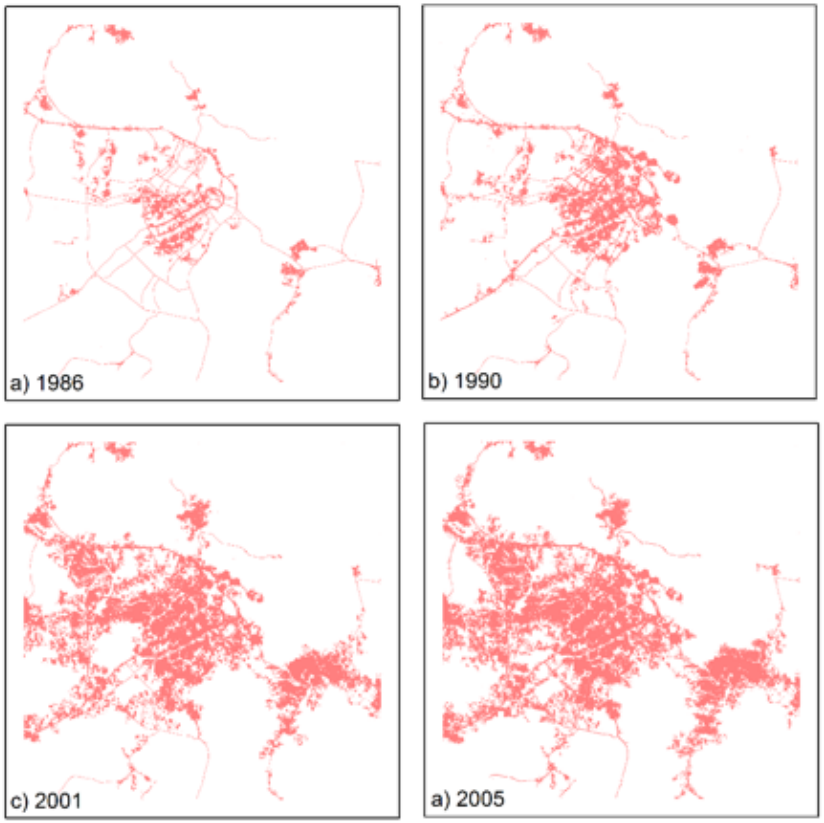

Figure 3.7. Urban area of the city of Abuja, Nigeria.

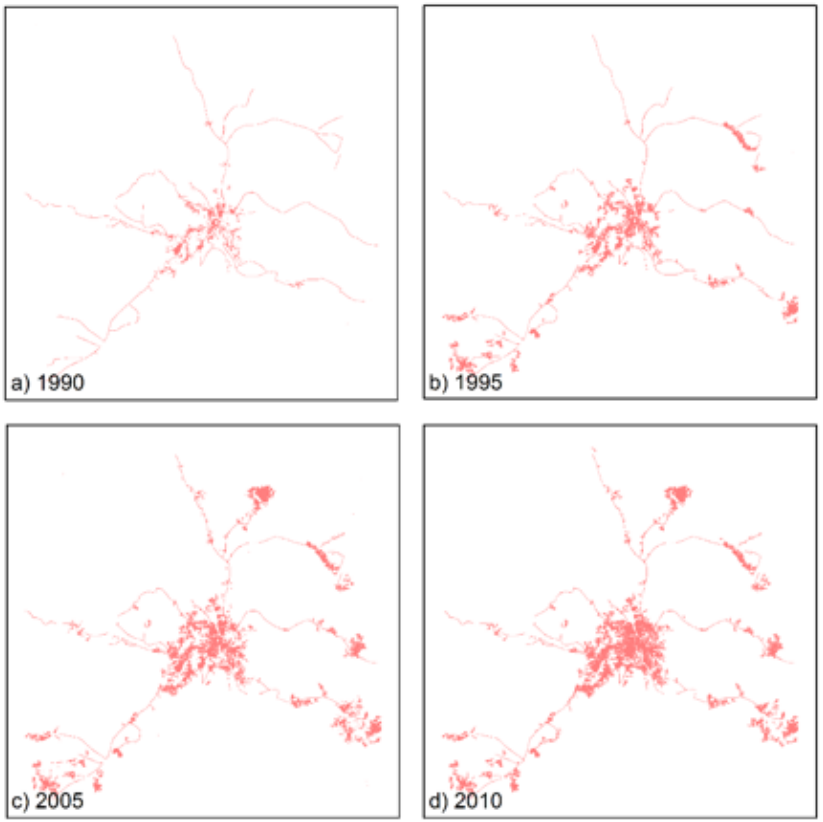

Figure 3.8. Urban area of the city of Kindia, Guinea.

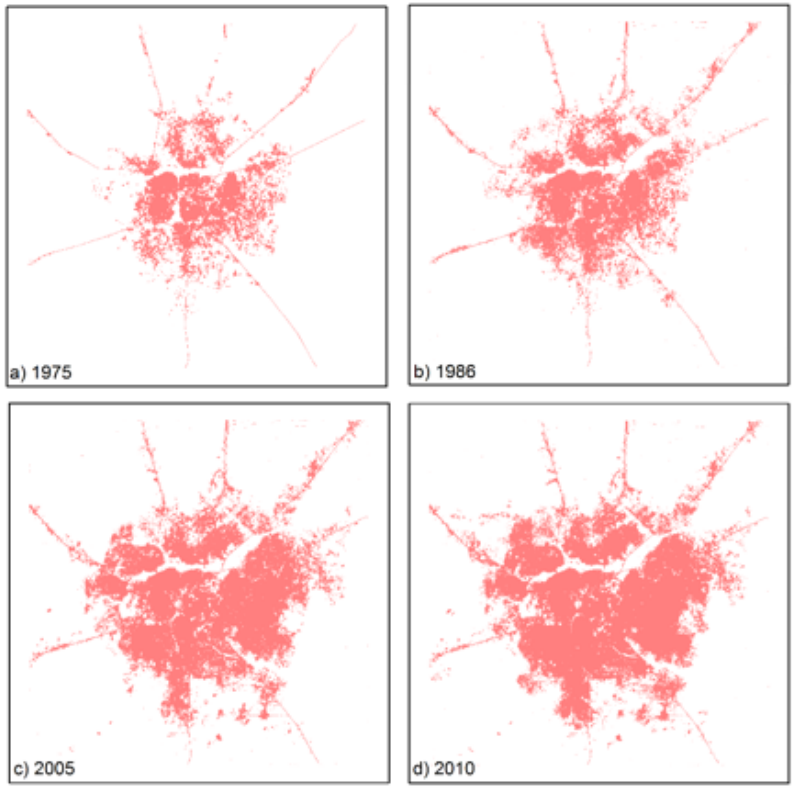

Figure 3.9. Urban area of the city of Ouagadougou, Burkina Faso.

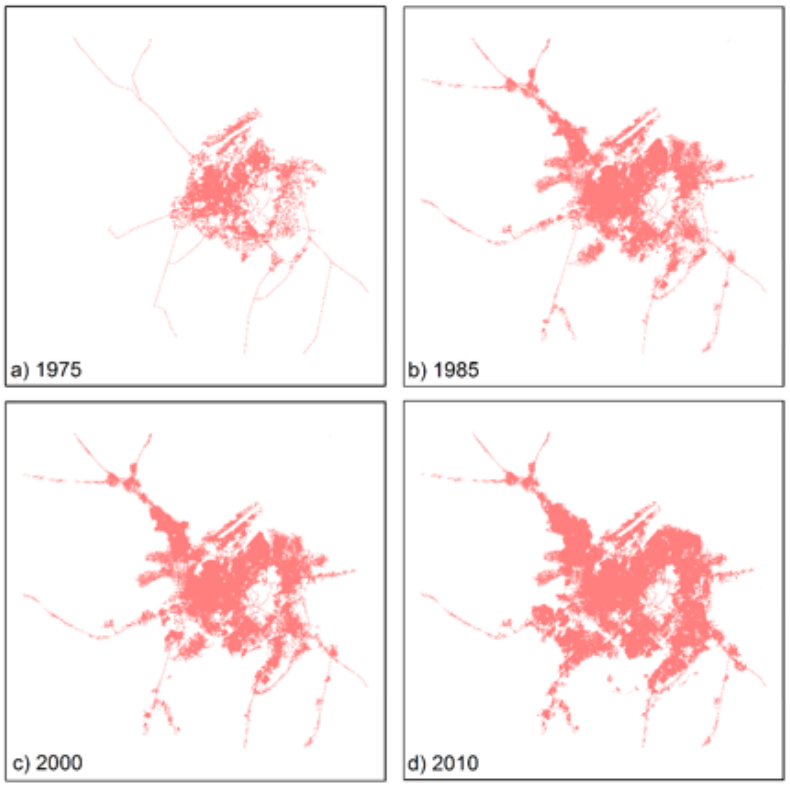

Figure 3.10. Urban area of the city of Kano, Nigeria.

Urban growth-Transition matrices growth

Based on the urban area maps derived in section 3.1 we prepared three pixel based transition matrices for each city (Table 3.6-3.11). These matrices show how many non-urban pixels, from an earlier time step, converted to urban in a later time step and the proportion of such change. For example, in the city of Kumasi a total of 29,867 non-urban pixels from the year 1973 turned into urban pixels in 1986 (Table 3.6A). These newly converted pixels constitute 22% of the total urban pixels in 1986. The conversion from non-urban to urban pixels were much higher, 45%, for the period 1986-2005 (Table 3.6-B) while for the period 2005-2010 it fell slightly to 39% (Table 3.6-C).

The conversion from non-urban pixels to urban is very high in all cities except for Daloa. In Daloa, the changes were 13% or below (Table 3.7A-C). In the rest of the cities the conversion were as high as 54% (Abuja and Kindia, Tables 3.8A-C, 3.9A-C). In Kindia, the trend of conversion of non-urban to urban pixels was high, but decreasing from 54% to 28% (Table 3.9A-C). In the city of Kumasi, Abuja and Ouagadougou the conversion started high at the beginning (22-41%), continued to grow higher (42-54%) and started to fall (13-39%) for the recent time periods (Table 3.6A-C, Table 3.8A-C and Table 3.10A-C). The city of Kano revealed a different trajectory of non-urban to urban conversion (Table 3.11A-C). The conversion was 49% at the beginning time period (1990-1995), which dropped to 10% in the middle time steps (1995-2005) and picking up again to 25% in recent time period (2005-2010).

A year to year comparison of the non-urban to urban conversion between cities from the same or different ecoregion is not possible—except in the case of Kumasi,

Ouagadougou and, to some extent to Kano—as the urban area maps belong to different years. Despite this limitation, we can see trends for certain time periods. We could not find any similarity in the conversion of non-urban land to urban between the cities from the same eco-region. For example, the city of Kumasi and Daloa fall in the same ecoregion of Eastern Guinean Forest (EGF), but the conversion is much higher in Kumasi than in Daloa. In Daloa, the periods 1986-1991 and 1991-2000 saw a 13% and 4% change from non-urban to urban conversion, respectively. In Kumasi, for the period 1986-2005, which compasses both periods 1986-1991 and 1991-2000 of Daloa, the conversion from non-urban to urban is 45%, much higher than in Daloa for the period 1986-2005 both Kumasi and Ouagadougou which are cities from two different eco-regions: EGF and West Sudanian Savanna (WSS) have added almost equal percentage (45% and 42% respectively), of non-urban pixels to urban. But for the next time period, 2005-2010, Kumasi still added 39% non-urban pixels as urban while Ouagadougou added only 13%, only a third that the city of Kumasi added. Similarly the city of Kindia, in Guinean Forest-Savanna Mosaic (GFSM) ecoregion, has a comparable conversion of non-urban pixels to urban with the city of Kano, from the WSS eco-region, for the period 2005 and 2010 which is 28% and 25% respectively. Although, overall there were large areas converting to urban land use in the cities but no comparable trends were observed for the cities from the same eco-region or country for that matter.

Table 3.6. Transition matrices-Kumasi, Ghana.

(A)		1973		
		Non-Urban	Urban	**Total**
1986	Non-Urban	866,646	--	**866,646**
	Urban	29,867 (22%)	103,487 (78%)	**133,354**
	Total	**896,513**	**103,487**	**1,000,000**

(B)		1986		
		Non-Urban	Urban	**Total**
2005	Non-Urban	757,310	--	**757,310**
	Urban	109,336 (45%)	133,354 (55%)	**242,690**
	Total	**866,646**	**133,354**	**1,000,000**

(C)		2005		
		Non-Urban	Urban	**Total**
2010	Non-Urban	604,608	--	**604,608**
	Urban	152,702 (39%)	242,690 (61%)	**395,392**
	TOTAL	**752,310**	**242,690**	**1,000,000**

Table 3.7. Transition matrices-Daloa, Cote d'Ivoire.

(A)		1986		
		Non-Urban	Urban	**Total**
1991	Non-Urban	964,645	--	**964,645**
	Urban	4,444 (13%)	30,911 (87%)	**35,355**
	Total	**969,089**	**30,911**	**1,000,000**

(B)		1991		
		Non-Urban	Urban	**Total**
2000	Non-Urban	963,045	--	**963,045**
	Urban	1,600 (4%)	35,355 (96%)	**36,955**
	Total	**964,645**	**35,792**	**1,000,000**

(C)		2000		
		Non-Urban	Urban	**Total**
2008	Non-Urban	948,788	--	**948,788**
	Urban	14,257 (28%)	36,955 (72%)	**51,212**
	Total	**963,045**	**36,955**	**1,000,000**

Table 3.8. Transition matrix – Abuja, Nigeria.

(A)		1986		
		Non-Urban	Urban	**Total**
1990	Non-Urban	919,726	--	**919,726**
	Urban	32,965 (41%)	47,309 (59%)	**80,274**
	Total	**952,691**	**47,309**	**1,000,000**

(B)		1990		
		Non-Urban	Urban	**Total**
2001	Non-Urban	823,727	--	**823,727**
	Urban	95,999 (54%)	80,274 (46%)	**176,273**
	Total	**919,736**	**133,354**	**1,000,000**

(C)		2001		
		Non-Urban	Urban	**Total**
2005	Non-Urban	788,863	--	**788,863**
	Urban	34,864 (17%)	176,273 (83%)	**211,137**
	Total	**823,727**	**242,690**	**1,000,000**

Table 3.9. Transition matrices – Kindia, Guinea.

(A)		1990		
		Non-Urban	Urban	**Total**
1995	Non-Urban	969,765	--	**969,765**
	Urban	16,308 (54%)	13,927 (46%)	**30,235**
	Total	**986,073**	**13,927**	**1,000,000**

(B)		1995		
		Non-Urban	Urban	**Total**
2005	Non-Urban	955,252	--	**955,252**
	Urban	14,513 (32%)	30,235 (68%)	**44,748**
	Total	**875,898**	**124,102**	**1,000,000**

(C)		2005		
		Non-Urban	Urban	**Total**
2010	Non-Urban	937,718	--	**937,718**
	Urban	17,534 (28%)	44,748 (72%)	**62,282**
	Total	**862,209**	**137,791**	**1,000,000**

Table 3.10. Transition matrix – Ouagadougou, Burkina Faso.

(A)		1975		
		Non-Urban	Urban	**Total**
1986	Non-Urban	868,208	--	**868,208**
	Urban	42,784 (32%)	89,008 (68%)	**131,792**
	Total	**897,962**	**89,008**	**1,000,000**

(B)		1986		
		Non-Urban	Urban	**Total**
2005	Non-Urban	773,236	--	**773,236**
	Urban	94,972 (42%)	131,792 (58%)	**226,764**
	Total	**868,208**	**131,792**	**1,000,000**

(C)		2005		
		Non-Urban	Urban	**Total**
2010	Non-Urban	738,903	--	**738,903**
	Urban	34,333 (13%)	226,764 (87%)	**261,097**
	Total	**773,236**	**226,764**	**1,000,000**

Table 3.11. Transition matrix – Kano, Nigeria.

(A)		1975		
		Non-Urban	Urban	**Total**
1985	Non-Urban	875,898	--	**875,898**
	Urban	60,293 (49%)	63,809 (51%)	**124,102**
	Total	**936,191**	**63,809**	**1,000,000**

(B)		1985		
		Non-Urban	Urban	**Total**
2000	Non-Urban	862,209	--	**862,209**
	Urban	13,689 (10%)	124,102 (90%)	**137,791**
	Total	**875,898**	**124,102**	**1,000,000**

(C)		2000		
		Non-Urban	Urban	**Total**
2010	Non-Urban	817,068	--	**817,068**
	Urban	45,141 (25%)	137,791 (75%)	**182,932**
	Total	**862,209**	**137,791**	**1,000,000**

Rate of growth in urban land use

We also calculated the overall and annual growth of the cities over the three different time periods. Overall, the growth of the cities are high but inconsistent over the past several decades. Also, the path of the growth is different in each city. We also calculated the overall and annual growth rate of the cities over the three different time periods. Overall, the growth of the cities are high but inconsistent over the past several decades. Also, the path of the growth is different in each city. For example, the urban land area in Kumasi had been continuously growing annually, since 1973 to 2010—the highest rate being 12.6% (Table 3.12) for the most recent period 2005-2010. The city of Daloa, Kindia, and Kano have a slightly different path of urban land area growth compared to Kumasi.

The city of Daloa, Kindia, and Kano have the slightly different path of the urban land area growth compared to Kumasi. All three cities saw a higher growth (3 to 5.5%) at the beginning followed by a marginal drop for some time in the middle (1.9 to 4.1%) and grew again (3-4.8%) for the most recent time periods. (Tables 3.13, 3.15, and 3.17). The growth is slowest in Daloa among all six cities.

In contrast, the annual growth of the urban area had been decreasing in Abuja and Ouagadougou in recent time periods. In Abuja, the annual growth rate was 4.9% for the period 2001-2005 compared to 10.2% during 1990-2001 (Table 3.14). Similarly, in Ouagadougou, the annual growth rate was 3.0% for 2000-2010 which was 4.1% in 1986-2010 (Table 3.16). The remaining cities have mixed trends on the growth of the urban area.

Table 3.12. Kumasi, Ghana - Growth of urban area.

Details	1973	1986	2005	2010
No. of pixels	103,487	133,354	242,690	395,392
Total area (in hectare)	9,314	12,002	21,842	35,585
Growth (%) over 1973		28.8 % (+2,688 ha)	134.5 % (+12,528 ha)	282.1 % (+26,271 ha)
Annual growth (%) over 1973		2.2 % (+207 ha)	4.2% (+392 ha)	7.6 % (+710 ha)
Growth (%) over 1986			81.9 % (+9,840 ha)	196.5 % (+23,583 ha)
Annual growth (%) over 1986			4.3 % (+518 ha)	8.2 % (+983 ha)
Growth (%) over 2005				62.9 % (+13,743 ha)
Annual growth (%) over 2005				12.6 % (+2,749 ha)

Table 3.13. Daloa, Cote d'Ivoire - Growth of urban area.

Details	1986	1991	2000	2008
No. of pixels	30,911	35,355	36,955	51,212
Total area (in hectare, ha)	2,782	3,182	3,326	4,609
Growth (%) over 1986		14.4 % (+400 ha)	19.6 % (+544 ha)	65.7 % (+1,827 ha)
Annual growth (%) over 1986		2.9 % (+80 ha)	1.4 % (+39 ha)	3.0 % (+83 ha)
Growth (%) over 1991			4.5 % (+144 ha)	44.9 % (+1,427 ha)
Annual growth (%) over 1991			0.5 % (+16 ha)	2.6 % (+84 ha)
Growth (%) over 2000				38.6 % (+1,283 ha)
Annual growth (%) over 2000				4.8 % (+160 ha)

Table 3.14. Abuja, Nigeria - Growth of urban area.

Details	1986	1990	2001	2005
No. of pixels	47,309	80,274	176,273	211,137
Total area (in hectare)	4,258	7,225	15,865	19,002
Growth (%) over 1986		69.7 % (+2,967 ha)	272.6 % (+11,607 ha)	346.3 % (+14,745 ha)
Annual growth (%) over 1986		17.4 % (+742 ha)	18.2 % (+774 ha)	18.2 % (+776 ha)
Growth (%) over 1990			119.6 (+8,640 ha)	163.0 % (+11,778 ha)
Annual growth (%) over 1990			10.9 % (+785 ha)	10.9 % (+785 ha)
Growth (%) over 2001				19.8% (+3,138 ha)
Annual growth (%) over 2001				4.9% (+784 ha)

Table 3.15. Kindia, Guinea - Growth of urban area.

Details	1990	1995	2005	2010
No. of pixels	13,927	30,235	44,748	62,282
Total area (in hectare)	1,253	2,721	4,027	5,605
Growth (%) over 1990		117.3 % (+1,468 ha)	221.3 % (+2,774 ha)	347.3 % (+4,352 ha)
Annual growth (%) over 1990		29.3 % (+367 ha)	14.8 % (+185 ha)	17.36 % (+229 ha)
Growth (%) over 1995			48 % (+1,306 ha)	106 % (+2884 ha)
Annual growth (%) over 1995			4.4 % (+119 ha)	7.1 % (+192ha)
Growth (%) over 2005				39.2 % (+1,578 ha)
Annual growth (%) over 2005				9.8 % (+395 ha)

Table 3.16. Ouagadougou, Burkina Faso - Growth of urban area.

Details	1975	1986	2005	2010
No. of pixels	89,008	131,792	226,764	261,097
Total area (in hectare)	8,011	11,861	20,409	23,499
Growth (%) over 1975		48.1 % (+3,851 ha)	154.8 % (+12,398 ha)	193.3 % (+15,488 ha)
Annual growth (%) over 1975		4.4 % (+350 ha)	5.2 % (+413 ha)	5.5 % (+443 ha)
Growth (%) over 1986			72.1 % (+8,547 ha)	98.1 % (+11,637 ha)
Annual growth (%) over 1986			3.8 % (+450 ha)	4.1 % (+485 ha)
Growth (%) over 2005				15.1 % (+3,090 ha)
Annual growth (%) over 2005				3.0 % (+618 ha)

Table 3.17. Kano, Nigeria - Growth of urban area.

Details	1975	1985	2000	2010
No. of pixels	63,809	124,102	137,791	182,932
Total area (in hectare)	5,743	11,169	12,401	16,464
Growth (%) over 1975		94.5 % (+5,426 ha)	115.9 % (+6,658 ha)	186.7 % (+10,721 ha)
Annual growth (%) over 1975		9.4 % (+543 ha)	4.6 % (+266 ha)	5.3 % (+306 ha)
Growth (%) over 1985			11.0 % (+1,232 ha)	47.4 % (+5,295 ha)
Annual growth (%) over 1985			0.7 % (+82 ha)	1.9 % (+212 ha)
Growth (%) over 2000				32.8 % (+4,063 ha)
Annual growth (%) over 2000				3.3 % (+406 ha)

The physical growth of the urban area is consistently high for Kumasi. In Abuja, Kindia and Ouagadougou urban growth can be observed during the past four decades, but the rate of growth has gradually decreased since the late 1970s or early 1980s. In Daloa and Kano, urban growth has not been consistent over the past four decades. During some time periods, the growth is very high which decreased for some time, and started to increase in recent times. Conversion of non-urban to urban is inevitable as the population grow in the cities creating a demand for more services such as transportation, housing and industries. Such infrastructures development are changing the urban land area.

When we compare the growth of the urban land use with the population growth in the selected cities (Table 3.1) we have mixed trends. The city of Kumasi, Daloa, Kindia and Kano's urban land area grew quicker than the population growth. For example, the city of Kumasi's urban land area grew by 12.6% annually while its population grew by 6.3% for circa 2010. In contrast, Abuja and Ouagadougou physical growth were outpaced by the population growth. Abuja saw a surge in its population by about 16% (for 2000-2010) while its area grew only by 4.5% (2001-2005) annually.

Discussion

At the global scale, there are at least ten different land cover datasets which can be used to identify urban areas. But it is difficult to pick one dataset over the others as the total urban land area among the datasets varies widely (Potere et al., 2009). Also, very few datasets are available for multiple years to study the growth of urban land use in an area. In addition, the resolution of global datasets varies from 300 m to 1000 m

(Gong et al., 2013) making their usefulness limited for subnational and national level studies. Recently, Gong et al. (2013) have created a global land cover map at 30 m × 30 m resolution using Landsat TM/ETM+ images. Most of the Landsat images used in Gong et al. (2013) were from circa 2010.

Gong et al. (2013) land cover data has an overall accuracy of about 65%. However, the user's and producer's accuracies for the impervious surface, which includes urban areas, are 31% and 11%, respectively. This new dataset drastically underestimates urban land area in West Africa. For example, for the city of Kindia Gong et al. (2013) estimates the area of impervious surface to be around one two thousandth of the area obtained here in this study. Big cities such as Abuja and Kano, were also underestimated in the order of one-fifth to one-seventh. This shows limitation of image classification techniques adopted for a large global scale mapping to identify urban land use at a subnational level.

The Lincoln Institute of Land Policy has prepared an Atlas of Urban Expansion which contains map of 120 cities around the world for two time periods: circa 1990 and 2000 using Landsat MSS and TM/ETM+ images. Only five cities in the Atlas are from West Africa (Angle et al., 2011). Ouagadougou was the only city which was part of our study as well. We found that the urban land area in Ouagadougou was about 6,660 and 14,940 hectares in circa 1990 and circa 2000 respectively. The urban land use area in the Atlas is comparable with our results, which is about 11,900 (for 1986) and 23,500 hectares (for 2010).

Ade and Afolabi (2013) mapped the city of Abuja in Nigeria for three years; 1987, 1999 and 2007. According to this study the built up area grew from 7,875 to

14,722 hectares for the period 1987-1999. In 2007, the built up area was found to be about 41,622 hectares. We found that the urban land use area in Abuja was d 4,260 and 15,870 hectares for 1986 and 2001 respectively. But for the year 2005 our estimation was almost 50% less than the results obtained by Ade and Afolabi (2013) for 2007, demonstrating the inconsistencies of image classification methods to estimate the urban land use.

Attua and Fisher (2010) studied the urban land cover change in New Juaben municipality of Ghana, which is located 160 Km South East of Kumasi. The municipality grew by 35% from 1985-to 2003, with the majority of growth in peri-urban areas. This rate is about 2% per annum compared to 4% we obtained for the city of Kumasi for around the same time period.

The long term average annual physical growth in the six cities is about 9.5%, which is about 4% for a sample of 30 cities used in Angel et al. (2011) study. The physical growth could be attributed to the growth in the population. But we find that the growth in physical area and population manifested differently in six cities. The city of Kumasi, Daloa, Kindia and Kano have more growth in their urban land area while Abuja and Ouagadougou have more growth in their population. The result from Abuja and Ouagadougou contrasts the result obtained from the sample of 120 cities, where the growth of urban land used outpaced the population growth (Angel et al., 2011).

The urban land use maps prepared in this study show that for the past four decades the cities in the region have experienced extensive transformations. The city centers were infilling and the fringes around the core city area were transforming to urban landscape. Another major feature of the growth was expansion along the major

transportation corridors and some pockets along the road network. This pattern of the growth looks similar to the urban growth reported from other cities in Africa (Abebe, 2013; Olayiwola and Igbavboa, 2014; Ade and Afolabi, 2013) but the rate of growth in urban land use varies among the cities in the same eco-region or country.

Conclusions

Despite many shortcomings of remote sensing data either in terms of spectral quality and atmospheric effects or sub-pixel mixing within the urban space (Potere et al. 2009, Strahler et al. 2006) we mapped the urban land use in six cities of West Africa from early 1970s to 2010 with fair accuracy. The uniqueness of a geographical area to map using remote sensing data is also evident in the study. For example, the NDVI threshold applied in this study to improve the spectral separability of different land cover types has different ranges for different Landsat images used in this study. This variability in NDVI threshold also depends on the season at which the images were captured. So, the same threshold for a particular land cover class across the different Landsat images to map urban area could not be used.

In some of the cities, our estimations were comparable to other studies as discussed in the previous section. We observed that the physical growth of the city is happening but the rate of such growth varies in the study area. At the same time, the rate of population rise and physical growth of the cities do not match proportionally indicating likely changes in the intensity of urban land use. Such changes in the intensity of urban land use can be studied using finer resolution remote sensing images. Finer resolution data will also help improve the understanding the impacts of urban land

use on the urban ecosystem, urban heat islands and microclimate, and urban landscape pattern (Jansen et al. 2004; Du et al., 2014; Meinel et al 2001).

Literature cited

Abebe, G. A. (2013). Quantifying urban growth pattern in developing countries using remote sensing and spatial metrics: A case study in Kampala, Uganda, A Master Thesis, Faculty of geo-Information Science and Earth Observation of University of Twente, The Netherlands, available online from http://www.itc.nl/library/papers_2013/msc/upm/abebe.pdf accessed on July 2015.

Ade, M. A., and Y.D. Afolabi (2013). Monitoring urban sprawl in the Federal Capital Territory of Nigeria using remote sensing and GIS techniques, *Ethiopian Journal of Environmental Studies and Management, 6*(1), 82-95

Alberti, M. (2005). The effects of urban patterns on ecosystem function, *International Regional Science Review* 28(2): 168-192.

Angel, S., J. Parent, D. L. Civco and A. M. Blei, (2010). Atlas of Urban Expansion, Cambridge MA: Lincoln Institute of Land Policy, online at http://www.lincolninst.edu/subcenters/atlas-urban-expansion/ accessed on January 2016

Attua, E. M. and J. B. Fisher (2011). Historical and future land-cover change in a municipality of Ghana. *Earth Interactions* 15.

Bauer, M. E., N. J. Heinert, et al. (2004). *Impervious surface mapping and change monitoring using Landsat remote sensing*. ASPRS annual conference proceedings, Denver, Colorado.

Brinkmann, K., J. Schumacher, et al. (2012). Analysis of landscape transformation processes in and around four West African cities over the last 50 years. *Landscape and Urban Planning* 105(1–2): 94-105.

Center for International Earth Science Information Network - CIESIN - Columbia University, and Information Technology Outreach Services - ITOS - University of Georgia (2013). Global Roads Open Access Data Set, Version 1 (gROADSv1).

Palisades, NY: NASA Socioeconomic Data and Applications Center (SEDAC). http://dx.doi.org/10.7927/H4VD6WCT. Accessed on August-September 2014.

Chen, J., X. Zhu, et al. (2011). A simple and effective method for filling gaps in Landsat ETM+ SLC-off images. *Remote Sensing of Environment* 115(4): 1053-1064.

Cui, L and J Shi (2012). Urbanization and its environmental effects in Shanghai, China. *Urban Climate* 2: 1-15.

Dawson, RJ, J W Hall, S L Barr, M Batty, A L Bristow, S Carney, A Dagoumas, S Evans, A Ford, H Harwatt, J Köhler, M R Tight, C LWalsh, and A M Zanni (2009). A blueprint for the integrated assessment of climate change in cities. Tyndall Working Paper 129, pp. 26.

de Berg, M., M. van Kreveld, M. Overmars, and O. Schwarzkopf (2002). Delaunay triangulations in *Computational Geometry: Algorithms and Applications*, 183-210.

DESA/UN (2011) Population Distribution, Urbanization, Internal Migration and Development: An International Perspective, Department of Economic and Social Affairs, Population Division of the United Nations available from www.unpopulation.org.

Du, P., et al. (2014) Remote Sensing Image Interpretation for Urban Environment Analysis: Methods, System and Examples. *Remote Sensing* **6**(10): 9458.

Fan, F., and W. Fan (2014). Understanding spatial-temporal urban expansion pattern (1990–2009) using impervious surface data and landscape indexes: a case study in Guangzhou (China), *Journal of Applied Remote Sensing*, *8*(1), 083609-083609.

Forkuor, G. and O. Cofie (2011) Dynamics of land-use and land-cover change in Freetown, Sierra Leone and its effects on urban and peri-urban agriculture–a remote sensing approach, *International Journal of Remote Sensing* 32(4): 1017-1037.

Gillies, R. R., J. Brim Box, et al. (2003) Effects of urbanization on the aquatic fauna of the Line Creek watershed, Atlanta—a satellite perspective, *Remote Sensing of Environment* 86(3): 411-422.

Google Earth Help https://support.google.com/earth/

Herold M and D A Roberts (2010) The Spectral Dimension in Urban Remote Sensing in T. Rashed and C. Jürgens (eds.), Remote Sensing of Urban and Suburban Areas, *Remote Sensing and Digital Image Processing* 10, DOI 10.1007/978-1-4020-4385-7_4

Hope T (1942) Process of Urbanization, *Social Forces*, Vol. 20 (3), Pp311-316, available from http://heinonline.org accessed on February 2014

Hu, X. and Q. Weng (2009) Estimating impervious surfaces from medium spatial resolution imagery using the self-organizing map and multi-layer perceptron neural networks, *Remote Sensing of Environment* 113(10): 2089-2102.

Irish, R. R., J. L. Barker, et al. (2006) Characterization of the Landsat-7 ETM+ automated cloud-cover assessment (ACCA) algorithm, *Photogrammetric Engineering and Remote Sensing* 72(10): 1179-1188.

Jansen J R (2007). Remote sensing of the environment: An earth resource perspective, Upper Saddle River, N.J., Prentice Hall.

Jansen J.R. (2005) Introductory digital image processing: a remote sensing perspective (3rd ed.), Upper Saddle River, N.J., Prentice Hall.

Kalnay, E. and M. Cai (2003) Impact of urbanization and land-use change on climate, *Nature* 423(6939): 528-531.

Kamh, S., M. Ashmawy, et al. (2012) Evaluating urban land cover change in the Hurghada area, Egypt, by using GIS and remote sensing, *International Journal of Remote Sensing* 33(1): 41-68.

Karnieli, A., Agam, N., Pinker, R. T., Anderson, M., Imhoff, M. L., Gutman, G. G., et al. (2010). Use of NDVI and land surface temperature for drought assessment: merits and limitations, *Journal of Climate, 23*(3), 618-633

Karolien, V., V.R. Anton, L. Maarten, S. Eria, M. Pau (2012). Urban growth of Kampala, Uganda: Pattern analysis and scenario development, *Landscape and Urban Planning* **106**(2): 199-206.

Knorn, J., Rabe, A., Radeloff, V. C., Kuemmerle, T., Kozak, J., & Hostert, P. (2009) Land cover mapping of large areas using chain classification of neighboring Landsat satellite images. *Remote Sensing of Environment*, *113*(5), 957-964.

Lambin, E. F., B. L. Turner, et al. (2001). The causes of land-use and land-cover change: moving beyond the myths, *Global Environmental Change* 11(4): 261-269.

Lee, D. T. and B.J. Schachter (1980) Two Algorithms for Constructing a Delaunay Triangulation, *International Journal of Computer and Information Sciences*, Vol. 9, No. 3, 1980

Lee, S. and R. G. Lathrop (2005) Sub-pixel estimation of urban land cover components with linear mixture model analysis and Landsat Thematic Mapper imagery. *International Journal of Remote Sensing* 26(22): 4885-4905.

Lillesand T M, R W Kiefer and J W Chipman (2006) Remote sensing and image interpretation, 4th ed., John Wiley and Sons, New York.

Linard, C., A. J. Tatem, et al. (2013) Modelling spatial patterns of urban growth in Africa, *Applied Geography* 44: 23-32.

Liu, Y. S., J. Y. Wang, et al. (2010) Analysis of arable land loss and its impact on rural sustainability in Southern Jiangsu Province of China, *Journal of Environmental Management* 91(3): 646-653.

Lu, D. and Q. Weng (2005). Urban classification using full spectral information of Landsat ETM+ imagery in Marion County, Indiana, *Photogrammetric Engineering & Remote Sensing* 71(11): 1275-1284.

Lu, D. and Q. Weng (2006). Use of impervious surface in urban land-use classification. *Remote Sensing of Environment* 102(1-2): 146-160.

Luck, M., & Wu, J. (2002). A gradient analysis of urban landscape pattern: a case study from the Phoenix metropolitan region, Arizona, USA. *Landscape ecology*, *17*(4), 327-339.

Marcotullio, P. J. and W. Solecki (2013). What is a city? An essential definition for sustainability. *Urbanization and Sustainability*, Springer: 11-25.

Masek, J., F. Lindsay, et al. (2000). Dynamics of urban growth in the Washington DC metropolitan area, 1973-1996, from Landsat observations, *International Journal of Remote Sensing* 21(18): 3473-3486.

Masek, J.G., E.F. Vermote, N. Saleous, R. Wolfe, F.G. Hall, F. Huemmrich, F. Gao, J. Kutler, and T.K. Lim. 2013. LEDAPS Calibration, Reflectance, Atmospheric Correction Preprocessing Code, Version 2. Model product. Available on-line [http://daac.ornl.gov] from Oak Ridge National Laboratory Distributed Active Archive Center, Oak Ridge, Tennessee, U.S.A. http://dx.doi.org/10.3334/ORNLDAAC/1146

McDonnell, M J and S T Pickett (1990). Ecosystem structure and function along urban-rural gradients: an unexploited opportunity for ecology, *Ecology:* 1232-1237.

Meinel, G., Neubert, M., & Reder, J. (2001). The potential use of very high resolution satellite data for urban areas—First experiences with IKONOS data, their classification and application in urban planning and environmental monitoring. *Regensburger Geographische Schriften*, *35*, 196-205.

Mohapatra R., C. Wu (2008) Subpixel Imperviousness Estimation with IKONOS Imagery: an Artificial Neural Network Approach., Taylor & Francis Group , London, UK.

Mundia, C. and M. Aniya (2005) Analysis of land use/cover changes and urban expansion of Nairobi city using remote sensing and GIS, *International Journal of Remote Sensing* 26(13): 2831-2849.

Olayiwola, A. M. and O.E. Igbavboa (2014). Land Use Dynamics and Expansion of the Built-Up Area in Benin City, Nigeria, *Mediterranean Journal of Social Sciences*, *5*(20), 2506

Olson, D. M., E. Dinerstein, et al. (2001) Terrestrial Ecoregions of the World: A New Map of Life on Earth: A new global map of terrestrial ecoregions provides an innovative tool for conserving biodiversity, *Bio-Science* 51(11): 933-938.

Otukei, J. and T. Blaschke (2010). Land cover change assessment using decision trees, support vector machines and maximum likelihood classification algorithms, *International Journal of Applied Earth Observation and Geo-information* 12: S27-S31.

Posa, M. R. C. and N. S. Sodhi (2006). Effects of anthropogenic land use on forest birds and butterflies in Subic Bay, Philippines, *Biological Conservation* 129(2): 256-270.

Potere, D. (2008). Horizontal positional accuracy of Google Earth's high-resolution imagery archive, *Sensors*, 8(12), 7973-7981.

Rashed, T. et al. (2001). Revealing the anatomy of cities through spectral mixture analysis of multispectral satellite imagery: a case study of the Greater Cairo region, Egypt, *Geocarto Int.* 16, (4), Pp 7 –18.

Richards J. A. (2013). Remote Sensing Digital Image Analysis: An Introduction, Springer

Rodríguez, J. and G. Martine (2008) Urbanization in Latin America and the Caribbean: experiences and lessons learned. *The New Global Frontier: Urbanization, Poverty and Environment in the 21st Century*: 353-367.

Sadler, J., E. Small, et al. (2006) Investigating environmental variation and landscape characteristics of an urban–rural gradient using woodland carabid assemblages, *Journal of Biogeography* 33(6): 1126-1138.

Satterthwaite, D., G. McGranahan, et al. (2010). Urbanization and its implications for food and farming, *Philosophical Transactions of the Royal Society B: Biological Sciences* 365(1554): 2809-2820.

Seto, K C, M Fragkias, B Güneralp, and M K Reilly (2011). A meta-analysis of global urban land expansion, *PLoS ONE*, 6 (8), e23777.

Seto, K C, S Parnell, et al. (2013). A Global Outlook on Urbanization. *Urbanization, Biodiversity and Ecosystem Services: Challenges and Opportunities*, in Urbanization, Biodiversity and Ecosystem Services: Challenges and Opportunities: A Global Assessment, T. Elmqvist et al. (eds.), DOI 10.1007/978-94-007-7088-1_1, Springer 9-12

Strahler, A, L. Boschetti, G. Foody, M. Friedl, M. Hansen, M. Herold, P. Mayaux, J. Morisette, S. Stehman, and C. E. Woodcock, Global Land Cover Validation: Recommendations for Evaluation and Accuracy Assessment of Global Land Cover Maps. GOFC-GOLD Report No. 25, 2006.

Thapa, R. B. and Y. Murayama (2009). Examining spatiotemporal urbanization patterns in Kathmandu Valley, Nepal: Remote sensing and spatial metrics approaches, *Remote Sensing* 1(3): 534-556.

Tian, G., J. Jiang, et al. (2011). The urban growth, size distribution and spatio-temporal dynamic pattern of the Yangtze River Delta megalopolitan region, China, *Ecological Modelling* 222(3): 865-878.

UN-Habitat (2014). The State of African Cities 2014: Re-imagining sustainable urban transitions, United Nations Human Settlements Program, available online http://unhabitat.org/books/state-of-african-cities-2014-re-imagining-sustainable-urban-transitions/

Vermote, E., N. El Saleous, et al. (1997). Atmospheric correction of visible to middle-infrared EOS-MODIS data over land surfaces: Background, operational algorithm and validation, *Journal of Geophysical Research: Atmospheres (1984–2012)* 102(D14): 17131-17141.

Wania, A., T. Kemper, et al. (2014). Mapping recent built-up area changes in the city of Harare with high resolution satellite imagery, *Applied Geography* 46: 35-44.

Weng, Q. (2012). Remote sensing of impervious surfaces in the urban areas: Requirements, methods, and trends, *Remote Sensing of Environment* 117(0): 34-49.

Wu, C. S. (2009). Quantifying high-resolution impervious surfaces using spectral mixture analysis, *International Journal of Remote Sensing* 30(11): 2915-2932.

Wu, Y., X. Zhang, et al. (2011). The impact of urbanization policy on land use change: A scenario analysis, *Cities* 28(2): 147-159.

Xian, G. and M. Crane (2005). Assessments of urban growth in the Tampa Bay watershed using remote sensing data, *Remote Sensing of Environment* 97(2): 203-215.

Yang, L. M., C. Q. Huang, et al. (2003). An approach for mapping large-area impervious surfaces: synergistic use of Landsat-7 ETM+ and high spatial resolution imagery, *Canadian Journal of Remote Sensing* 29(2): 230-240.

Yeboah, I. E. A. (2000). Structural adjustment and emerging urban form in Accra, Ghana, *Africa Today* 47(2): 61-89.

Yeboah, I. E. A. (2003) Demographic and housing aspects of structural adjustment and emerging urban form in Accra, Ghana, *Africa Today* 50(1): 107-119.

Websites:

Earth Resources Observation and Science Center (EROS) (http://glovis.usgs.gov/) January 2014- July 2015

City population http://www.citypopulation.de

Chapter 4: Identifying and Analyzing Factors of Urban Growth in West African Cities

Pradeep Adhikari

Kirsten M. de Beurs

Department of Geography and Environmental Sustainability

University of Oklahoma, Norman, OK 73019

(To be submitted to the journal of Urban Ecosystems)

Abstract: The urban land use system is a complex system. Understanding the growth of the city's land use system is an important task to devise a plan for sustainable urban development. In this study, we identified that Normalized Difference Vegetation Index (NDVI) and distance to the urban area showed strong associations with the growth of six cities in West Africa. The six cities include Kumasi, Daloa, Abuja, Kindia, Ouagadougou, and Kano. We found that none of the factors showed a consistent association with urban land use. Out of the six cities, Ouagadougou and Kano showed some level of agreement in associating the urban growth with NDVI at different time periods. In the rest of the cities, proximity parameters such as distance to the nearest urban area and distance to the core city area showed some level of association to urban growth.

Key words: Urban land use; West Africa; Logistic Regression; NDVI; Urban pixel.

Introduction

The global share of urban land use is estimated to be in the range of 1% to 6% of the Earth's surface (UNEP-IRP, 2013; Gong et al. 2013; Alberti et al., 2013; Lambin et

al. 2001). Although the share of urban land use is small, the ecological footprint of such land use is large (Alberti et al. 2003). The ecological footprint is large for urban land use because urban area expansion causes extensive alteration of the landscape (McDonnell and Pickett 1990). Losses of arable lands and increased imperviousness surface area (Arnold and Gibbons, 1996; Tian et al., 2011; Eppler et al., 2015; UN-Habitat 2014) are some aspects of this alteration. These types of alterations directly impact the geomorphology and hydrology of the landscape ultimately affecting its ecosystem dynamics in urban areas (Alberti et al. 2003). A comprehensive and multidisciplinary approach understanding urban expansion processes (Veldkamp and Lambin, 2001) is a precondition to devise a sustainable urban development plan.

One way to analyze the effect of urban area expansion or the conversion of non-urban to urban land use is the use of simulation and empirical models. Several simulation and empirical models have been developed to study the land use dynamics including urban land use system (EPA, 2000; Briassoulis, 2000; Agarwal et al., 2001). A review of the literature shows four broad categories of land use change models: a) statistical and empirical models, b) spatial interaction models, c) optimization models, and d) integrated models (Briassoulis, 2000; Agarwal et al., 2002; Cheng and Masser, 2003; Robinson et al., 2006). The use of particular type of model depends on the scope, scale and extent of analysis (Agarwal et al., 2002).

Statistical and empirical models derive a mathematical relationship between the dependent (also called response variable) and independent variables (also called predictor or explanatory variables) based on historical data (Hu and Lo, 2007). Empirical models such as logistic regression models have been used in the study of

urban growth, agriculture, deforestation, invasive species and landslide susceptibility mapping (EPA, 2000; Agarwal et al., 2001; Geoghegan et al., 2001; Schneider and Pontius, 2001; Serneels and Lambin, 2001; Walsh et al., 2001; Allen and Lu, 2003; Cheng and Masser, 2003; Zhu and Huang, 2006; Hu and Lo, 2007; Aguayo et al., 2007). The advantage of logistic models is that they identify the influence of independent variables and also provide a degree of confidence regarding their contribution to the dependent variable (Hu and Lo, 2007; Irwin and Geoghegan, 2001). Furthermore, logistic regression models are data driven and do not need intensive computational capabilities (Hu and Lo, 2007). Therefore, the objectives of this study are to model and quantify the probability of urban land use growth with a set causative factors that include environmental and social variables. Furthermore, we analyze whether or not causative factors identified for the cities of the same eco-region or country show a similar level of association to urban growth.

Materials and methods

Study area

The study area covers six cities from five countries and three eco-regions (Olson et al., 2001) of West Africa (Fig. 4.1). The countries in West Africa are located along a climatic gradient from the Sahel region in the north to the Guineo-Congolese zone in the south (FAO, 2001). The general climate in the region is dictated by the tropical continental air mass, dry and dusty from the Sahara Desert and another mass of tropical maritime air, warm and humid from the south Atlantic forming the Inter Tropical

Convergence Zone (ITCZ). The ITCZ also dominates the annual rainfall variability in the region (AIACC, 2006).

West Africa has a population of a little over 300 million people as of 2010 and is expected to reach 570 million in 2050 and 735 million by the end of 21st century (DESA/UN 2011). The average urban population growth rate since 1950 is the second highest compared to the other regions of Africa despite the countries in the region witnessing severe droughts since the late 1970s (Druyan, 2011; Wang and Eltahir, 2000; Tarhule and Woo, 1997). The growth in urban population in SSA, in part, is credited to rural to urban migration driven by climatic variability, social, and economic factors (Barrios et al., 2006; Parnell and Walawege 2011). In a region like West Africa where the agricultural sector employs 60 percent of the active labor force as subsistence farmers (Jalloh et al. 2013), any changes in the rainfall amount or onset of rainfall trigger crop failures ultimately driving rural population to the urban area in search of jobs and improved livelihood (Barrios et al. 2006). But recent literature on rural-urban migration in West Africa shows that that the share of such migration is not an important component of the urban growth (Beauchemin, 2011).

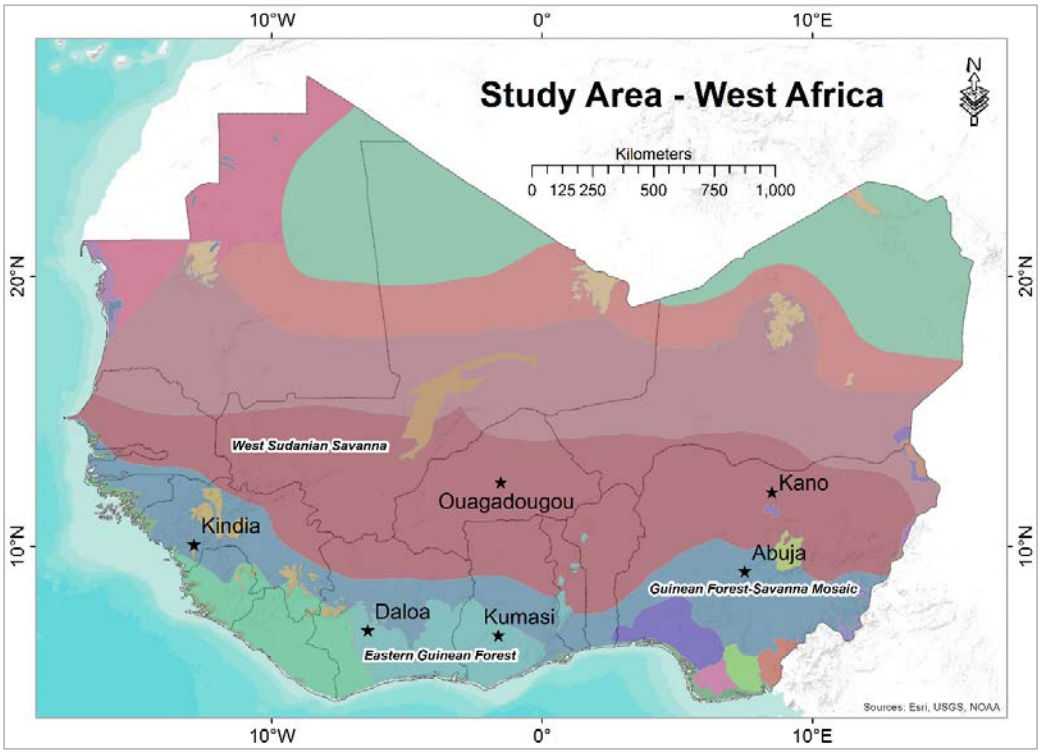

Figure 4.1. Location of six cities in West Africa.

The selected six cities are medium to large in size but fast growing cities in West Africa. They are from five different countries: Ghana, Cote d'Ivoire, Nigeria, Guinea, and Burkina Faso. The cities are selected in such a way that at least two cities are from the same three eco-regions in West Africa: Eastern Guinean Forest (EGF), Guinean Forest-Savanna Mosaic (GFM), and West Sudanian Savanna (WSS) of West Africa (Table 4.1). Although by definition an ecoregion has a relatively uniform climate and houses unique ecological communities (Olson et al. 2001), climatic parameters like annual rainfall vary (Table 4.1).

Table 4.1. Features of selected cities.

Cities	Countries	Eco-regions	Mean annual rainfall (mm, 2001-10)	Population (Year 2000, in '000)*	Population (Year 2010 in '000)*	Annual rate of pop. growth (%)
1. Kumasi	Ghana	Eastern Guinean Forest	1,146	1,187	1,935	6.3
2. Daloa	Cote d'Ivoire		1,026	185	248	3.4
3. Abuja	Nigeria	Guinean Forest-Savanna Mosaic	1,436	833	2,153	15.8
4. Kindia	Guinea		730	96	135	4.1
5. Ouagadougou	Burkina Faso	West Sudanian Savanna	812	921	1,911	10.7
6. Kano	Nigeria		712	2,602	3,271	2.6

**Sources: DESA/UN, 2011 and http://www.citypopulation.de*

To capture variability at least two cities from the same eco-region with different annual rainfall are selected for this study. In addition, as urban growth may have been affected by governmental policies (Wu et al., 2011) the selected cities capture variability that exists in the region both in terms of climate and country specific land policy. The selected cities had populations as low as 96 thousand (Kindia) to more than two million (Kano) in 2000. The population in the cities has grown substantially for the period 2000-2010. Abuja grew the most with 15.8% followed by Ouagadougou's 10.7% and Kumasi at 6.3%. Among the six cities Kano grew the least, by 2.6%.

Logistic regression

A logistic regression model is used to study the urban growth with socio-economic and environmental variables as causative factors and to generate (predict) urban growth. The model is set-up in a raster modeling environment to form a grid of cells at 30 m × 30 m spatial resolution. In this case, the nature of the urban land use of a

cell is dichotomous: either the presence or absence of urban. I used binary values to represent urban and non-urban and I assumed that the probability of a cell changing to urban follows a logistic curve (Kleinbaum and Klein, 2010):

$$f(z) = \frac{1}{1+e^{-z}} \text{ ----- (4.1)}$$

The probability of a pixel to be urbanized can be estimated with the following logistic regression model:

$$P(Y = 1|X_1, X_2, \ldots\ldots X_k) = \frac{1}{1+e^{-(\alpha+\sum_{i=1}^{k}\beta_i X_i)}} \text{ ----- (4.2)}$$

Where,

P($Y = 1|X_1, X_2, \ldots, X_k$) is the probability of the response(or dependent) variable Y being 1 given ($X_1, X_2, \ldots, X_k$), i.e. the probability of a pixel being converted to urban; X_i is an explanatory (or an independent) variable representing a causal factor for urban growth. The explanatory variables can be of interval, ordinal or categorical type variable; and β_i is the coefficient for variable X_i. The logistic regression model is implemented using IBM SPSS Statistics Software, Version 22.0.

Data

Response variable

The response variable is the urban or non-urban pixel obtained from the six city maps (Chapter 3, Figures 3.5 through 3.10). Also, the methods used to create the urban

land cover data are presented in Chapter 3 section 2.3. The years for which the urban area map are available do not match one to one in all cities (Table 4.2). I used the first available year as the base year and applied the logistic regression analysis to the remaining three year. The causative factors and their association with the conversion of non-urban to the urban pixel are compared to the following three years for each city. As the land covered data are prepared at 30m × 30m spatial resolution, a total number of pixels for each city for this analysis were close to 1 million.

Table 4.2. Cities and years for which the urban area are used in the study.

Cities/Country	Year of urban area maps
Kumasi, Ghana	1973, 1986, 2005, 2010
Daloa, Cote d'Ivoire	1986, 1991, 2000, 2008
Abuja, Nigeria	1986, 1990, 2001, 2005
Kindia, Guinea	1990, 1995, 2005, 2010
Ouagadougou, Burkina Faso	1975, 1986, 2005, 2010
Kano, Nigeria	1975, 1985, 2000, 2010

Explanatory variables

Several environmental and socio-economic factors are used as explanatory variables in the logistic model. In general, these variables alone or in combination reflect the overall physical setting of the city. An overview of all selected explanatory variables can be found in table 4.3. The details about each variable follow after the table.

Table 4.3. A list of explanatory variables used in the logistic regression model.

Explanatory Variables	Units	Explanatory Variables	Units
Elevation	Meters	NDVI, minimum (×10)	No unit
Slope	Percent	Precipitation anomaly, maximum	mm
Distance to major roads	Kilometers	Precipitation anomaly, minimum	mm
Distance to core city area	Kilometers	PDSI, maximum	No unit
Distance to nearest urban pixels	Kilometers	PDSI minimum	No unit
Distance to rivers	Kilometers	Population (total, natural growth and migrated) (in ‘000)	Individual
Distance to water bodies	Kilometers	Conflict (Categorical)	No unit
NDVI, maximum (×10)	No unit	Human Influence Index	No unit

Physical and environmental

Elevation and slope

I downloaded the Global Digital Elevation Model-GDEM (Version 2) from NASA's Earth Observing System Data and Information System. The data has a spatial resolution of 1 arc-second (~30 meters). For the logistic regression, we extracted elevation (in meters) for each pixel within a 30 Km × 30 Km city boundary. The same elevation data is used to calculate the slope as a rate of change in elevation (in percentage) for a pixel.

Distance to the major roads

Major road data was obtained from the Center for International Earth Science Information Network (CIESIN 2013). The road data is presented in polyline vector format. The Euclidean distance (in meters) to the major roads from each pixel within the city are calculated in ESRI's ArcGIS and used in the regression. As we have road data for only one time period, the same road data is used for all three years.

Distance to the core city area

Generally, the core city area in developing countries has highest population density (Suzuki et al., 2013). Therefore, the core city area was demarcated based on the population data mentioned in the subsection *Population* under *Scoio-Economic Variables (Page 118 below)*. The Euclidean distance (in meters) to the core city area from each pixels within the city is calculated in ESRI's ArcGIS.

Distance to the nearest urban pixels

Based on the urban land cover maps (e.g. 1973, 1986, 2005 and 2010 for Kumasi), the Euclidean distance to the nearest urban pixels from each pixels within the 30Km × 30Km city boundary is obtained for the year for which the land cover maps are available. For example, while making predictions for 1986, in Kumasi, we used the distance to urban pixel in 1973 as the distance to the nearest urban pixel. Similarly for 2005 we used the distance to urban pixels in 1986.

Distance to the river

I obtained river polyline data from the Unites States Geological Survey (http://hydrosheds.cr.usgs.gov/index.php). The Euclidean distance to the rivers (in meters) from each pixel within city boundary were obtained in ArcGIS. For all years the same river data used to calculate the distance to the river.

Distance to other water bodies

Data for other water bodies is obtained in vector form from the Digital Chart of the World (http://www.diva-gis.org/gdata). For each pixel, within the city boundary I calculated the Euclidean distance to the nearest water body.

Vegetation indices

The normalized difference vegetation index (NDVI) is one of the most commonly used vegetation indices (Pettorelli et al., 2005). Research has shown that NDVI can be used as a proxy for yield in semi-arid rain fed agro-ecosystems in the

developing world (Buerkert et al., 1995; Funk and Budde, 2009; Maselli et al., 2000; Rasmussen, 1998; Reynolds et al., 2000). NDVI is derived from the red and near-infrared (NIR) reflectance ratio as follows

$$\text{NDVI} = \frac{\text{NIR} - \text{RED}}{\text{NIR} + \text{RED}} - - - - - (4.3)$$

Here NIR and RED are the percentages of near-infrared and red light reflected by the vegetation and captured by satellite sensors (Karnieli et al., 2010). NDVI data was obtained from Global Inventory Modeling and Mapping Studies (GIMMS) which is a 15-day maximum value composite and available from mid of 1981 to 2012 at 8 km spatial resolution (Tucker et al. 2005). For our purpose, the maximum and minimum NDVI were extracted over the cropped areas of the country that the city belongs to. The cropland area was masked using Moderate Resolution Imaging Spectroradiometer MODIS-Type 2 land cover data for the period since 2001. For example, in the case of Abuja 2005, I used the crop mask for Nigeria using Moderate Resolution Imaging Spectroradiometer MODIS-Type 2 land cover data of 2005. For the time before 2001, we used data from other sources listed in Chapter 2 (Chapter 2, Table 2) that are closest to the year for which the urban land use data is available.

To address any time lag between a change in NDVI and movement of people to the cities a 5-year average maximum and minimum NDVI prior to the year, for which urban land use data was available, were derived. For example, to study the role of NDVI on urban growth in 2005, the average maximum and minimum NDVI for past five years (from 2000 to 2004) were obtained for the cropland area over the country the city belonged.

Now, we used the same Landsat image that was used to create the urban land use map and calculated NDVI for that year. The NDVI thus obtained was then normalized by the maximum NDVI for that year. For example, for the year 2005, we calculated NDVI for each pixels within the city boundary of 30 Km × 30 Km. Then the NDVI for 2005 was normalized. This normalized raster is then multiplied using the maximum and minimum NDVI obtained for the country cropland area as explained in previous paragraph for the city for 2005.

Precipitation anomalies

Precipitation anomaly (mm/month) data was used to investigate the impact of climatic conditions in the country during the time the city expanded. Precipitation anomaly provides a deviation (departure) in the amount of precipitation compared to a long-term average (normal). The monthly precipitation anomaly data is obtained from the Climate Anomaly Monitoring System (CAMS) of the NOAA Climate Prediction Center's. The data is available at 2.5^{o} lat/lon resolution (~280 Km × 280 Km) for the period 1979 to 2014 (Janowiak and Xie, 1999). Both the wettest and driest values during the past five years for which the urban area maps are available are used in this analysis to address the any lag between the precipitation anomaly and its likely impacts on agriculture. I resampled the precipitation anomaly data to 30m × 30m to match the urban land cover data.

Palmar Drought Severity Index

The PDSI measures the departure of the moisture supply and was developed by W.C. Palmer in 1965 (Guttman, 1998). We used PDSI as it is calculated based on precipitation, temperature, and local available water content of the soil making it better suited to represent the soil water content. Soil water content is critical for the crop growth (Shaxson and Barber, 2003) and potentially better represent the dry and wet seasons in the study area. This dataset has a spatial resolution of $2.5^{o} \times 2.5^{o}$ and is available from (http://www.cgd.ucar.edu/cas/catalog/climind/pdsi.html). The PDSI incorporates the duration of the dry or wet period and ranges in values from -10 to 10 and lag emerging droughts by several months. The value -10 indicates extreme drought while the +10 shows the wettest period. I resampled the data to 30m × 30m.

Socio-Economic Variables

Population

The global country and city level yearly population data are available from various international agencies including the World Bank, the United Nations since 1950. But most of these datasets are tabular data. There are some gridded population data, such as the one from United Nations Environment Program, but they are available at $2.5^{o} \times 2.5^{o}$ spatial resolution. A much finer gridded global population data is available since 2001 from the LandScan™ (Bright et al. 2012).

To create gridded population data, matching the urban area data for the selected cities, we used the 2012 Landscan™ data. The 2012 Landscan™ data was first resampled at 30m × 30m. Then each pixels were normalized with the total population

that fall within the city boundary of 30 Km × 30 Km. The total population data is disaggregated to naturally grown and migrated populations. We assumed that a city has the same population growth rate (World Development Indicators, data.worldbank.org) as that of the country that it belongs. Based on five year average population growth rate we first calculated the naturally grown population for each year by multiplying the normalized gridded population with the population for the year. For example, the normalized gridded data is multiplied by 397,000 to get the gridded population for 1973 in the city of Kumasi. Similarly, the normalized gridded data is multiplied by 385,527 to get the naturally grown population. Finally, migrated population was calculated by deducting naturally grown population from the total population. The disaggregated population data used in this study are presented for each city in Tables 4.4 through 4.9.

Table 4.4. Population - Kumasi, Ghana.

Population	**1972**	**1973**	**1986**	**2005**	**2010**
Total population	374,300	397,000	532,000	1,537,000	1,935,000
Annual growth rate (%)		2.89	3.00	2.60	2.38
Naturally grown population		385,527	519,087	794,663	1,734,441
Migrated population		11,473	12,913	742,337	200,559

Table 4.5. Population - Daloa, Cote d'Ivoire.

Population	**1985**	**1986**	**1991**	**2000**	**2008**
Total population	111,800	116,620	138,280	184,800	234,720
Annual growth rate (%)		4.12	3.52	2.71	1.47
Naturally grown population		116,421	120,731	142,029	187,521
Migrated population		199	17,549	42,771	47,199

Table 4.6. Population - Abuja, Nigeria.

Population	1985	1986	1990	2001	2005
Total population	204,000	229,200	330,000	929,600	1,316,000
Annual growth rate (%)		2.59	2.61	2.50	2.53
Naturally grown population		209,290	235,185	338,258	953,130
Migrated population		19,910	94,815	591,342	362,870

Table 4.7. Population - Kindia, Guinea.

Population	1989	1990	1995	2005	2010
Total population	53,255	57,148	76,611	96,074	135,000
Annual growth rate (%)		3.10	5.35	1.73	2.43
Naturally grown population		54,905	60,205	77,939	98,412
Migrated population		2,243	16,406	18,135	36,588

Table 4.8. Population - Ouagadougou, Burkina Faso.

Population	1974	1975	1986	2005	2010
Total population	68,600	157,000	446,600	1,328,000	1,911,000
Annual growth rate (%)		1.77	2.49	2.89	2.94
Naturally grown population		69,815	160,911	459,496	1,366,985
Migrated population		87,185	285,689	868,504	544,015

Table 4.9. Population - Kano, Nigeria.

Population	1974	1975	1985	2000	2010
Total population	64,300	77,000	204,000	2,602,000	3,271,000
Annual growth rate (%)		2.40	2.65	2.50	2.66
Naturally grown population		65,844	79,042	209,099	2,671,333
Migrated population		11,156	124,958	2,392,901	599,667

Security and conflict

Poor security and conflict (a war, a non-state conflict and one sided violence) especially in rural areas have been mentioned as one of the reasons of migration to the cities of Africa (Barrios et al., 2006; DESA/UN, 2011). Therefore, in this study, the security situation was used as one of the variables in the logistic regression model. A global armed conflict database (V.4-2014) is available from the Department of Peace and Conflict Research of the Uppsala University (http://www.pcr.uu.se/). This country level dataset has the information on armed conflict in a country with at least 25 battle-related deaths and at least one party is the government of a state in the time period 1946-2013 (Gleditsch et al., 2002; Themner et al., 2014). Based on this data, a value of "1" was assigned to the city data if the country it belongs to had a record of a conflict during the time period of urban growth; otherwise a value of "0" was assigned.

Human Influence Index

The Global Human Influence Index is a global dataset, available at 1Km spatial resolution which indicates the human impact on earth's land use. It is based on nine global data sets covering human population pressure, human land use and infrastructure,

and human access (WCS and CIESIN, 2005). This data was released in 2005 and covers the period from 1995-2004. Therefore, this data was used as a response variable only in or after 2005 prediction.

Once the data were compiled for all cities, they were tested for multicollinearity. As expected two groups: one of maximum and minimum NDVI, and the other of the total population, naturally grown and migrated population are found to be highly correlated (CC > 0.9). So, only one of such highly correlated variables is used in the model at a time. While implementing the model, explanatory variables were added one by one and also in combinations and the performance of the models was noted against model's capability to correctly predict the urban pixels (i.e. the response variable) with pseudo R^2 (Nagelkerke R^2) values.

Results

The results from the multiple runs of logistic regression for each city are presented in the tables below (Tables 4.10a-c through 4.15a-c). Explanatory variables which failed to predict the conversion of urban land use ($p > 0.05$) are not included in the table. The variables that are not reported include both elevation and slope, precipitation anomaly, PDSI, and conflict. Also, we did not find a difference between disaggregated population data as explanatory variables. So, we used only total population as an explanatory variable. Furthermore, if an explanatory variable has odd ratio of 1, we dropped the variable in the regression model as the variable could predict urban and non-urban area equally (Onlinecourses.science.psu.edu).

As expected, we observed total population playing a role in predicting urban land use. But the accuracy level of prediction varied both within the city, at different time steps, and across the cities. For example, in the case of Kumasi, total population alone predicted 28% urban land use in 1986 but it failed to predict urban area in 2010. Daloa which is located in the same eco-region—Eastern Guinean Forest—as Kumasi, total population predicted 43% urban land use correctly in 2008 (Table 4.11c). But in 2005 and 2010 NDVI predicted as high as 65% in 2005 and 88% in 2010 correctly in Kumasi (Table 4.10b and 4.10c).

In Abuja and Kindia, both of which falls on Guinean Forest-Savanna Mosaic eco-region, total population can predict much less urban land use compared to the city of Kumasi and Daloa. In the case of Abuja, population predicted 19% (1990) to 44% (2005) of urban land use correctly. Whereas NDVI alone predicted 23% in 2005 (Table 4.12c) to 60% in 2001 (Table 4.12b) urban area correctly. Furthermore, the distance to the urban area is an important parameter that could predict 63 % urban area in 2001 (Table 4.12b) while it could predict 91% urban land use correctly in 2005 (Table 4.12c). The city of Kindia had been the one of the least affected cities in the group by total population, only about 5%, in 2008 (Table 4.13b) urban land use was predicted accurately. In 2005 none of the parameters correctly predicted the urban land use in Kumasi.

In contrast to the cities reported earlier, the city of Ouagadougou and Kano, from the West Sudanian Savanna eco-region, have some commonalities. In both cities, population growth alone predicted of 21% (Kano in 1985, Table 4.15a) to 38% (Ouagadougou in 2010, Table 4.14c) of urban land use. The population size of these

cities in 2010 is also very similar, about 2 million and a little about 3 million for Ouagadougou and Kano respectively. In 2010, distance to the urban area alone predicted 90- 94 % of the urban land use in Ouagadougou and Kano (Tables 4.15c and 4.14c). Whereas NDVI predicted 62% of urban land use in Kano in 1985 (Table 4.15a) whereas it predicted about 21% urban land use in Ouagadougou in 1986 (Table 4.14a).

We observed that the explanatory variables —as well as their degree of impacts on urban land use conversion—are not consistent for different time periods even for the city. Distance to urban area, distance to the core city area, population growth and NDVI are the most common factors affecting the urban growth across all cities. But the scale of impacts vary at different time periods within a city. Two of the largest cities in the group, the city of Ouagadougou and Kano, reveal— distance to the urban area—predict 90%-94% urban land use correctly. Furthermore, we observed that total population growth increased the odds of urban land conversion while the distance to the city area and NDVI decreased the odds of urban land conversion.

Table 4.10a. Kumasi - Odds ratios and R^2 to predict urban pixels for 1986.

Explanatory Variables (Significant at 0.05)	Correctly predicted pixels (%)	Nagelkerke R^2	Odds ratios
Distance to core city area	41.4	0.37	0.665
NDVI, maximum	16.0	0.18	0.526
NDVI, minimum	20.2	0.17	0.001
Population, natural growth	28.3	0.30	1.002
Population, migrated	28.3	0.30	1.002
Population, total	28.3	0.30	1.001
Distance to core city area +Distance to nearest urban pixels	52.1	0.45	0.793 0.162
Distance to core city area +Distance to nearest urban pixels + NDVI maximum	48.2	0.46	0.832 0.171 0.810
Distance to core city area +Distance to nearest urban pixels + NDVI minimum	48.6	0.46	0.830 0.171 0.116

Table 4.10b. Kumasi - Odds ratios and R^2 to predict urban pixels for 2005.

Explanatory Variables (Significant at 0.05)	Correctly predicted pixels (%)	Nagelkerke R^2	Odds ratios
NDVI, maximum	65.2	0.57	0.147
Distance to core city area +Distance to nearest urban pixels	63.2	0.55	0.778 0.003
Distance to core city area +Distance to nearest urban pixels + NDVI maximum	71.4	0.66	0.982 0.006 0.227

Table 4.10c. Kumasi - Odds ratios and R^2 to predict urban pixels for 2010.

Explanatory Variables (Significant at 0.05)	Correctly predicted pixels (%)	Nagelkerke R^2	Odds ratios
Human Influence Index	66.6	0.43	1.142
NDVI, maximum	88.2	0.79	0.127
NDVI, minimum	85.3	0.76	0.001
Distance to core city area	69.1	0.46	0.648
Distance to nearest urban pixels	86.8	0.61	0.001
Distance to core city area + NDVI maximum	88.2	0.81	0.834 0.149

Table 4.11a. Daloa - Odds ratios and R^2 to predict urban pixels for 1985.

Explanatory Variables (Significant at 0.05)	Correctly predicted urban pixels (%)	Nagelkerke R^2	Odds ratios
NDVI, maximum	58.3	0.60	0.066
NDVI, minimum	58.0	0.58	0.001
Population, Total	33.8	0.39	1.002
NDVI, maximum + Population, Total	60.6	0.61	0.001 1.001
Distance to nearest urban pixels	87.4	0.72	0.963

Table 4.11b. Daloa - Odds ratios and R^2 to predict urban pixels for 2000.

Explanatory Variables (Significant at 0.05)	Correctly predicted urban pixels (%)	Nagelkerke R^2	Odds ratios
Population, total	37.5	0.42	1.002
Distance to nearest urban pixels	95.7	0.92	0.847
NDVI, maximum	60.5	0.61	0.060
NDVI, minimum	57.2	0.59	0.001

Table 4.11c. Daloa - Odds ratios and R^2 to predict urban pixels for 2008.

Explanatory Variables (Significant at 0.05)	Correctly predicted urban pixels (%)	Nagelkerke R^2	Odds ratios
Human Influence Index	1.6	0.24	1.125
Population, total	42.8	0.45	1.002
NDVI, maximum	66.7	0.66	0.053
NDVI, minimum	68.2	0.66	0.001
Distance to nearest urban pixels	80.8	0.64	0.983
Distance to nearest urban pixels + NDVI, maximum	76.0	0.80	0.989 0.117
Distance to nearest urban pixels + Population Total	62.3	0.71	0.987 1.001

Table 4.12a. Abuja - Odds ratios and R^2 to predict urban pixels for 1990.

Explanatory Variables (Significant at 0.05)	Correctly predicted urban pixels (%)	Nagelkerke R^2	Odds ratios
NDVI, maximum	41.3	0.44	0.135
NDVI, minimum	46.3	0.44	0.001
Population, Total	19.3	0.29	1.001

Table 4.12b. Abuja - Odds ratios and R^2 to predict urban pixels for 2001.

Explanatory Variables (Significant at 0.05)	Correctly predicted urban pixels (%)	Nagelkerke R^2	Odds ratio
Population, total	42.1	0.36	1.002
Distance to nearest urban pixels	62.9	0.49	0.996
NDVI, maximum	47.9	0.44	0.065
NDVI, minimum	59.5	0.43	0.001

Table 4.12c. Abuja - Odds ratios and R^2 to predict urban pixels for 2005.

Explanatory Variables (Significant at 0.05)	Correctly predicted urban pixels (%)	Nagelkerke R^2	Odds ratio
Human Influence Index	30.1	0.43	1.110
Population, total	44.1	0.34	1.001
NDVI, maximum	23.4	0.27	0.127
NDVI, minimum	24.1	0.26	0.001
Distance to nearest urban pixels	90.7	0.64	0.985

Table 4.13a. Kindia - Odds ratios and R^2 to predict urban pixels for 1995.

Explanatory Variables (Significant at 0.05)	Correctly predicted urban pixels (%)	Nagelkerke R^2	Odds ratio
NDVI, maximum	0.1	0.21	0.243
NDVI, minimum	0.1	0.21	0.002
Distance to nearest urban pixels	100	1.00	0.001

Table 4.13b. Kindia - Odds ratios and R^2 to predict urban pixels for 2008.

Explanatory Variables (Significant at 0.05)	Correctly predicted urban pixels (%)	Nagelkerke R^2	Odds ratio
Population, Total	5.5	0.07	1.001
Distance to nearest urban pixels	86.6	0.80	0.931

Table 4.14a. Ouagadougou - Odds ratios and R^2 to predict urban pixels for 1986.

Explanatory Variables (Significant at 0.05)	Correctly predicted urban pixels (%)	Nagelkerke R^2	Odds ratio
NDVI, maximum	21.4	0.34	0.002
NDVI, minimum	8.2	0.27	0.001
Population, Total	25.0	0.27	1.001
NDVI, maximum + Population, Total	46.4	0.48	0.004 1.001
Distance to nearest urban pixels	82.8	0.63	0.990
Distance to core city area + Distance to nearest urban pixels + NDVI maximum	78.1	0.71	0.993 0.992 0.016

Table 4.14b. Ouagadougou - Odds ratios and R^2 to predict urban pixels for 2005.

Explanatory Variables (Significant at 0.05)	Correctly predicted urban pixels (%)	Nagelkerke R^2	Odds ratio
Distance to core city area	2.1	0.02	0.993
Distance to nearest urban pixels	81.2	0.50	0.996
NDVI, maximum	22.3	0.18	0.396
NDVI, minimum	22.3	0.27	0.083
Distance to core city area +Distance to nearest urban pixels	81.2	0.51	0.848 0.996
Distance to core city area +Distance to nearest urban pixels + NDVI, maximum	76.0	0.57	0.586 0.996 0.360

Table 4.14c. Ouagadougou - Odds ratios and R^2 to predict urban pixels for 2010.

Explanatory Variables (Significant at 0.05)	Correctly predicted urban pixels (%)	Nagelkerke R^2	Odds ratio
Human Influence Index	53.7	0.38	1.143
NDVI, maximum	23.4	0.27	0.127
Distance to nearest urban pixels	94.4	0.73	0.976
Distance to core city area + Distance to nearest urban pixels	94.4	0.74	2.373 0.976
Distance to nearest urban pixels + Population, total + NDVI, maximum	92.2	0.80	6.895 0.982 0.096
Distance to core city area + Distance to nearest urban pixels	94.4	0.74	2.373 0.976

Table 4.15a. Kano - Odds ratios and R^2 to predict urban pixels for 1985.

Explanatory Variables (Significant at 0.05)	Correctly predicted urban pixels (%)	Nagelkerke R^2	Odds ratio
NDVI, maximum	62.1	0.58	0.001
NDVI, minimum	62.1	0.54	0.001
Population, Total	21.0	0.25	1.002
NDVI, maximum + Population, Total	60.8	0.61	0.001 1.001

Table 4.15b. Kano - Odds ratios and R^2 to predict urban pixels for 2000.

Explanatory Variables (Significant at 0.05)	Correctly predicted urban pixels (%)	Nagelkerke R^2	Odds ratio
Distance to nearest urban pixels	95.1	0.80	0.959

Table 4.15c. Kano - Odds ratios and R^2 to predict urban pixels for 2010.

Explanatory Variables (Significant at 0.05)	Correctly predicted urban pixels (%)	Nagelkerke R^2	Odds ratio
Human Influence Index	42.1	0.43	1.205
NDVI, maximum	23.4	0.27	0.127
NDVI, minimum	24.1	0.26	0.001
Distance to nearest urban pixels	89.9	0.71	0.990

The accuracy of the predicted urban area maps using the logistic regression for three different time periods for each city (with an exception of Kindia where none of the variables correctly predicted urban land use in 2005) are presented in figures 4.2 through 4.7. The maps presented shows the pixels with 50% or higher probability to convert to the urban pixels in that particular year. When we compared the predicted urban area to the actual urban area maps described in the *Data section, Response variable,* we found mix results (Table 4.16 through 4.21). The logistic regression models underestimated urban area for all time steps for the city of Kumasi (Table 4.16), Kindia (Table 4.19) and Kano (Table 4.21) varying from about 0.5% to 27%. Whereas the models overestimated the urban area in Ouagadougou by 16%-28% (Table 4.20) in all time steps. In the city of Daloa, the logistic regression models underestimated the urban area for 1991 (by 13%) and 2000 (by 3%) while it overestimated the urban area in 2008 by 7% 1990 (Table 4.17). Similarly, for the city of Abuja the logistic regression model underestimate urban area by 24% (in 1990) and by about 5% (in 2001) while in 2005 it overestimated the area by almost 19% (Table 4.18).

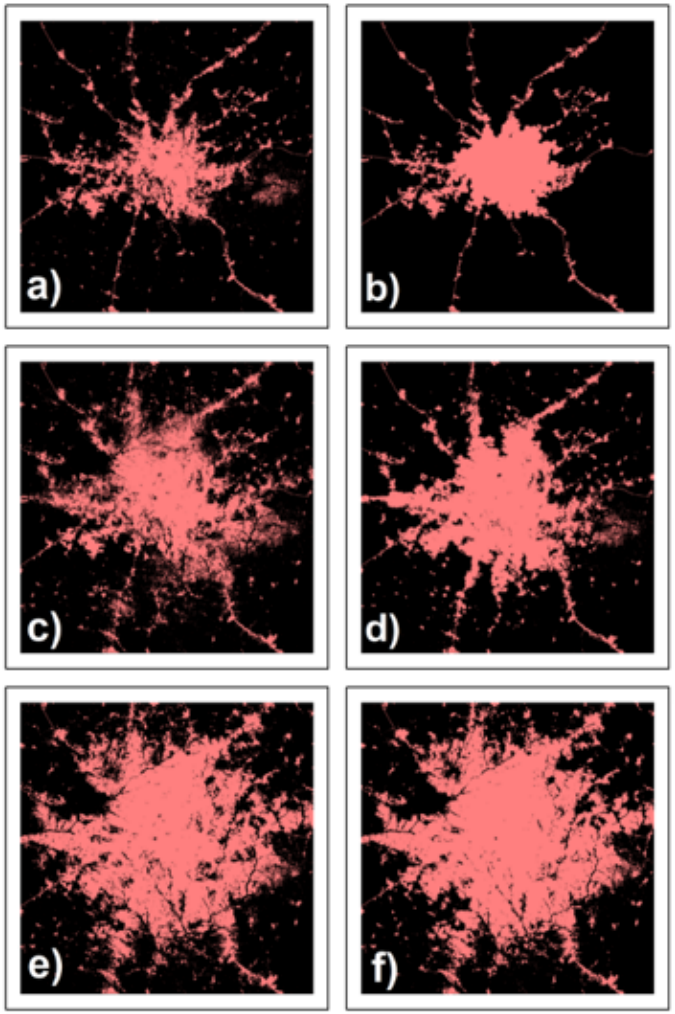

Figure 4.2. Actual (a, c and d) vs Predicted (b, d and f) urban pixels for 1986, 2005 and 2010 for Kumasi.

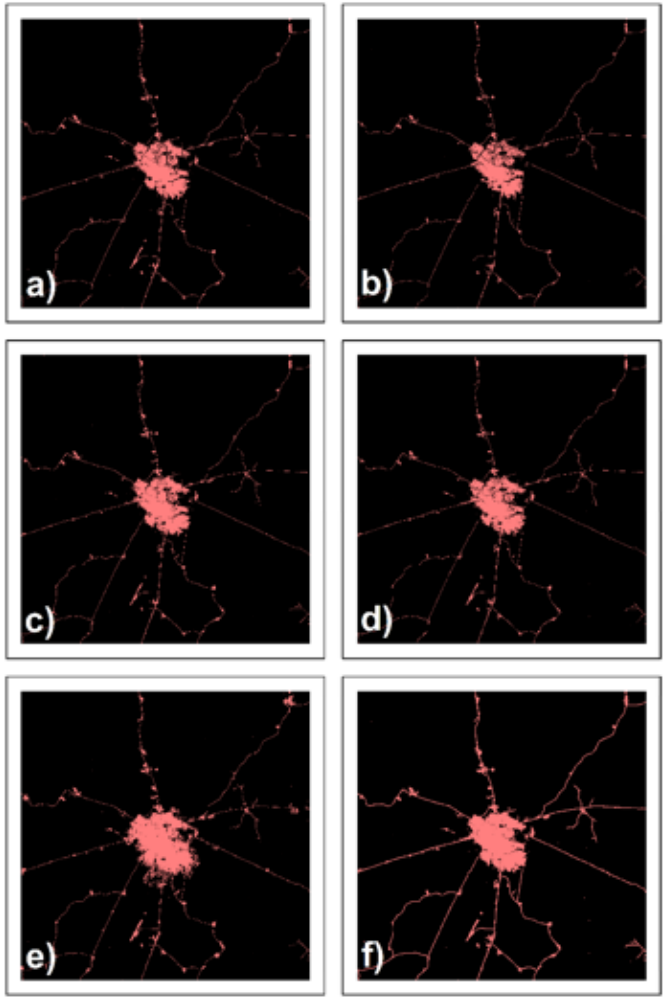

Figure 4.3. Actual (a,c and d) vs Predicted (b, d and f) urban pixels for 1991, 2000 and 2008 for Daloa.

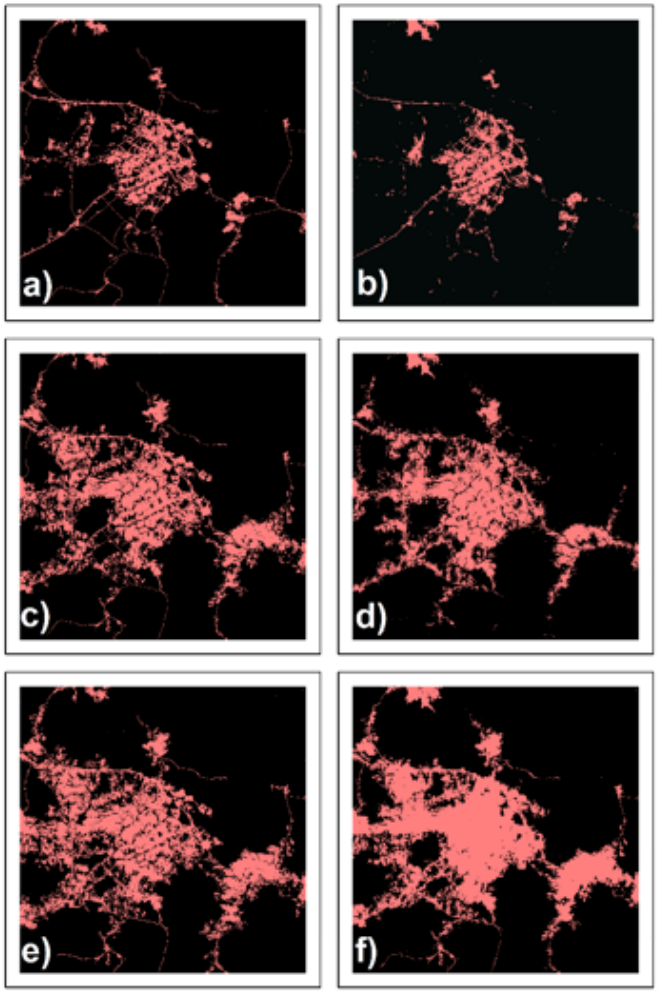

Figure 4.4. Actual (a, c and d) vs Predicted (b, d and f) urban pixels for 1990, 2001 and 2005 for Abuja.

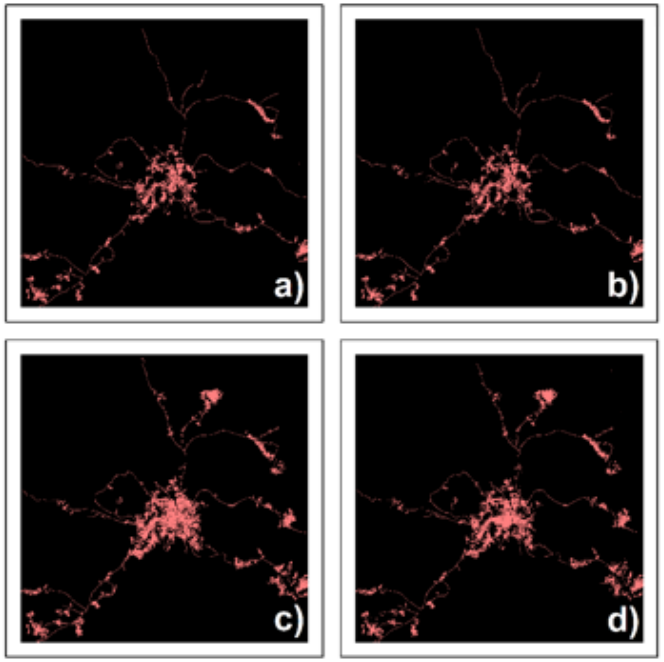

Figure 4.5. Actual (a and c) vs Predicted (b and d) urban pixels for 1995 and 2010 for Kindia.

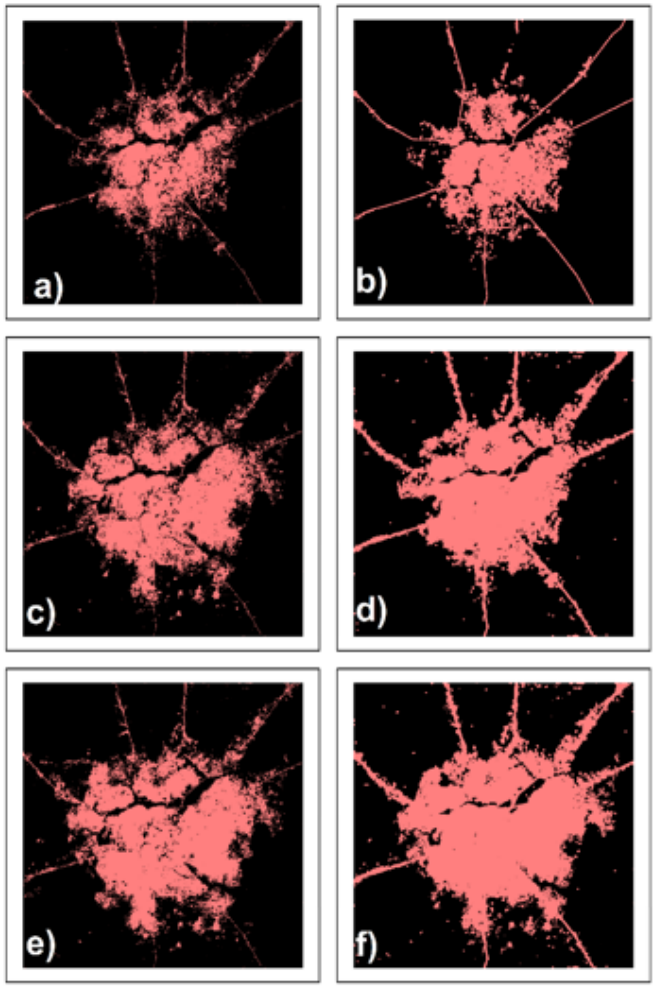

Figure 4.6. Actual (a, c and d) vs Predicted (b, d and f) urban pixels for 1986, 2005 and 2010 for Ouagadougou.

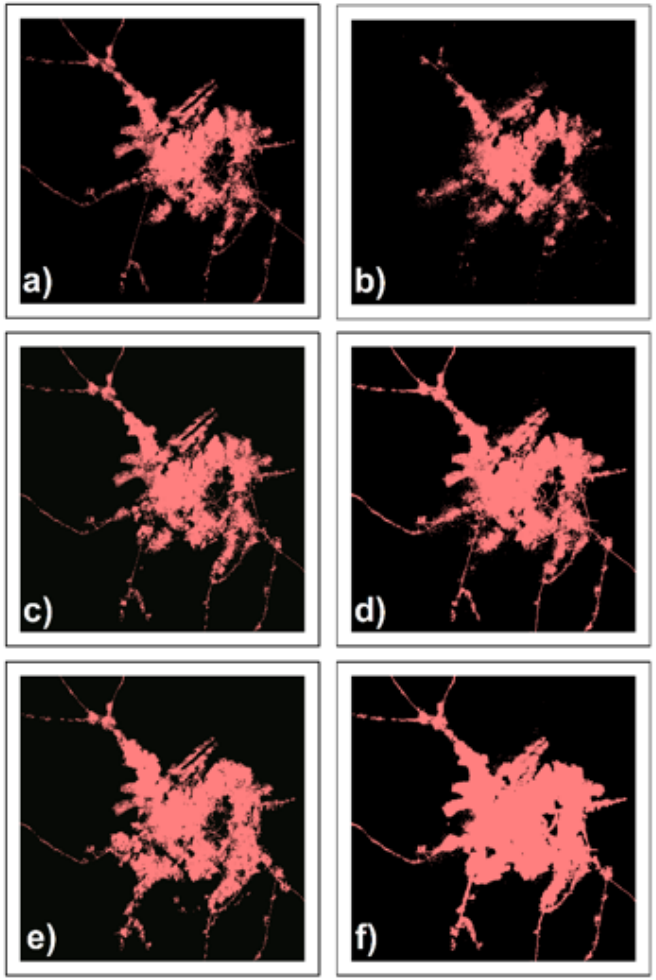

Figure 4.7. Actual (a, c and d) vs Predicted (b, d and f) urban pixels for 1985, 2000 and 2010 for Kano.

Table 4.16. Kumasi-Accuracy of predicted of urban pixels.

Year	Actual (Pixels)	Predicted (Pixels)	Difference (%)
1986	133,354	112,644	-15.53
2005	242,690	197,807	-18.50
2010	395,392	374,725	-5.23

Table 4.17. Daloa-Accuracy of predicted of urban pixels.

Year	Actual (Pixels)	Predicted (Pixels)	Difference (%)
1991	35,355	30,911	-12.57
2000	36,955	35,810	-3.10
2008	51,212	54,793	+7.00

Table 4.18. Abuja-Accuracy of predicted of urban pixels.

Year	Actual (Pixels)	Predicted (Pixels)	Difference (%)
1990	80,274	60,994	-24.02
2001	176,273	167,740	-4.84
2005	211,137	250,213	+18.51

Table 4.19. Kindia-Accuracy of predicted of urban pixels.

Year	Actual (Pixels)	Predicted (Pixels)	Difference (%)
1995	30,235	30,092	-0.47
2010	62,282	45,373	-27.15

Table 4.20. Ouagadougou-Accuracy of predicted of urban pixels.

Year	Actual (Pixels)	Predicted (Pixels)	Difference (%)
1986	131,792	157,428	+19.45
2005	226,764	263,738	+16.31
2010	261,097	335,109	+28.35

Table 4.21. Kano-Accuracy of predicted of urban pixels.

Year	Actual (Pixels)	Predicted (Pixels)	Difference (%)
1985	124,102	104,353	-15.91
2000	137,791	172,809	-25.41
2010	182,932	219,495	-19.98

Discussion

Urban growth and underlying determinants of such growth need special attention from planners and urban development professionals especially in a region, such as West Africa, which has a high population growth. In this study we identified and quantified the causative factors that are driving the growth of urban land use in six cities of West Africa. To my knowledge this is the first time that such attempt has been made for West Africa.

All cities except the city of Daloa revealed urban area spread away from the city center in recent years. This is comparable to what has been shown for other cities around the world (Henríquez and Azócar 2006; Schneider et al., 2008).

We used sixteen different explanatory variables that potentially have an association with urban growth in the region. Some of the data for the explanatory

variables were too coarse to be useful in our study. For example, the precipitation anomaly and Palmer Drought Severity Index (PDSI) are important variables to understand the impact of climatic variability in the region which has faced long and severe droughts over the past 4-5 decades. Drought is thought to be one of the factors driving the rural to urban migration (Barrios et al., 2006; Parnell and Walawege 2011). However these two sets of data were available only at very coarse resolutions of 2.5º × 2.5º which failed to capture the variability within the 30 Km × 30 Km city boundary used in our study. Another important socio-economic variable, believed to have triggered rural to urban migration in the region, is conflict. This data is also available at the country level. These two variables did not reveal a significant relationship.

Among the environmental parameters, NDVI played a role in predicting the urban land use. In some years, NDVI predicted urban land use by as high as 65% in the case of Kumasi (for the year 2005), 62% in the case of Kano for the year 1985, 61% in Daloa for the year 2000. But in the case of Abuja, Kano and Ouagadougou NDVI prediction were around 23% only for 2005 or later years. We did not observe clear trends in the prediction of the urban pixel in the region. Records show that Nigeria (Abuja and Kano) in 1983, Guinea (Kindia) in 1998, Burkina Faso (Ouagadougou) in 1995, and again in 1998-2001 have droughts (Tarhule and Woo, 1997; Jalloh et al., 2013). But we did not observe any effect of drought on the trend of the predictive capability of the logistic regression model using NDVI as the explanatory variables in those cities.

Higher level of association of proximity parameters such as distance to the core city area or distance to the urban area have been extensively used in earlier studies and

found to be important in explaining land use transitions (Luo and Wei, 2009). The result from this study also demonstrates proximity parameters playing a key role in the transformation of urban land use in West African cities. The proximity parameters explained 40 to 100 percent of the urban transition in West Africa.

Conclusions

Well planned and managed cities with better mobility and services play an important role in a national development agenda (Kessides, 2005). But while providing such services, a city goes on extensive transformations affecting the urban ecosystem negatively. Therefore, understanding such transformation is an important step for the city planners, managers and researchers to come up with a sustainable urban development plan.

Logistic regression is a way to analyze the complex process of urban transformation. The logistic regression model, though data intensive, can integrate various thematic variables concerning the urban transformation and predict their association with the urban transformation. In this study, we identified factors that have played a role in such transformation in six cities of West Africa.

We observed that the factors related to proximity parameters and Normalized Difference Vegetation Index are the major factors in the region for the urban transformation but the levels of such transformation were inconsistent in cities whether or not they belong to the same country or same eco-region. This shows the uniqueness of the cities going urban transformation.

Literature cited

Agarwal, C, G M Green et al. (2002). A review and assessment of land-use change models: dynamics of space, time, and human choice.

Aguayo, M I, T Wiegand et al. (2007). Revealing the Driving Forces of Mid-Cities Urban Growth Patterns Using Spatial Modeling: a Case Study of Los Ángeles, Chile. *Ecology and Society* 12(1).

Aguayo, M I, T Wiegand et al. (2007). Revealing the Driving Forces of Mid-Cities Urban Growth Patterns Using Spatial Modeling: a Case Study of Los Ángeles, Chile. *Ecology and Society* 12(1).

Alberti, M., Marzluff, J. M., Shulenberger, E., Bradley, G., Ryan, C., & Zumbrunnen, C. (2003). Integrating humans into ecology: opportunities and challenges for studying urban ecosystems. *BioScience*, *53*(12), 1169-1179.

Allen, J. and K. Lu (2003). Modeling and Prediction of Future Urban Growth in the Charleston Region of South Carolina: a GIS-based Integrated Approach. *Ecology and Society* 8(2).

Arnold Jr, C. L. and C. J. Gibbons (1996). Impervious surface coverage: the emergence of a key environmental indicator. *Journal of the American planning Association* **62**(2): 243-258.

Barrios, S., L. Bertinelli, et al. (2006). Climatic change and rural–urban migration: The case of sub-Saharan Africa. *Journal of Urban Economics* 60(3): 357-371.

Briassoulis, H (2000) Analysis of Land Use Change: Theoretical and Modeling Approaches, available online from http://www.rri.wvu.edu/Webbook/Briassoulis/contents.htm assessed on August-September 2014.

Buerkert, A., Lawrence, P.R., Williams, J.H., & Marschner, H. (1995). Non-destructive Measurements of Biomass in Millet, Cowpea, Groundnut, Weeds and Grass

Swards using Reflectance and their Application for Growth Analysis. *Experimental Agriculture, 31*, 1-11

Chen, N., P. Valente and H Zlotnik (1998). What do we know about recent trends in urbanization? In Migration, urbanization, and development: New directions and issues: 59-88.

Cheng, J. and I. Masser (2003). Urban growth pattern modeling: a case study of Wuhan city, PR China. *Landscape and Urban Planning* 62(4): 199-217.

Cheng, J. and I. Masser (2003). Urban growth pattern modeling: a case study of Wuhan city, PR China. *Landscape and Urban Planning* 62(4): 199-217.

DESA/UN (2011) Population Distribution, Urbanization, Internal Migration and Development: An International Perspective, Department of Economic and Social Affairs, Population Division of the United Nations available from www.unpopulation.org.

EPA (2000) Projecting Land-Use Change: A Summary of Models for Assessing the Effects of Community Growth and Change on Land-Use Patterns. EPA/600/R-00/098. U.S. Environmental Protection Agency, Office of Research and Development, Cincinnati, OH.

Funk, C.C., Budde, M.E. (2009) Phenologically-tuned MODIS NDVI-based production anomaly estimates for Zimbabwe. *Remote Sensing of Environment* 113, 115-125.

Geoghegan, J., S. C. Villar, et al. (2001). Modeling tropical deforestation in the southern Yucatan peninsular region: comparing survey and satellite data. *Agriculture Ecosystems & Environment* 85(1-3): 25-46.

Gleditsch, Nils Petter, Peter Wallensteen, Mikael Eriksson, Margareta Sollenberg, and Håvard Strand (2002) Armed Conflict 1946-2001: A New Dataset. *Journal of Peace Research* 39(5).

Guttman, N. B. (1998). Comparing the palmer drought index and the standardized precipitation index, Wiley Online Library.

Hu, Z. and C. Lo (2007). Modeling urban growth in Atlanta using logistic regression. *Computers, Environment and Urban Systems* 31(6): 667-688.

Irwin, E. G. and J. Geoghegan (2001). Theory, data, methods: developing spatially explicit economic models of land use change. *Agriculture, Ecosystems & Environment* 85(1): 7-24.

Jalloh, Abdulai; Nelson, G.C.; Thomas, T.S.; Zougmoré, R. B.; Roy-Macauley, H. eds. West African agriculture and climate change: a comprehensive analysis. Intl Food Policy Res Inst, 2013.

Janowiak, J. E. and P. Xie, 1999: CAMS_OPI: A Global Satellite-Rain Gauge Merged Product for Real-Time Precipitation Monitoring Applications. *J. Climate*, vol. 12, 3335-3342.

Kleinbaum, D G, and M Klein (2010) Logistic Regression, Statistics for Biology and Health, DOI 10.1007/978-1-4419-1742-3_1, # Springer Science Business Media, LLC 2010

Maselli, F., Romanelli, L., Bottai, L., Maracchi, G. (2000) Processing of GAC NDVI data for yield forecasting in the Sahelian region. *International Journal of Remote Sensing* 21, 3509-3523.

McDonnell, M J and S T Pickett (1990) Ecosystem structure and function along urban-rural gradients: an unexploited opportunity for ecology. *Ecology*: 1232-1237.

Onlinecourses.science.psu.edu. "Welcome To STAT 504! | STAT 504". N.p., 2016. Web. 14 Feb. 2016.

Parnell, S. and R. Walawege (2011). Sub-Saharan African urbanisation and global environmental change. *Global Environmental Change* 21, Supplement 1(0): S12-S20.

Pettorelli, N., Vik, J.O., Mysterud, A., Gaillard, J.-M., Tucker, C.J., & Stenseth, N.C. (2005). Using the satellite-derived NDVI to assess ecological responses to environmental change. *Trends in Ecology & Evolution*, 20, 503-510

Rasmussen, M S (1998) Developing simple, operational, consistent NDVI-vegetation models by applying environmental and climatic information. Part I: Assessment of net primary production. *International Journal of Remote Sensing* 19, 97-119.

Reynolds, C A, M Yitayew, et al. (2000). Estimating crop yields and production by integrating the FAO Crop Specific Water Balance model with real-time satellite data and ground-based ancillary data. *International Journal of Remote Sensing 21, 3487-3508*.

Robinson, D. T., D. G. Brown, et al. (2007). Comparison of empirical methods for building agent-based models in land use science. *Journal of Land Use Science* 2(1): 31-55.

Schneider, A. and C. E. Woodcock (2008). Compact, Dispersed, Fragmented, Extensive? A Comparison of Urban Growth in Twenty-five Global Cities using Remotely Sensed Data, Pattern Metrics and Census Information. *Urban Studies* 45(3): 659-692.

Serneels, S. and E. F. Lambin (2001). Proximate causes of land-use change in Narok District, Kenya: a spatial statistical model. *Agriculture, Ecosystems & Environment* 85(1): 65-81.

Tarhule, Aondover, and Ming-Ko Woo. Towards an interpretation of historical droughts in northern Nigeria. *Climatic Change* 37, no. 4 (1997): 601-616.

Tucker, C.J., J. E. Pinzon, M. E. Brown, D. Slayback, E. W. Pak, R. Mahoney, E. Vermote and N. El Saleous (2005), An Extended AVHRR 8-km NDVI Data Set Compatible with MODIS and SPOT Vegetation NDVI Data. *International Journal of Remote Sensing*, Vol 26:20, pp 4485-5598.

UN-Habitat (2014) The State of African Cities 2014: Re-imagining sustainable urban transitions, United Nations Human Settlements Program, available online http://unhabitat.org/books/state-of-african-cities-2014-re-imagining-sustainable-urban-transitions/

Veldkamp, A. and E. F. Lambin (2001). Predicting land-use change. *Agriculture Ecosystems & Environment* 85(1-3): 1-6.

Walsh, S. J., T. W. Crawford, et al. (2001). A multiscale analysis of LULC and NDVI variation in Nang Rong district, northeast Thailand. *Agriculture Ecosystems & Environment* 85(1-3): 47-64.

Zhu, L. and J.-f. Huang (2006). GIS-based logistic regression method for landslide susceptibility mapping in regional scale. *Journal of Zhejiang University Science* 7(12): 2007-2017.

Chapter 5: Conclusions

This dissertation research has focused on West Africa, one of the fastest-growing regions of the world. The average urban population growth rate since 1950 is the second highest in West Africa compared to the other regions of Africa. In 1900, the growth rate was 5% which rose to 12% in 1950, 28% in 1980 and 17% in 2000 (Fuwape and Onyekwelu 2010). This region is also one of the rapidly urbanizing sub-regions in Africa (UN-Habitat, 2014).

The pressures on the land resources are palpable in the region as the result of the growing population and rapid growth of the small towns and cities. Therefore, understanding the current state of land cover and land use in the region is, therefore, critically important. Also, this is the region which has endured most severe and longest droughts since the late 1970s (Tarhule and Woo, 1997; Jalloh et al., 2013; Druyan, 2011; Wang and Eltahir, 2000) showing its vulnerability to climatic variability.

Many countries in the region lack resources to prepare a long term land cover data which play a critical role to formulate a sustainable land development policies. So, we investigated if the global land cover data that are available freely could be used for such purposes. We compared twelve datasets at the pixel, country and eco-region levels to estimate croplands. We choose to evaluate the datasets on the basis of cropland because of two prime reasons, the importance of agriculture in the region as well as in land cover change studies. Agriculture is a crucial livelihood for over 50 percent of people in the region. Also, land use change is mainly characterized by the expansion of urban and infrastructure areas into cropland while the expansion of cropland occurred at the cost of grasslands, savannahs and forest areas (Holmgren, 2006). The eco-region

and country level analysis showed high variability in cropland estimation. At the pixel level, the IIASA-IFPRI and GLC-SHARE showed better accuracies to estimate croplands in the region newer datasets agreed better to estimate the cropland.

With regards to the urban land use growth, this dissertation attempted to understand the phenomenon investigating six small to large but rapidly growing cities: Kumasi of Ghana, Daloa of Cote d'Ivoire, Abuja and Kano in Nigeria, Kindia of Guinea, and Ouagadougou of Burkina Faso in the region. We found that all the cities, except Daloa, have a large number area of non-urban converted to urban in the past three to four decades. The growth of the urban area is high, 13 to 54%, but the trends of the growth were not consistent. Abuja and Ouagadougou were growing but the rate of growth had been decreasing in the recent times. Kumasi has been growing consistently since 1975 at a much higher rate and still growing, about 13% annually. Also, most of the cities have shown a higher rate of growth of urban land use than population except Abuja and Ouagadougou. Abuja and Ouagadougou have higher population growth, in the range of 10.7 to 15.8% than the growth of the urban land use which varies from 3 to 4.5%. We did not observe any similarities on the growth of the urban area of the cities from the same eco-region.

Finally, this research identified and quantified environmental and socio-economic variables such as Normalized Difference Vegetation Index (NDVI), distance to the urban area and population showed strong associations with the growth of the six cities in West Africa. We found out that none of the variables showed consistency in their association of predicting urban land use for multiple years. Out of the six cities, two cities Ouagadougou and Kano showed some level of agreement in associating the

urban growth with the NDVI at different time periods. In the rest of the cities, accessibility such as distance to the nearest urban area and distance to the core city area are the dominating factors in the growth of six cities in West Africa. We also observed that among all variables except the population growth and human influence index tend to decrease the odds of non-urban conversion to urban.

This study revealed that the growth of the cities in the same country or eco-region had different drivers of the urban growth at different times. Also, the association of the drivers for the growth were different within a city at the different time periods or in other cities from the same eco-region. So the Null hypothesis is rejected. Instead, the urban growth factors were localized and playing out a different level of associations in the conversion of urban land uses in the cities of West Africa.

Literature cited

Fuwape, J. and J C Onyekwelu (2011). Urban forest development in West Africa: benefits and challenges. *Journal of Biodiversity and Ecological Sciences*, Vol. 1, No. 1: 77-94.

UN-Habitat (2014) The State of African Cities 2014: Re-imagining sustainable urban transitions, United Nations Human Settlements Program, available online http://unhabitat.org/books/state-of-african-cities-2014-re-imagining-sustainable-urban-transitions/

Jalloh, A.; Nelson, G.C.; Thomas, T.S.; Zougmoré, R. B.; Roy-Macauley, H. eds. West African agriculture and climate change: a comprehensive analysis. Intl Food Policy Res Inst, 2013.

Tarhule, A., and Ming-Ko Woo. Towards an interpretation of historical droughts in northern Nigeria. Climatic Change 37, no. 4 (1997): 601-616.

Druyan, L. M. (2011) Studies of 21st-century precipitation trends over West Africa, *International Journal of Climatology 31(10),* 1415-1424.

Wang, G. and E. A. B. Eltahir (2000). Biosphere atmosphere interactions over West Africa. II: Multiple climate equilibria, *Quarterly Journal of the Royal Meteorological Society* 126(565): 1261-1280.